DOI:10.14753/SE.2024.3001

SEMMELWEIS EGYETEM

DOKTORI ISKOLA

Ph.D. értekezések

3001.

HORVÁTH KRISZTINA

Neuroendokrinológia
című program

Programvezető: Dr. Fekete Csaba, tudományos tanácsadó

Témavezető: Dr. Kovács Krisztina, tudományos tanácsadó

DOI:10.14753/SE.2024.3001

IMPACT OF CRH NEURONS IN THE STRESS RESPONSE

PhD thesis

Krisztina Horváth

János Szentágothai Neurosciences Doctoral School

Semmelweis University

Supervisor: Krisztina Kovács, D.Sc.

Official reviewers: Attila Patócs, MD, D.Sc.
Máté Tóth, Ph.D.

Head of the Complex Examination Committee: Dániel Bereczki, MD, D.Sc.

Members of the Complex Examination Committee: Árpád Dobolyi, D.Sc.
Tibor Kovács, MD, Ph.D.

Budapest
2024

DOI:10.14753/SE.2024.3001

Table of Contents

DOI:10.14753/SE.2024.3001

DOI:10.14753/SE.2024.3001

DOI:10.14753/SE.2024.3001

Abbreviations

3V – Third ventricle

4V – Fourth ventricle

AAV8 – Adeno-associated virus serotype 8

ACA – Anterior cingulate area

act. DREADD – activator DREADD

ADX – Adrenalectomy

AHNc – Anterior hypothalamic nucleus

AHNp – Anterior hypothalamic nucleus, posterior part

AId – Agranular insular area, dorsal part

AON – Anterior olfactory nucleus

AP – Area postrema

AP-1 – Activator protein-1

ARH – Arcuate hypothalamic nucleus

AVP – Arginine vasopressin

B – Barrington's nucleus (Pontine Urinary Center)

BAC – Bed nucleus of the anterior commissure

BNST – Bed nuclei of the stria terminalis

BSTa – Bed nuclei of the stria terminalis, anterior division

BSTad – Bed nuclei of the stria terminalis, anterior division, dorsal part

BSTav – Bed nuclei of the stria terminalis, anterior division, ventral part

BSTp – Bed nuclei of the stria terminalis, posterior division

BW – Body weight

CA – Ammon's horn (Hippocampal Formation)

CA3 – Field CA3

CEA – Central amygdalar nucleus

CL – Central lateral nucleus of the thalamus

CLA – Claustrum

CM – Central medial nucleus of the thalamus

CN – Cochlear nuclei

CNO – Clozapine-N-oxide

CNS – Central nervous system

COA – Cortical amygdalar area

CORT – Corticosterone

CRH – Corticotropin-releasing hormone

CRH-R1 – CRH receptor-1

CRH-R2 – CRH receptor-2

CRS – Chronic repeated restraint stress

CVS – Chronic variable stress

CTXsp – Cortical subplate

CU – Cuneate nucleus

CS – Superior central nucleus raphe

DG – Dentate gyrus

DIO – Double-floxed inverted open-reading frame

DMX – Dorsal motor nucleus of the vagus nerve

DMH – Dorsomedial nucleus of the hypothalamus

DP – Dorsal peduncular area

DpMe – Deep mesencephalic nucleus

DREADD – Designer Receptors Exclusively Activated by Designer Drug

DTr – Dorsal transition zone

ECU – External cuneate nucleus

Epd – Endopiriform nucleus, dorsal part

EW – Edinger-Westphal nucleus

FS – Fundus of striatum

G – Geniculate nucleus

GABA – Gamma-aminobutyric acid

GAS – General Adaptation Syndrome

GLU – Glutamate

GR – Glucocorticoid receptor

GU – Gustatory areas

hM3D(Gq) – Gq coupled human M3 muscarinic receptor

HPA – Hypothalamo-pituitary-adrenal

hSyn – human *synapsin 1*

IEG – Immediate-early gene

IF – Interfascicular nucleus raphe

ILA – Infralimbic area

IO – Inferior olivary complex

IP – Intraperitoneal

IPN – Interpeduncular nucleus

ISH – In Situ Hybridization

LC – Locus coeruleus

LGv – Ventral part of the lateral geniculate complex

LHA – Lateral hypothalamic area

LPS – lipopolysaccharide

LRN – Lateral reticular nucleus

LS – Lateral septal nucleus

LV – Lateral ventricles

LVOV – Lateral and ventral orbital cortex ventral part

MC2R – Melanocortin type II receptor

MCLHD – Magnocellular nucleus, lateral hypothalamic area dorsal part

MCLHV – Magnocellular nucleus, lateral hypothalamic area ventral part

ME – Median eminence

MEA – Medial amygdalar nucleus

Mm – Mus musculus

MOBgl – Main olfactory bulb, glomerular layer

MOBopl – Main olfactory bulb, outer plexiform layer

Mop – Primary motor area

MOs – Secondary motor area

MPN – Medial preoptic nucleus

MR – Mineralocorticoid receptor

MV – Medial vestibular nucleus

NB – Nest building

NCBI – National Center for Biotechnology Information

NE – Novel environment

NLOT – Nucleus of the lateral olfactory tract

NTS – Nucleus of the solitary tract

O – Orbital cortex

OF – Open field

OT – Olfactory tubercle

PAG – Periaqueductal gray

PCG – Pontine central gray

PeF – Perifornical nucleus

PG – Pontine gray

PGdm – Pontine nucleus, dorsomedial part

PHd – Posterior hypothalamic nucleus, dorsal part

PHp – Posterior hypothalamic nucleus, posterior

PHv – Posterior hypothalamic nucleus, ventral part

PIL – Posterior intralaminar thalamic nucleus

PIR – Piriform area

PL – Prelimbic area

PM – Premammillary nucleus

PMTH – Posteromedial thalamic area [intermediodorsal nu of the thalamus; subparafascicular area]

POMC – Pro-opiomelanocortin

PRC – Precommissural nucleus

PRP – Nucleus prepositus

PSTN – Parasubthalamic nucleus

PVH – Paraventricular hypothalamic nucleus

PVR – Periventricular region

PVTa – Paraventricular nucleus of the thalamus, anterior

PVTp – Paraventricular nucleus of the thalamus, posterior

RE – Nucleus reuniens

RFP – Red fluorescent protein

RH – Rhomboid nucleus

ROI – Regions of interest

RPA – Nucleus raphe pallidus

RSP – Retrosplenial area

SAM – Sympathetic-adreno-medullar

SCH – Suprachiasmatic nucleus

SCs – Superior colliculus, sensory related

SHRP – Stress hyporesponsive period

SNc – Substantia nigra, compact part

SO – Supraoptic nucleus

SSp – Primary somatosensory area

SSs – Supplemental somatosensory area

STN – Subthalamic nucleus

SUM – Supramammillary nucleus

TRN – Tegmental reticular nucleus

TST – Tail suspension test

TTv – Taenia tecta, ventral part

VMH – Ventromedial hypothalamic nucleus

X – Nucleus x

XII – Hypoglossal nucleus

ZI – Zona incerta

DOI:10.14753/SE.2024.3001

1. Introduction

1.1. Dynamic equilibrium from the aspect of an organism

The concept of homeostasis stands as a fundamental principle crucial for preserving the stability of living systems. The term – which was conceived to elucidate the concept of "milieu intérieur" previously described by Claude Bernard (1) – was coined by Walter Cannon in 1926 (2) and gained widespread recognition in 1932 with the publication of his book, The Wisdom of the Body (3). Cannon postulated that physiological variables (e.g. blood pressure, pH, body temperature) are maintained within a specific range through the control of feedback system, which regulation ensures the stability of the internal environment (4). The concept was extended by Carl Richter, who acknowledged that the maintenance of homeostasis involves not only the internal control system but also the significant contribution of behavioral responses (5). In the late 20th century, James Hardy proposed the idea that values of physiological variables are perpetually compared to a predetermined "set point" through homeostatic mechanisms to keep them within a sufficient range (6). Therefore, while it is possible to designate a mean value for each physiological parameter, general tendency is for that value to fluctuate within a defined range, thereby engendering dynamic equilibrium.

Any external or internal stimulus that disrupts homeostasis − commonly referred to as a stressor − elicits stress response. This non specific, adaptive reaction of the organism confers adaptability to the changing environment through behavioral, metabolic and autonomic nervous system responses. The concept of stress was initially introduced by Hans Selye in 1936. He wrote: *„Stress is a nonspecific response of the living organism to any demand for change."* (7). Hans Selye further delineated three stages of the stress response (alarm reaction, active resistance and exhaustion) through General Adaptation Syndrome (GAS) (8, 9) and defined the pathological „triad of stress" that he observed to appear consistently after exposure to various stressors, regardless of their nature: enlargement of adrenal glands, involution of thymus and appearance of gastrointestinal ulceration (10). He asserted that "*Stress is the spice of life*", underscoring its essential role as a vital component of existence.

The absence of stress can potentially lead to a state of inactivity and boredom, ultimately resulting in a diminished quality of life (11). Thus, stress is indeed a

fundamental element of our existence. However, it is crucial to distinguish between eustress, which yields favorable effects, and distress, which has a negative impact. The aftermath of the stress reaction is contingent upon the nature of the triggering stimuli, the duration of exposure and the individual's unique perception and physiological response to the specific stressor (12). From the aspect of stimulus type, stressors can be differentiated based on their mode of action (e.g. physical, psychological) (13). In terms of duration, stress can be categorized as short-term (acute) and chronic stress. In case of chronic stress, the organism is exposed to a stressor for an extended period or is frequently exposed to various stressors over time (14). To gain a better understanding of the uniqueness of an individual's reaction to a stressor, it is essential to consider the match/mismatch and cumulative stress hypotheses. According to these hypotheses, the likelihood of an individual experiencing distress increases with the greater the disparity between conditions in early and adult life environments, or with an overall increase in adversity (15, 16).

In summary, while mild stress can enhance the efficiency of one's performance, excessively intense, repetitive or prolonged exposure to stress can ultimately result in failure of coping strategies. Development of behavioral biases, involving alterations in cognition, memory, learning, and emotional reactions or pathological conditions such as anxiety, depression, and cognitive impairment can occur (17-19) (Figure 1).

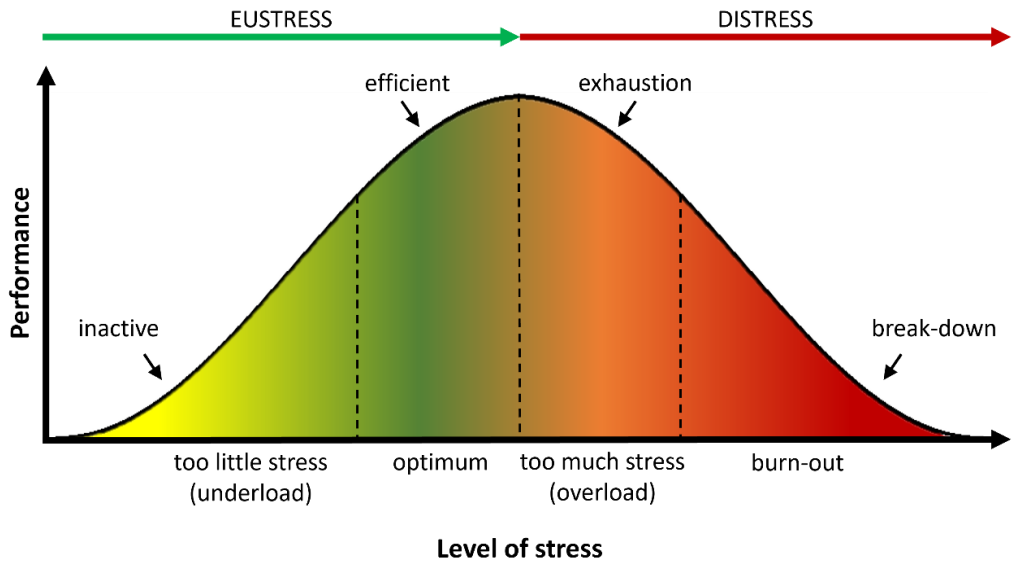

Figure 1. ***Stress curve.*** *Efficiency of the performance is highly dependent on the level of stress exposure.*

DOI:10.14753/SE.2024.3001

1.2. Stress in general

Since the discoveries of Walter Canon and Hans Selye in the past century, our understanding of *stress* has significantly expanded, owing to the numerous research conducted within the field. It is established, that a diverse array of brain structures – *stress system* – participates in the generation and regulation of stress response. While various stressors necessitate the collaboration of diverse cell types and neuronal networks across distinct brain regions, the precise mechanisms through which each type of stressor acts remain incompletely understood to date (20).

There is an immediate response to a threatening external or internal stimulus. The interplay of nervous, endocrine and immune systems promptly leads to activation of the sympathetic-adreno-medullar (SAM)-, and the hypothalamo-pituitary-adrenal (HPA) axis (21). SAM response is orchestrated by the sympathetic nervous system and is primarily mediated by catecholamines (epinephrine and norepinephrine) secreted by adrenal medulla (22). In contrast, HPA axis operates through regulation of hormonal secretion. Alterations stemming from activation of both axes occur within a few seconds to minutes, leading to heightened alertness and vigilance of the subject, which enables a more precise assessment of the ongoing situation. Beyond behavioral changes, a cascade of physiological adaptations takes place. In order to provide sufficient energy to confront the emerging crisis, physical adaptation facilitates the redirection of vital substrates by mobilizing all available resources (increasing blood glucose, lipolysis and proteolysis). Simultaneously, energy-consuming processes, including digestion and reproduction, are suppressed (23). These adaptations afford the subject opportunity to react quickly, even in life-threatening situations and enable a rapid decision on whether it is advisable to confront the challenge (fight) or to retreat (flight). This concept is referred to as fight-or-flight response (24, 25).

Stress response should be proportionate to the degree of threat posed by the stessor. The rate and temporality of induced alterations must provide the organism with sufficient resources and time to restore its steady state and maintain the homeostasis. However, it is essential to avoid under- or overshooting of the response, leading to a pathologic stress response, which may result in lasting damages (23).

Although the two aforementioned axes jointly orchestrate the stress response – as optimal functioning of SAM and HPA systems necessitates their complementary co-activation (26) – they are often examined independently. SAM system is recognized for initiating responses within seconds, leading to short-term effects that typically subside 20-60 minutes post-challenge (20). In contrast, HPA system is generally characterized as having a slower but prolonged and permissive impact, allowing normalization of defense responses over time (27, 28).

1.3. Hypothalamo-pituitary-adrenal (HPA) axis

1.3.1. Paraventricular nucleus of the hypothalamus (PVH)

The operation of the hypothalamo-pituitary-adrenal axis is orchestrated by the paraventricular nucleus (PVH) of the hypothalamus. This specific brain region is in the perfect position to integrate stress-related information (nociceptive, visual, somatosensory, acoustic, visceral and blood derived signals) and initiate neuroendocrine stress response through adaptive neuroendocrine-, autonomic-, metabolic- and behavioral responses (29-31). Systemic stress related afferents ascend from the brainstem (solitary tract, locus coeruleus, ventrolateral medulla) and convey their information directly through catecholaminergic (noradrenergic) pathways. In contrast, psychological stressors are mediated by various indirect inputs. For instance, limbic structures (e.g. lateral septum, hippocampus, central and medial amygdala) affect the stress axis through interconnections with other brain regions, mainly acting on neurons of bed nuclei of the stria terminalis (BNST) or the peri-PVH region (32, 33).

According to literature, various stressors evoke different patterns of neuronal activation within the PVH, which reflects the structural complexity of the region (13, 34). PVH neurons can be categorized into three classes: magnocellular cells, hypophyseotropic parvocellular cells and preautonomic (extrahypophyseotropic) parvocellular cells. Each type can be distinguished based on their morphology and function. Magnocellular neurons have large and round cell bodies with fewer dendritic arbors. These cells synthesize arginine vasopressin (AVP) and oxytocin, which they release into the general circulation through direct axonal transport that terminates in the neurohypophysis. AVP is best known for its role in maintaining the osmotic balance of the organism, while oxytocin is mainly recognized for its involvement in reproduction

and bonding. In contrast to the magnocellular cells, the smaller parvocellular neurons exhibit a greater number of dendritic branches. Corticotropin-releasing hormone (CRH) neurons of the PVH also belong to the cluster of parvocellular neurons. These CRH cells can be further divided into two subgroups. Preautonomic parvocellular CRH cells project to the brainstem (e.g. locus coeruleus, parabrachial nucleus) and to the spinal cord and mediate autonomic stress reaction. In contrast, hypophyseotropic CRH neurons are the key regulator cells of HPA axis and innervate the external zone of median eminence (ME) and release CRH into the portal system of the adenohypophysis (anterior lobe of the pituitary gland) (31, 35). Hypophyseotropic parvocellular cells have been shown to co-release AVP and oxytocin as well. These peptide hormones play an essential role in the regulation of stress cascade via potentiating CRH action at the pituitary (33).

Numerous stimulatory and inhibitory pathways ensure the optimal responsiveness of HPA axis by acting on the CRH^{PVH} neurons. CRH cells of the region are mainly regulated by three neurotransmitters (Figure 2). Principal inhibitory neurotransmitter is the gamma-aminobutyric acid (GABA), which binds to $GABA_A$ receptors. PVH receives GABAerg imputs from the area surrounding the supraoptic nucleus (SO), perifornical nucleus (PeF), anterior hypothalamic nucleus (AHNp), bed nuclei of the stria terminalis, posterior division (BSTp), prefrontal cortex, hippocampus (HC), peri-PVH region and from the anterior part of the PVH itself. Another crucial neurotransmitter, that plays a key role in direct excitatory actions is glutamate (GLU). Several subtypes of metabotropic and ionotropic glutamate receptors have been identified within the region. Glutamatergic afferents of the PVH have been reported to originate from the ventromedial hypothalamic nucleus (VMH), posterior hypothalamic nucleus (PH), dorsomedial nucleus of the hypothalamus (DMH), anterior hypothalamic nucleus (AHNc), lateral hypothalamic area (LHA), paraventricular nucleus of the thalamus (PVT), medial amygdalar nucleus (MEA), peri-PVH region and from intra-PVH areas. Third neurotransmitter, that also regulates the neurons of the PVH is norepinephrine (NE). The most significant NE innervation of the PVH originates from the nucleus of the solitary tract (NTS) of the brainstem. By acting on alpha-1 (α1) and beta (β) adrenergic receptors, NE plays both excitatory and inhibitory role. While it can

stimulate CRH^{PVH} neurons through triggering glutamatergic afferents, it can also modulate GABA release (35).

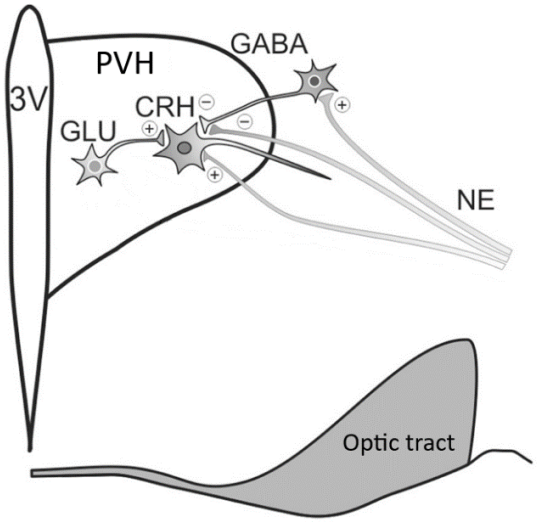

Figure 2. ***Activity of CRH^{PVH} neurons is mainly regulated by three neurotransmitters: gamma-aminobutyric acid (GABA), glutamate (GLU) and norepinephrine (NE).*** *Paraventricular hypothalamic nucleus (PVH); Corticotropin-releasing hormone (CRH); Third ventricle (3V) (35).*

1.3.2. Neuroendocrine stress cascade

Homeostatic challenges activate the HPA axis through the initiation of CRH release from the hypophyseotropic parvocellular neurons of the PVH into the portal vasculature of the adenohypophysis. Upon binding to CRH receptor-1 (CRH-R1) on the corticotrope cells, CRH initiates ACTH secretion. ACTH is derived from pro-opiomelanocortin (POMC) precursor polypeptide, along with α-, β- and γ-MSH, CLIP, β-lipotroin, γ-lipotropin and β-endorfin. The peak of ACTH in the plasma can be detected 5-15 minutes post-stress (36). ACTH then reaches the adrenal glands through systemic circulation. The adrenal cortex consists of three layers. The outer part (zona glomerulosa) synthesizes aldosterone (fluid, mineral homeostasis). The middle part (zona fasciculata) produces glucocorticoids (and androgens). The inner part (zona reticularis) also synthesizes androgens. It is important to highlight that the principal glucocorticoid in humans is cortisol, while corticosterone (CORT) in mice. Elevated ACTH, acting through melanocortin type II receptors (MC2R), stimulates the two inner zones of adrenal cortex, thereby resulting in glucocorticoid and androgen release. Deficiency of ACTH leads to atrophy of the two regions. The level of circulating

glucocorticoids peaks 15-30 minutes post-stress (31, 33). In target tissues, CORT acts on two types of nuclear receptors, the mineralocorticoid (MR, NR3C2) and glucocorticoid (GR, NR3C1) receptors. Basal and stress induced occupancy along with the distribution of the receptors differs. As MR exhibits a 10 times greater affinity for CORT compared to GR, mineralocorticoid receptors are almost fully occupied even in the basal state of the organism. Thus, MR mostly plays role in the early-phase of stress response and CORT mainly exerts its effect through glucocorticoid receptors in stress reactions. Presence of MR has been described in the region of CA1 and lateral septum (LS), while GR can be found in LS, dentate gyrus (DG), NTS, central nucleus of amygdala (CEA), PVH and locus coeruleus (LC) (23, 32, 33).

1.3.3. Regulation of HPA axis

The adaptability of the neuroendocrine stress response is ensured by a multistep negative feedback system. The activity of HPA axis is mainly modulated by glucocorticoids via various direct and indirect ways. CORT exerts negative feedback directly at the levels of hypothalamus and anterior pituitary: in addition to inhibiting the secretion of CRH and ACTH, CORT also suppresses the expression of the CRH and the precursor of ACTH (POMC) (37). Furthermore, through non-genomic mechanisms, glucocorticoids induce endocannabinoid synthesis and release from the CRH cells. Endocannabinoids inhibit the CRH neurons via inhibiting the presynaptic excitatory cells (38). CORT also has a remarkable impact on the half-life of CRH transcripts as its presence induces the degradation of CRH mRNA (31). Glucocorticoids exert indirect inhibitory effects through acting on neuronal pathways afferent to the PVH. Significant glucocorticoid negative feedback can be observed on the level of limbic areas (e.g. hippocampal neurons) (33). The effect of glucocorticoids is region specific. While CORT decreases CRH mRNA in the PVH, it has an opposite effect in the CEA and BNST. This phenomenon can be explained by the diversity of tissue specific steroid receptor coactivators, such as SRC-1 (31). Experiments have shown that adrenalectomy (ADX), which leads to CORT deficit, results in increase of HPA axis activity (31). Contrarily, administration of dexamethasone – a synthetic corticosteroid agonist – inhibits the activity of the axis (38). Schematic image of the HPA axis and the feedback system is shown in Figure 3.

DOI:10.14753/SE.2024.3001

Feedback system also has a crucial role in regulating the non stress state rhythmicity of the neuroendocrine stress axis elements. First, a suprachiasmatic nucleus (SCH) drived circadian pattern (period of 24 hours) in the CRH, ATCH and CORT release can be observed. The peak of these hormones is detected at the beginning of the active phase of the subject: occurring in the morning for humans and in the evening for mice. The main role of this rhythmicity is to ensure the availability of the necessary energy for the active phase of the subject. Ultradian rhythmicity (less than 24 hours) can also be observed. Although further studies are needed to confirm the presence of an ultradian pattern in CRH release, ACTH and CORT release do show detectable 60-90 minutes rhythmicity during the active phase of the subject. In the context of this cyclicity, the main driver is not SCH, but the feedback loop system. The role of ultradian rhythmicity is to maintain the responsiveness of the axis, and it also exerts significant impact on brain functions. Natural CORT rhythm is essential for the proper functioning of working memory, sleep and recognition. It is worth mentioning, that seasonal changes also occur: during long-photoperiod summer, a general lowering of the HPA axis activity can be detected (39, 40).

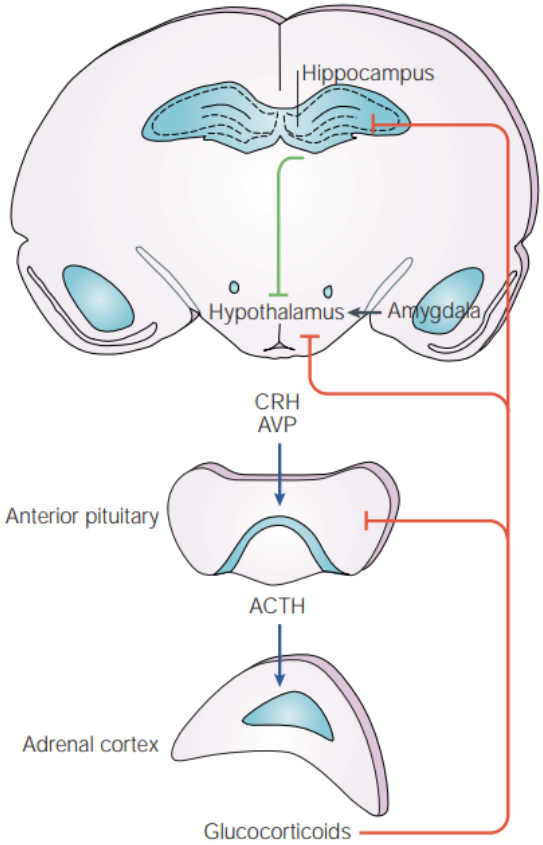

Figure 3. ***Feedback system of the hypothalamo-pituitary-adrenal axis*** *(41).*

1.3.4. Impact of the neuroendocrine stress cascade

Neuroendocrine stress response provides optimal arousal through various changes. Initially, stress cascade affects cognition, metabolism, thermogenesis and cardiovascular system through stimulating noradrenergic^{LC} cells. It also has an impact on food intake (amount and quality), reproduction (CRH supresses the gonadotropin-releasing hormone pulse generator), behavior (CRH induces grooming, decreases rearing and sleeping and increases locomotion in case of familiar surroundings, while decreases exploration in novel environment), memory (Lupien et al. observed that chronic elevation of CORT reduces performance of HC dependent learning (42)), fear and anxiety (NE release from the LC to the basolateral amygdala influences stress-activated memory storage (43)), coping strategy (actively coping mice have higher CRH mRNA in the hypothalamus) and immune defense (direct cytokine effects, bone marrow and thymus influence through NE) (31).

While stress response has to ensure the adequate adaptability of the organism, under- or overshooting must be avoided. Long-term success of neuroendocrine stress cascade mainly depends on the characteristics of the glucocorticoid response. Impairment of CORT production results in serious damages of the functions listed above, consequently leading to a decline in resilience. In human, pathological hypocortisolism leads to Addison's disease, while hypercortisolism results in Cushing's syndrome (44).

1.4. Corticotropin-releasing hormone (CRH)

1.4.1. CRH in general

Corticotropin-releasing hormone (CRH) – a 41 amino acid neuropeptide – was initially isolated, and its essential role in the neuroendocrine stress response was elucidated in 1981 by Vale et al. (45). Studies have demonstrated that CRH peptide first appears on the 13th embryonic day in the hypothalamus of mice. Development of the mouse HPA axis from the perspective of CRH can be divided into two phases after birth. Until postnatal day 12 (p12), a phenomenon known as stress hypo-responsive period (SHRP) dominates: level of CRH^{PVH} is high, while basal corticosterone is low. During SHRP mild stress does not result in robust elevation of CORT or ACTH. Level of urocortin 3 (another member of the CRH family) along with GR elevates rapidly and

reaches its maximum on the last day of the phase. In contrast, during the second stage, CRH expression decreases, while basal CORT levels reach the normal adult level and the optimal responsiveness of HPA axis develops (46).

CRH provides ligands for CRH receptor-1 and CRH receptor-2 (CRH-R2) (47) to serve neurotransmitter and neuromodulatory functions (48, 49). In mammals, CRH-R1 is primarily expressed in the brain (especially in neocortex and cerebellum) and in the anterior lobe of the pituitary, while its presence in the periphery is less common (e.g. adrenal gland, reproductive tract, skin, gastrointestinal tract and adipose tissue). Simultaneously, CRH-R2 has been identified predominantly in peripherial regions (e.g. heart, lung, skeletal muscle), but it also occurs in the brain in small quantities (e.g. LS, amygdala, hypothalamus and brainstem) (50). LC, cerebellar cortex, thalamus and striatum have been shown to exclusively harbour CRH-R1, whereas BNST predominantly expresses CRH-R2 (23). The interaction between CRH and its receptors is modulated by the presence of CRH binding protein. The highest expression level of CRH binding protein has been detected in the brain and the pituitary gland, but it also occurs at the periphery (e.g. in the skin) (50). Both receptors belong to the B1 subfamily of 7-transmembrane (7TM) receptors and primarily signal by coupling to G proteins, thereby stimulating adenylate cyclase. Several CRH receptor isoforms exist due to alternative splicing. Only CRH-R1α is adenylate cyclase coupled directly. CRH-R1α has greater affinify to CRH and urocortin 1 while CRH-R2α/β has lower affinity to CRH and higher for urocortin 1, urocortin 2 and urocortin 3 (51). Urocortins have an essential role in stress recovery, while they also modulate the immune response and appetite. In stressful situations, the absence of CRH-R1 disrupts neuroendocrine stress reactivity, while the absence of CRH-R2 results in elevated stress induced ACTH and CORT levels (52).

The amino acid sequence of secreted CRH is highly conserved between humans, rats and mice. Its expression pattern is also conserved in vertebrates, which indicates its specific cell and tissue dependent roles (17). CRH expressing neurons are widely distributed in the central nervous system (CNS) and several parts of the periphery, where it mostly acts via paracrine and autocrine actions. Peripheral CRH has been detected in the skin (53), gastrointestinal tract (54), immune system (55), reproductive system (55), adrenal gland (56), etc.

1.4.2. CRH neurons in the central nervous system

While structure and function of CRH^{PVH} neurons are well established, much less is known about the stress-related organization of CRH cells outside the hypothalamus. CRH neurons have already been described throughout the brain e.g. in the cortical region, BNST, CEA, tegmental reticular nucleus (TRN), Barrington's nucleus (B), periaqueductal gray (PAG), external cuneate nucleus (ECU) and inferior olivary complex (IO) in the mouse brain (57-59). It has been shown that central (intracerebroventricular) administration of CRH reproduces many of the autonomic- (60), behavioral- (61), neurochemical- (62) and electrophysiological (63) responses seen during stress. Simultaneously, Sztainberg and Chen specified that administration of CRH into distinct brain regions (e.g. BNST, CEA, LC, HC) results in various functional and behavioral changes (64). Therefore, it is evident that there are several CRH expressing neuron populations throughout the mouse brain and CRH in distinct brain regions serve different functions, but to comprehensively understand their exact role in the stress response, further research in this field is imperative.

Detecting and visualizing CRH-positive neurons in the brain is rather challenging due to their low basal expression within the cell bodies and the lack of highly sensitive CRH antibodies. To address this limitation, previous studies have used colchicine treatment to enhance the concentration of the neuropeptide in the perikaryon via blockade of axonal transport (65). However, use of colchicine raises concerns about the physiological relevance of approach (66). Introduction of CRH Cre-driver mouse lines (67) serves as adequate detecting strategy. In Crh-IRES-Cre (B6(Cg)-$Crh^{tm1(cre)Zjh}$/J) mice, 3' untranslated region of the corticotropin-releasing hormone locus (*Crh*) harbors an internal ribosome entry site and a Cre recombinase. Thus, *Cre* expression is directed by the endogenous *Crh* promoter/enhancer elements (Figure 4). Cre-driver mouse lines in combination with various reporter constructs provide easy tools with which to visualize CRH expressing neurons throughout the CNS (57, 67, 68). If Crh-IRES-Cre animals are bred with mice that harbor *loxP*-flanked sequences, Cre-mediated recombination occurs in the CRH cells of the offspring.

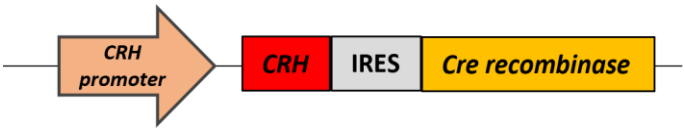

DOI:10.14753/SE.2024.3001

***Figure 4*. Concept of Crh-IRES-Cre mice.** *Expression of Cre recombinase is under the control of CRH promoter.*

Previous systematic studies have compared the distribution of natural CRH peptide and of reporter's expression in three transgenic mouse lines. Among these mouse models, a good overlap between endogenous CRH and the red fluorescence-producing reporter expression was found only in Crh-IRES-Cre;Ai14 tdTomato mice (69). Ai9 (B6;Cg-Gt(ROSA)26Sor$^{tm9(CAG\text{-}tdTomato)Hze}$/J) is a Cre reporter strain similar to Ai14, with the difference that the latter has an additional *att* site-flanked neo selection cassette at the 3' end of the targeted allele. Thus, crossing homozygous Crh-IRES-Cre and Ai9 mice also results in selective fluorophore expression in CRH neurons in F1 heterozygous Crh-IRES-Cre;Ai9 mice (Figure 5).

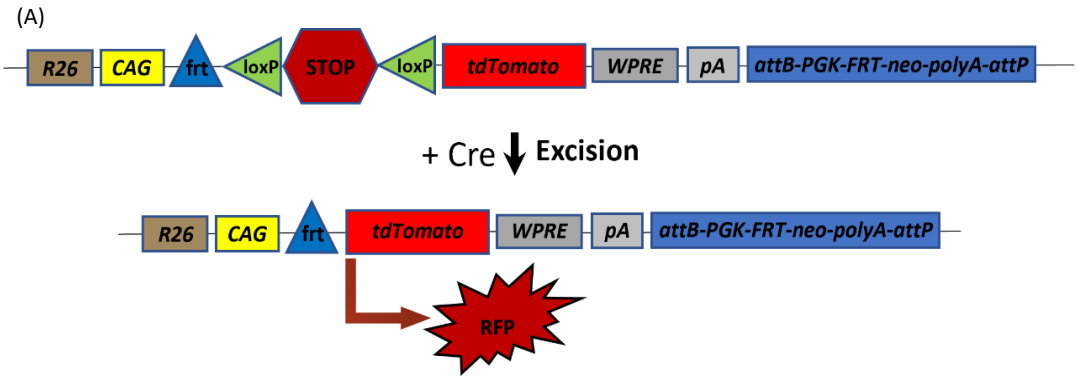

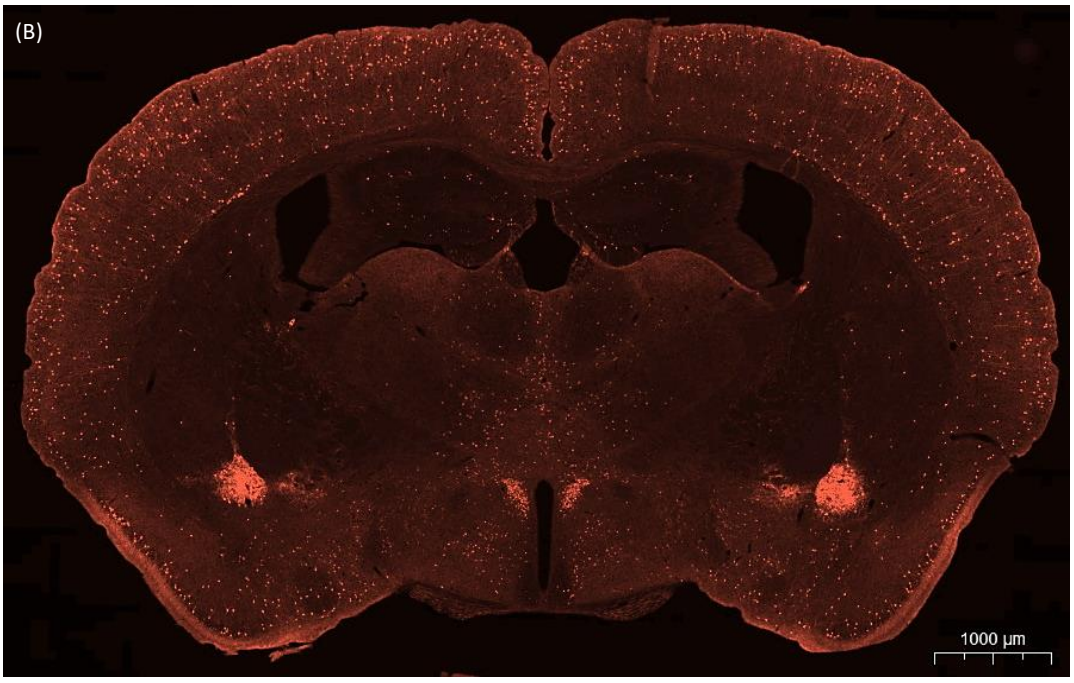

Figure 5*. Crh-IRES-Cre;Ai9 mice.** ***(A)*. In presence of Cre recombinase, STOP codon excision occurs, which results in the expression of tdTomato red fluorescent protein (RFP).* ***(B)****. Image of a Crh-IRES-Cre;Ai9 mouse (25-μm-thick) brain section. Cre-mediated recombination results in fluorophore expression in the CRH neurons.*

1.5. Neuronal activation

1.5.1. Detection

Cellular immediate-early genes (IEGs), such as members of the FOS family (34, 70), nerve growth factor-induced clone B (Ngfi-B) (71), or activity-regulated cytoskeleton-associated protein (Arc) (72) serve as versatile markers of neuronal activation. IEGs represent the "eukaryotic version" of retroviral protooncogenes, as their induction occurs within minutes and does not require de novo protein synthesis. Upon cellular activation, IEGs become triggered and via IEG-encoded transcription factors, they modulate (activate or inhibit) the expression of target genes. FOS has become a valuable marker for identifying stress induced cells. The FOS family of proteins consists of four protein members: c-Fos, FosB, Fra-1 and Fra-2 (34). Fra-2 is encoded by Fos-related antigen 2 (*Fosl2*) gene.

Utilization of *c-Fos*, along with its protein product (c-Fos) has become widespread in the identification of hypothalamic and extrahypothalamic circuits involved in acute stress (73-79). Their popularity in the field is based on several specific features. Firstly, they exhibit stereotypical inducibility. Their expression level is low under resting (no stress) conditions and their constitutive expression is only detectable in specific brain areas such as anterior and lateral preoptic areas and SCH. However, their expression rapidly and transiently increases in response to diverse external or internal stimuli or intense synaptic activity, leading to the reprogramming of the cell. IEG activation is inversely correlated with the burst-interval of action potentials. Another advantage of the IEGs is the transient nature of their responses. Additionally, their detection is straightforward and can be combined with the use of other markers (neurochemical markers, retrograde tracers, mRNA analysis). However, it is important to note the limitations of the technique; distinguishing between cells activated by different stressors can be challenging, especially if the insults occur within a short time window.

Additionally, this method does not provide an exact representation of the activation pathways (through which activated neurons are connected with each other), of the reactive neurons and necessitates the sacrifice of the animals (34). Acute stress results in elevation of c-Fos mRNA within minutes post-stress and it reaches its maximal rate in approximately half an hour. Expression of c-Fos protein peaks between 1-3 hours after stress, followed by a progressive decrease and it vanishes completely 4-6 hours after the challenge (80). C-Fos exerts its impact through activator protein-1 (AP-1) transcription factor, which it forms through heterodimerization with members of the Jun (another transcription factor) family. Binding of AP-1 to the regulatory region of target genes can have both stimulatory and inhibitory effects. The c-Fos/c-Jun complex has excitatory effects, while the c-Fos/JunB complex has repressive impact. Although c-Fos detection is an efficient method for cellular activity analysis in acute stress experiments, in chronic stress studies it is less profitable as repeated stress results in highly reduced c-Fos activation (34).

In contrast to c-Fos, FosB and Fos-related antigens (FRAs; Fra-1 and Fra-2) are involved in long term phenotypical changes following e.g. chronic stress. In comparison to c-Fos, basal level of FRAs is slightly higher, especially in magnocellular hypothalamic neurons. Furthermore, they exhibit a delayed and prolonged activation pattern accompanied by their accumulation within the nucleus, resulting in extended expression and half-life. They are well detectable 4-6 hours after an acute insult and can persist for up to 12-24 hours (34). Consequently, they are ideal for mapping chronically activated neurons when c-Fos expression has already diminished.

1.5.2. Chemogenetic activation of neurons

Chemogenetic innovations offer various methods to selectively and reversibly modify cell or even neuronal circuit activity in mice in vivo. Among chemogenetically designed proteins, usage of Designer Receptors Exclusively Activated by Designer Drugs (DREADDs) became highly popular. Gq coupled human M3 muscarinic receptor (hM3D(Gq)) is the most frequently used DREADD, enhancing neuronal activity through Gq signaling pathways that acts via mobilization of intracellular calcium (81).

The widely used pAAV8/hSyn-DIO-hM3D(Gq)-mCherry construct employs adeno-associated virus serotype 8 (AAV8) as a delivery system for the hM3D(Gq)

designer receptor. Moreover, the viral vector is facilitated by the neuron specific human *synapsin 1* promoter (hSyn) and the designer receptor is fused with the mCherry red fluorescent marker at the C-terminal. AAV8 has been reported to be effective in gene delivery in rodent experiments (82). The success of gene expression is facilitated by the double-floxed inverted open-reading frame (DIO) system: the transgene is floxed by two pairs of oppositely orientated heterotypic loxP-type recombination sites, while the open reading frame is inverted. Thus, the expression of transgene is restricted to cells that harbour Cre, as the presence of the recombinase is crucial for the reorientation of the inverted hM3D(Gq)-mCherry sequence (Figure 6) (83, 84).

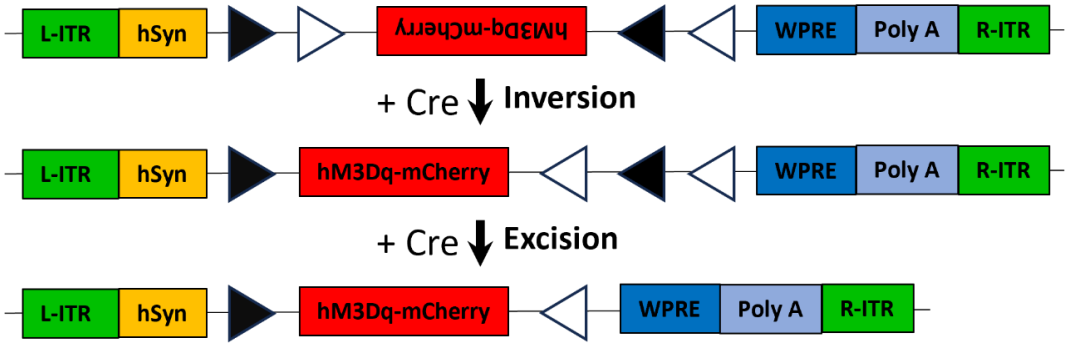

Figure 6. ***Operation of double-floxed inverted open-reading frame (DIO) system in the presence of Cre recombinase****. Triangles indicate the recombination sites (different colours represent different sequences) recognized by Cre.*

DREADD receptor can be activated by the metabolite of clozapine, clozapine-N-oxide (CNO). It is notable that CNO can convert back to clozapine. Despite this − due to its rare occurrence − CNO is considered to be inert and is reported to have no behavioral or pharmacological side-effects according to most published articles. However, to eliminate this potential risk, an alternative actuator, compound 21 (C21) is recommended to be used. C21 not only exclusively activates hM3Dq but also demonstrates minimal off-target activity (81).

DOI:10.14753/SE.2024.3001

2. Aims

My first aim was to study the recruitment of hypothalamic and extrahypothalamic CRH neurons in categorically distinct, acute stress reactions in Crh-IRES-Cre;Ai9 reporter mice. My main questions were:

> Is Crh-IRES-Cre;Ai9 mouse a proper model for my research?

> Where tdTomato positive profiles are found in the mouse brain?

> Where are the acute stress-activated neuron populations locate in the mouse brain?

> Which tdTomato positive (putative CRH) neurons are activated in response to various acute challenges in the mouse brain?

My second aim was to determine the impact of chronic stress exposure on mice and to elucidate anxiety-related behavior- and stress-related molecular differences resulting from the variability and unpredictability of chronic stressors.

Finally I compared hormonal-, behavioral- and molecular responses of mice in which CRH^{PVH} neurons were chemogenetically activated with those exposed to single or repeated restraint to investigate the role of CRH^{PVH} neurons in organization of stress reaction.

DOI:10.14753/SE.2024.3001

3. Materials and methods

3.1. Animals

In our experiments adult male C57BL/6J; Crh-IRES-Cre and Crh-IRES-Cre;Ai9 mice (8-12 weeks of age) were used. Animals were purchased from The Jackson Laboratory. Crh-IRES-Cre (B6(Cg)-Crh$^{tm1(cre)Zjh}$/J; stock number: 012704) and Ai9 mice (B6;Cg-Gt(ROSA)26Sor$^{tm9(CAG-tdTomato)Hze}$/J; stock number: 007905) lines were maintained as homozygotes at the Transgenic Facility of Institute of Experimental Medicine. The Crh-IRES-Cre;Ai9 reporter mice were generated by crossing these homozygote pairs. In F1 heterozygotes Cre-mediated recombination resulted in tdTomato fluorophore expression in CRH neurons. Animals had ad libitum access to standard laboratory chow and water and were kept under standard circumstances temperature: 21±1 °C, humidity: 65%, light: 400 lx with 12L-12D cycle with the light on at 07:00 AM.

All experiments were complied with the ARRIVE guidelines and performed in accordance with the guidelines of European Communities Council Directive (86/609 EEC), EU Directive (2010/63/EU) and the Hungarian Act of Animal Care and Experimentation (1998; XXVIII, Sect. 243/1998). All procedures and experiments were approved by the Animal Care and Use Committee of the Institute of Experimental Medicine, Hungarian Academy of Sciences (permit number: PEI/001/29-4/2013).

3.2. Acute stress

Mice were caged individually one day prior to stress exposure. Animals were exposed to ether, hypertonic salt, lipopolysaccharide (LPS), restraint or predator odor stress. Tests were carried out in a separate experimental room in the early light phase of the day. After stress, animals were placed back in their home cages until sacrifice.

3.2.1. Hypertonic salt

Mice were intraperitoneally injected with 1.5 M NaCl solution (0.6 mL/kg body weight) (85).

3.2.2. Lipopolysaccharide injection

Lipopolysaccharide (LPS, serotype: 0111:B4, Sigma L4391) was dissolved in sterile, pyrogen-free saline and administered intraperitoneally at dose of 1 mg/kg (0.6 mL/kg). The dose was selected to induce substantial systemic inflammation and maximal activation of the HPA axis.

3.2.3. Ether inhalation

For ether stress, mice were placed into a glass chamber saturated with diethyl-ether vapour. As animals became anesthetized (1–1.5 min), they were removed from the chamber and the ether exposure was maintained for total of 5 min using a nose cone with ether-soaked cotton (86).

3.2.4. Restraint

Mice were placed in 50 ml Falcon tubes, in which holes were cut at the end and along the sides to prevent overheating of the animals. To achieve comparable degree of restraint, packing with paper towels at the rear was used. This procedure minimized the space around the animal, prevented them from turning and provided stressful stimulus, without being harmful.

3.2.5. Predator odor

Mice were exposed to a synthetic analog of fox anogenital product 2-MT (87) (2-methyl-2-thiazoline, CAS 2346-00-1, Santa Cruz Biotechnology, Inc.) in a covered transparent plexiglass arena (40 x 20 x 20 cm) under a fume hood. One day prior to the experiment animals were habituated for 20 min to the test box in which an empty Eppendorf tube lid was placed into the corner. On the day of stress, animals were put into the testing box, where they could freely explore the environment for 10 min, then 2 μL of concentrated 2-MT was pipetted onto a filter paper and placed onto the lid inside the cage. The odor exposure was maintained for 10 min.

3.2.6. Controls

For the restraint and ether stressed animals, undisturbed mice were considered as control group (absolute control). In case of lipopolysaccharide and hypertonic salt

injected animals, controls were injected intraperitoneally with saline solution (0.6 mL/kg) (ip saline control). Control animals for the predator odor group went through the same procedure as the odor exposed ones, except that saline was pipetted onto the filter paper instead of 2-MT solution (Novel Environment group, NE).

3.3. Chronic repeated restraint stress (CRS)

During chronic repeated restraint stress, mice were exposed daily to one hour restraint stress as described in 3.2.4., but for three weeks. Control animals were left undisturbed except for changing the bedding.

3.4. Chronic variable stress (CVS)

Experimental mice were exposed in a semi-random order to one of the following stressors twice daily, for three weeks. More detailed protocol of the used stressors can be seen in Table 1.

- Social defeat – Experimental animals were put into the home cage of a dominant CD1 male mouse for 5 minutes.
- Water avoidance stress – Mice were placed for 1 hour onto a 8 cm diameter glass cylinder which stood in the center of a 40×40×30 cm plastic tank filled with water to 1 cm below the top of platform.
- Circadian rhythm disturbation – Mice were exposed to reversed or altered light/dark phase.
- Forced swim – Mice were placed into a 2L beaker filled with 23 °C water for 5 minutes.
- Soaked bedding – Tap water-soaked bedding was provided for mice in their home cage.
- Slanted cage – Home cage of the mice was tilted to 45° angle.
- Isolation – Mice were placed into a new clean cage alone for 4 hours.
- Crowding – 5 mice were cohoused in a 10×5×10 cm plastic cage.
- Shaking – Home cages of mice were placed on an orbital shaker with 30-50 rpm rotation.
- Foot shock – Mice received 0.5 mA shock every 20 seconds for 12 minutes with the help of DC Shocker Controller (Supertech Instruments).

> Rat feces odor – Perforated Falcon tube filled with feces of adult male rats was placed in the home cage of the experimental mice.

Table 1. ***Chronic variable stress (CVS) protocol.***

CVS protocol		
day	***a.m.***	***p.m.***
1.day	water avoidance (1h)	overnight light (12h)
2.day	social defeat (5min)	footshock (12min)
3.day	forced swimming (5min)	soaked bedding+slanted cages (4h)
4.day	crowding+shaking (30min)	crowding (30min)
5.day	restraint (30min)	isolation (12h)
6.day	social defeat (5min)	forced swimming (5min)
7.day	footshock (12min)	soaked bedding+slanted cages (4h)
8.day	forced swimming (5min)	footshock (12min)
9.day	water avoidance (1h)	overnight light (12h)
10.day	social defeat (5min)	footshock (12min)
11.day	isolation+rat feces odor (4h)	isolation+rat feces odor+dark (4h)
12.day	crowding+shaking (30min)	crowding+soaked bedding+slanted cages (30min)
13.day	forced swimming (5min)	forced swimming (5min)
14.day	crowding+shaking (30min)	restraint (30min)
15.day	rat feces odor+dark (4h)	social defeat (5min)
16.day	rat feces odor (4h)	footshock (12min)
17.day	forced swimming (5min)	restraint (30min)
18.day	social defeat (5min)	rat feces odor+dark (4h)
19.day	water avoidance (1h)	footshock (12min)
20.day	dark for (4h)	restraint (30min)
21.day	soaked bedding+slanted cages (30min)	rat feces odor (4h)

3.5. Virus construct administration

Mice were anesthetized with intraperitoneal injection of an anesthetic mixture (containing 8.3 mg/mL ketamine and 1.7 mg/mL xylazine hydrochloride in 0.9% saline, 10 ml/kg body weight); and were then mounted in a small animal stereotaxic frame (David Kopf Instruments, CA, USA). Using Nanoject II precision microinjector pump (Drummond, Broomall, PA) we injected virus construct bilaterally (30 nL/side) into hypothalamic paraventricular nucleus (coordinates: AP: -0.7, ML: ±0.035, DV: -0.5). Cre-dependent adeno-associated virus constructs, pAAV8/hSyn-DIO-hM3D(Gq)-mCherry (44361-AAV8, $\geq 4\times10^{12}$ vg/mL) and pAAV-hSyn-DIO-mCherry (5049-AAV8, 10^{13} vg/ml) were purchased from Addgene. For chemogenetic activation of CRH^{PVH} neurons 3 weeks after stereotaxic virus injections, DREADD agonist 21 (C21/compound 21; Hello Bio Cat. No. HB4888; dose: 1 mg/kg bw) was dissolved in

saline (1 mg/mL) and injected intraperitoneally. Control animals were injected intraperitoneally with saline (10 mL/kg bw).

3.6. Behavioral tests

3.6.1. Nest building

Mice were placed into clean individual cages at the beginning of light cycle between 9-12 AM, in which one white A4 sized shredded paper was uniformly distributed. Animals were given 24 hours to rearrange the bedding material and so complete the nest building trial. The nests were evaluated on a scale of 1-5 as described by Neely et al. (88).

3.6.2. Open field

The open field apparatus was a white, 40×40×30 cm, nontransparent plastic box. Each examined animal was placed in the center of the box in the same direction. Mice were allowed to explore the cage for 10 minutes. Animals were recorded from the top and the videos were analyzed with Noldus EthoVision and Solomon Coder. Movement pattern and several behavioral elements of the mice were monitored.

3.6.3. Tail suspension

Mice were suspended by the end of their tail with a tape for 6 minutes. Coping of the animals were recorded from the side and the videos were analyzed with Solomon Coder. Duration and frequency of struggling and immobile conditions were measured. Movements only of the front legs and swinging as a result of the previous movements were not considered as struggling.

3.7. Adrenalectomy

Crh-IRES-Cre;Ai9 mice were deeply anesthetized with intraperitoneal injection of an anesthetic mixture (ketamine, 83 mg/kg; xylazine-hydrochloride, 3.3 mg/kg in 0.9% NaCl, 10 mL/kg body weight). Adrenals were bilaterally removed from dorsal approach. Sham-operated animals were used as controls. After surgery, mice had a free choice to drink water or saline. Animals were sacrificed one week after surgery.

3.8. Perfusion and tissue processing

Mice, whose brain tissue was used for immuno-staining, were transcardially perfused under terminal anesthesia (Nembutal, Ceva-Phylaxia, Budapest, Hungary). 90 minutes after the beginning of stress (at the maximum of FOS protein (86)) animals were perfused with saline followed by 70 ml ice-cold fixative (4% formaldehyde in 0.1 M phosphate buffer, pH 7.2). Brains were removed and post-fixed in the same fixative supplemented with 10% sucrose for 3 hours and cryoprotected overnight in 10% sucrose in potassium phosphate buffered saline, KPBS. Four series of coronal brain sections (25 μm) were cut on freezing microtome. Sections were stored at -20 °C in antifreeze solution (30% ethylene glycol and 20% glycerol in 0.1M PBS).

Other cohorts of mice, (which were used to measure gene expression in the hypothalamus) were decapitated 90 minutes (in case of acute stress) or 24 hours (in case of CRS and CVS) after the beginning of stress exposure. Hypothalamus was dissected as described by Brown et al. (89), and the tissue were stored at -90 °C until assays.

3.9. Immunohistochemistry

After 30 min KPBS washing, free-floating brain sections were incubated in 2% normal donkey serum (017-000-121, Jackson ImmunoResearch Europe Ltd., St. Thomas Place, UK) in KPBS/0.3% Triton X100 at room temperature for 1 hour then either in rabbit anti-c-Fos IgG (sc-52 Santa Cruz Biotechnology, Santa Cruz, CA, 1:10000) or in sheep anti-tdTomato (provided by Cs. Fekete, Institute of Experimental Medicine, Hungary, 1:50000) at 4 °C overnight. The immunoreaction was visualized by donkey anti-rabbit IgG (ThermoFisher, 1:1000)/Alexa fluor 488 conjugate or by Alexa Fluor 488 donkey anti-sheep IgG/Alexa fluor 488 conjugate (ThermoFisher, 1:1000 dilution), respectively, at room temperature for 2 hours in dark. Sections were mounted onto gelatine coated slides and coverslipped with DAPI Fluoromount-G (SB. Cat. No. 0100-20) as a nuclear counterstain.

3.10. RNAscope In Situ Hybridization (ISH)

RNAscope assay was performed using RNAscope Multiplex Fluorescent Reagent Kit v. 2 (Advanced Cell Diagnostics, Newark, CA, USA) according to the manufacturer's protocol with modifications (90). After one hour of KPBS washing,

tissues were treated with 1% H_2O_2 in KPBS for 30 min. After another 30 min washing, sections were mounted on Superfrost Ultra Plus (Thermo Fisher Scientific, Waltham, MA, USA), then dried at room temperature. As the final step of pretreatment, slides were incubated at 60 °C for 60 min. After a further 20 min of washing in Milli-Q (MQ) water, slides were submerged in 4 °C PFA fixative for 2 min. Following another 30 min MQ water washing, they were put into 0.01 mg/mL proteinase K solution (PK000011, Geneaid Biotech, New Taipei, Taiwan) in 1 M Tris/HCl, pH = 8 and 0.5 M EDTA, pH = 8 buffer at 37 °C for 5 min. After MQ water rinsing tissues endured another 2 min 4 °C PFA treatment. After another 30 min of MQ water washing, sections were hybridized with 3-plex mouse positive or negative control or mouse specific Crh probe. Signal amplification and channel development were applied sequentially according to the manufacturer's protocol. Used probes and dilution of fluorophores are listed in Table 2. Sections were coverslipped with DAPI Fluoromount-G (SB. Cat. No. 0100-20) as nuclear counterstain.

Table 2. ***Used probes and dilution of fluorophores.***

Target	Catalog number	Fluorophores	Fluorophore dilution
Mm*-Crh	316091	Fluorescein Plus TSA	1:3000
3-plex Positive Control Probe-Mm	320881	Fluorescein Plus TSA	1:3000
3-plex Negative Control Probe	320871	Fluorescein Plus TSA	1:3000

*Mus musculus.

3.11. Imaging and data analysis

Digital images of brain sections were captured at 20x magnification in 3D HISTECH Pannoramic MIDI II. slide scanner. Regions of interest (ROI) were outlined on the basis of Allen Brain Atlas and analyzed with NIS Elements Imaging Software 5.21.01. DAPI-, tdTomato- and FOS-positive cells were monitored. Normalized CRH neuron ratio was calculated as number of tdTomato positive cells divided by the total cell number (DAPI positive profiles) in a specific region × 100. The ratio of activated neurons was calculated by dividing the number of FOS-immunoreactive cells with the total cell count of the specific region × 100. The ratio of stress-activated CRH neurons was calculated as number of double labeled (tdTomato + FOS) profiles divided by total cell count × 100 at ROI. Stress-induced changes in cases of FOS and FOS + tdTomato

double labeling were determined by fold change calculation compared to respective control values.

Images of ISH sections were evaluated using Nikon Ni-E C2+ laser-scanning confocal microscope equipped with a 1.4 NA Plan Apo VC DIC 60xOil objective.

3.12. Gene expression analysis

Frozen hypothalamus samples were homogenized, then, total mRNA was isolated by Total mRNA Mini Kit (Geneaid) according the manufacturer's instruction. To eliminate genomic DNA contamination, DNaseI (Fermentas) treatment was used. Sample quality control and the quantitative analysis were carried out by NanoDrop (Thermo Scientific). cDNA synthesis was performed with High Capacity DNA Reverse Transcription Kit (Applied Biosystems). Real-Time PCR was carried out in ABI StepOnePlus instrument (Applied Biosystems) with Fast EvaGreen quantitative PCR master mix (Biotium) and gene-specific primers. Primers (Microsynth) were designed in our laboratory using Primer-BLAST software of the National Center for Biotechnology Information (NCBI). The used forward and reverse primers are shown in Table 3. Gene expression was analyzed by the 2-DDCT method using the ABI StepOne Software v2.3 (Applied Biosystems). The amplicons were tested by melt curve analysis on ABI StepOnePlus instrument (Applied Biosystems). Relative changes in gene expression were normalized against GAPDH mRNA expression. Selection of the reference gene was made with the help of NormFinder software (91).

Table 3. ***Forward and reverse target sequence used for mRNA quantification.***

Genes	**Forward primer**	**Reverse primer**
GAPDH	*TGACGTGCCGCCTGGAGAAA*	*AGTGTAGCCCAAGATGCCCTTCAG*
Fos	*GAGAGCCTTTCCTACTACCATTCC*	*GGACAGATCTGCGCAAAAGTC*
Fosl2	*CACCGCGGATCATGTACCAG*	*TATCTACCCGGAACTTCTGCTG*
FosB	*CAGATCGACTTCAGGCGGAAAC*	*AATCTCTCACCTCGGCCAGC*

3.13. Corticosterone measurement

Retro-orbital sinus or trunk blood was collected, centrifuged and serum samples were stored at -20 °C. Corticosterone was determined by direct radioimmunoassay (RIA) as previously described (92).

3.14. Statistical analysis

All quantitative data are expressed as group mean ± SEM (standard error of the mean) for each treatment group. Data were analyzed using GraphPad Prism software (version 7; San Diego, CA, USA). One-way ANOVA with Tukey's multiple comparisons test (tdTomato neuron distribution; neuronal activation and colocalization; transcription factors; corticosterone; body weight; behavior) and unpaired t-test (neuronal activation and colocalization analysis; corticosterone; behavior) were performed. We considered p-value < 0.05 as statistically significant.

DOI:10.14753/SE.2024.3001

4. Results

4.1. Localization of tdTomato positive profiles

To reveal the distribution of CRH positive neurons in the adult mouse brain, Crh-IRES-Cre;Ai9 reporter mice (n = 44) were used.

4.1.1. Validation of Crh-IRES-Cre;Ai9 mice

Because Ai9 mice may express low levels of tdTomato prior to Cre recombination, first, we tested baseline tdTomato signal in Cre-negative controls. Most of the brain areas did not display any red fluorescence in Ai9 mice, however, within the circumventricular organs, such as the subfornical organ, the median eminence and the area postrema, significant red fluorescence was recognized. These non-neuronal profiles that showed red fluorescence, also displayed green fluorescence and may represent autofluorescence of the tissue. When the signal was checked by specific anti-tdTomato antibody and DAB chromogen, these areas were negative.

4.1.2. Distribution of tdTomato positive neurons in the mouse brain

Figure 7A shows the distribution of native tdTomato positive cellular profiles throughout the Crh-IRES-Cre;Ai9 mouse brain. Relatively high density of tdTomato positive profiles was found in the olfactory areas, striatum, pons and medulla. Medium density of tdTomato positive cells was detected in the isocortex, pallidum, thalamus, hypothalamus and midbrain. The hippocampal formation and cortical subplate contained the lowest level of tdTomato expression.

Next, we compared native tdTomato fluorescence observed in Crh-IRES-Cre;Ai9 mice with CRH mRNA distribution published in Allen Brain Atlas (experiment 292, probe RP_Baylor 102704) (Figure 7B). Good correlation between tdTomato density with the reported CRH mRNA raw expression values was seen in isocortex, hypothalamus and medulla. However, a mismatch between tdTomato and CRH mRNA expression was found in the striatum, thalamus, midbrain and pons, where the density of red fluorescent profiles exceeded those of CRH mRNA raw expression. By contrast,

DOI:10.14753/SE.2024.3001

in the olfactory areas, hippocampal formation and cortical subplate tdTomato expression was lower than the reported CRH mRNA.

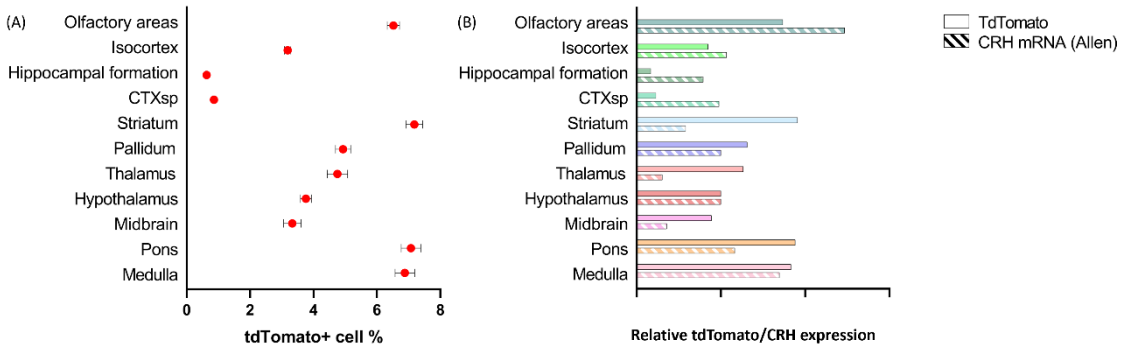

Figure 7. ***Overview of tdTomato marker expression in the brain of Crh-IRES-Cre;Ai9 mice.*** *(**A**). Density of tdTomato positive cells in major brain areas expressed as number of tdTomato positive cells/number of DAPI positive cells × 100. (**B**). Comparison of tdTomato and CRH mRNA expression (as reported in Allen Brain Atlas). Both markers have been normalized to the hypothalamic values.*

Then, RNAscope in situ hybridization was performed on critical match (PVH) and mismatch (PVTa) areas. This experiment confirmed >80% overlap between tdTomato and CRH expressing profiles in the hypothalamic paraventricular nucleus. By contrast, no CRH mRNA was detected in tdTomato+ cells in the thalamic region of the reporter mice (Figure 8).

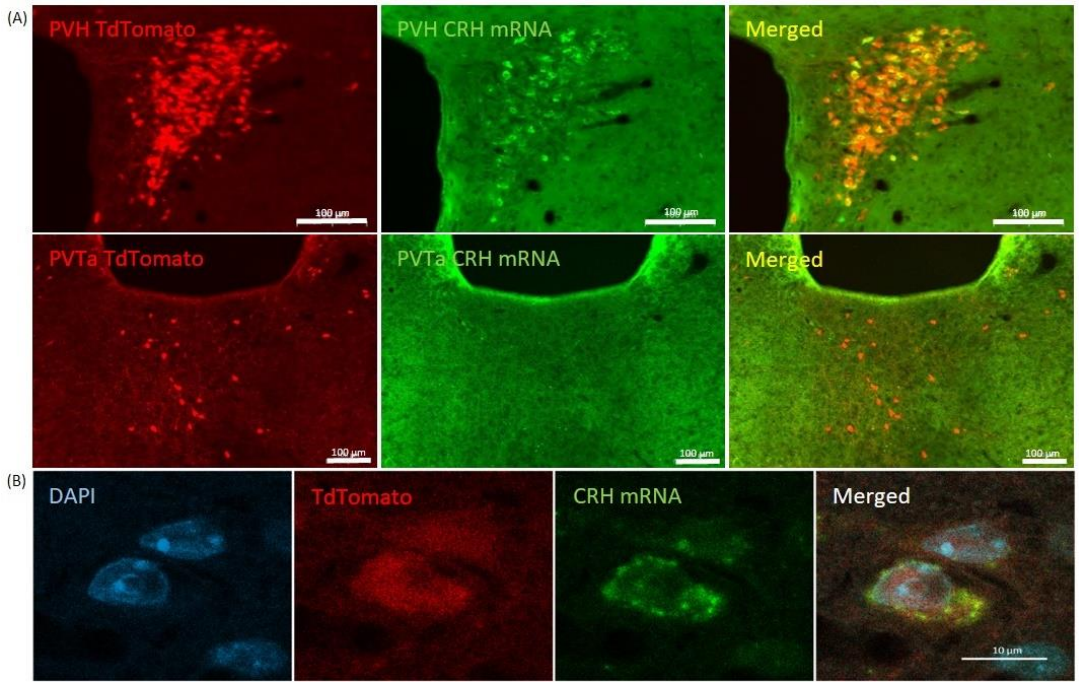

Figure 8. ***Co-expression of CRH mRNA and tdTomato marker in the hypothalamus and thalamus of Crh-IRES-Cre;Ai9 mice.*** *(**A**). CRH mRNA was visualized by RNAscope and tdTomato was immunostained. The vast majority of tdTomato positive cells display CRH mRNA signal in the PVH. No colocalization of the two markers is seen in the anterior thalamic region. High magnification of a pair of DAPI+, tdTomato+ and CRH mRNA+ cells from the PVH is shown in (**B**).*

Finally, we checked whether manipulation of hypothalamic CRH expression affects the appearance of tdTomato in Crh-IRES-Cre;Ai9 mice. Removal of the adrenals results in a significant upregulation of CRH expression in the hypothalamus (93). Adrenalectomized (ADX) male mice had the same number of tdTomato positive neurons in the PVH than sham-operated controls. The red fluorescence intensity on sections obtained from ADX mice was also comparable to that as seen in sham-operated controls (Figure 9).

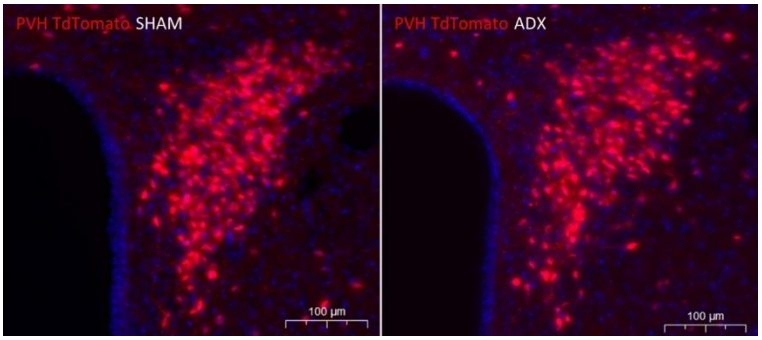

Figure 9. ***TdTomato staining in the hypothalamic paraventricular nucleus (PVH) of sham operated (SHAM) and adrenalectomized (ADX) Crh-IRES-Cre;Ai9 mice.***

Detailed analysis of tdTomato distribution throughout the Crh-IRES-Cre;Ai9 mouse brain is shown in Figure 10. In the hypothalamic paraventricular nucleus, 24.83% of DAPI positive profiles expressed the red fluorescent marker. Similarly, a high ratio (>20%) of tdTomato positive cells was found in the pyriform (PIR) and somatosensory cortices, Barrington's nucleus (B, the pontine urinary center) and inferior olive (IO). Moderate density (>10% <20%) of tdTomato signal has been detected in the olfactory bulb (MOBopl), in the olfactory tubercle (OT), lateral hypothalamic area (LHA), central amygdala (CEA), nucleus X and lateral reticular nucleus (LRN). Scattered tdTomato labeling with moderate density has been revealed throughout the bed nuclei of stria

DOI:10.14753/SE.2024.3001

terminalis (BNST) and in the fundus of striatum (FS). Within the precomissural nucleus (PRC) a moderate number of tdTomato positive cells were revealed.

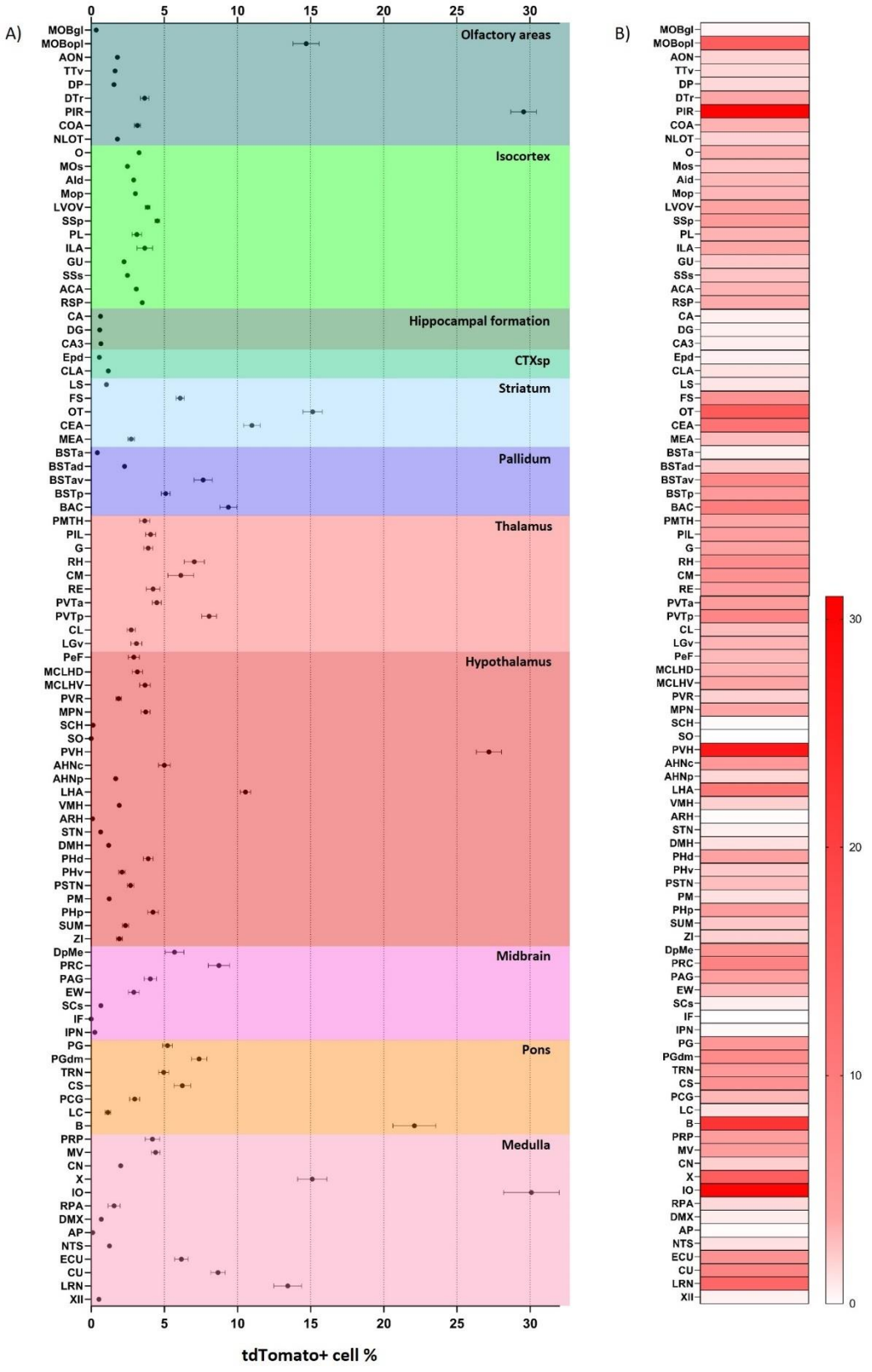

Figure 10. ***Density of tdTomato expressing neurons throughout the Crh-IRES-Cre;Ai9 mouse.*** *95 brain areas have been analyzed in detail. (**A**). Mean ± SEM values of tdTomato cell density in the brain of male, non-stressed control Crh-IRES-Cre;Ai9 mice. (**B**). "Heat map" of tdTomato cell density.*

4.1.3. Distribution of tdTomato positive fibers in the mouse brain

One major advantage of Crh-IRES-Cre;Ai9 mice is the visualization of tdTomato positive, presumably CRH fibers and varicosities. Some of these profiles have not been fully resolved by classic immunostaining. In addition to the well-recognized median eminence (ME), we have detected a dense network of tdTomato-positive varicosities in layer 1 tenia tecta, molecular layers of the piriform and cerebellar cortices as well as close to the substantia nigra, pars compacta (SNc) (Figure 11). According to the Allen Brain Atlas (experiment 297, probe RP Baylor 253895), most of these areas contain CRH-R1 receptors.

DOI:10.14753/SE.2024.3001

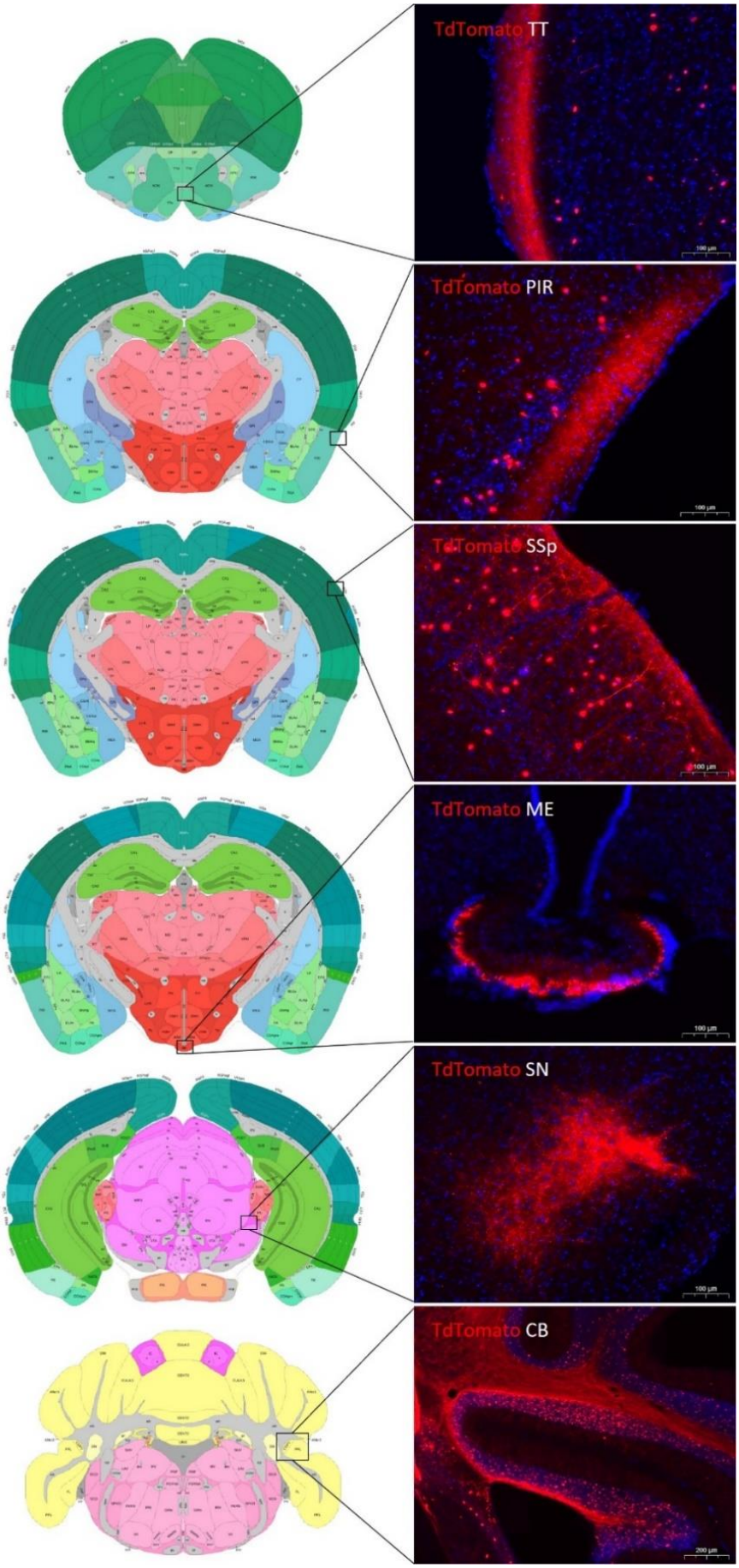

DOI:10.14753/SE.2024.3001

<u>Figure 11.</u> ***TdTomato immunoreactive fibers/terminals in Crh-IRES-Cre;Ai9 mouse brain.*** *TT-tenia tecta; PIR-Piriform area; SSp-primary somatosensory area; ME-median eminence; SN-substatia nigra; CB-cerebellum. Drawings on the left are from the Allen Brain Atlas.*

4.2. Acute stress-induced neuronal activation

Next, we aimed to monitor whether CRH neurons within and outside of the hypothalamus are recruited in a challenge-specific manner. Crh-IRES-Cre;Ai9 mice were exposed to ether- (*n* = 6), high salt- (*n* = 6), restraint- (*n* = 6), LPS (*n* = 4) or predator odor (*n* = 3) acute insults. To identify stress-activated neuron population throughout the mouse brain, the immediate-early gene, c-Fos, as a functional anatomical marker of acute neuronal activation has been used. Stress-induced CRH neurons were detected as colocalization of tdTomato signal (putative CRH) with FOS-immunoreactivity at cellular level. Stress response was confirmed by the measurement of plasma corticosterone levels.

4.2.1. Controls

There were several brain areas that displayed slight-to-moderate constitutive expression of FOS protein under *no stress* (control for ether and restraint stressed groups, *n* = 10) conditions. These areas included: olfactory bulb, prelimbic, infralimbic and piriform cortices, lateral septum, median and medial preoptic nuclei, suprachiasmatic nucleus, paraventricular thalamic nucleus, lateral hypothalamic area, dorsal hippocampus and dentate gyrus, midbrain periaqueductal area, pontine gray, nucleus of the solitary tract and lateral reticular nucleus.

Because intraperitoneal injection and placement of animals into a novel environment might be potentially stressful, first, we have checked neuronal activation (FOS) in general, and FOS+tdTomato coexpression in particular in the brain of these control animals.

Intraperitoneal saline injection (control for intraperitoneally injected hypertonic salt group and LPS treatment, *n* = 5) resulted in FOS activation (in addition to those seen in non-injected controls) in the cingulate cortex, bed nuclei of the stria terminalis (BNST), posterior PVH, in the thalamic stress-responsive complex (PVT, central medial-, paratenial- and mediolateral thalamic nuclei plus in the medial portion of the reuniens). Structures in which the difference between ip injected and non-injected groups reached significance were the primary motor area (Mop), pontine nucleus, dorsomedial part (PGdm) and hypoglossal nucleus (XII) (Figure 12A). Furthermore, intraperitoneally saline injected animals showed significantly higher colocalization rate

of CRH and FOS in magnocellular nucleus, lateral hypothalamic area dorsal part (MCLHD) and ventromedial hypothalamic nucleus (VMH) compared to the controls (Figure 12B).

Placing animals into a *novel environment* (control for the predator odor exposure, $n = 4$) resulted in moderate expression of FOS in all olfactory-related areas, increased rate of neurons expressing FOS in the prelimbic and infralimbic cortices, anterior cingulate area (ACA), lateral septum (LS), paraventricular hypothalamic nucleus (PVH), ventromedial hypothalamic nucleus (VMH), posterior hypothalamic area, thalamic stress-responsive complex, periaqueductal gray (PAG) and locus coeruleus (LC). Figure 12A indicates those areas where the difference is significant. Furthermore, central medial nucleus of the thalamus (CM), central lateral nucleus of the thalamus (CL) and PVH also showed significant elevation of activated CRH neuron rate compared to that of the control animals (Figure 12B).

DOI:10.14753/SE.2024.3001

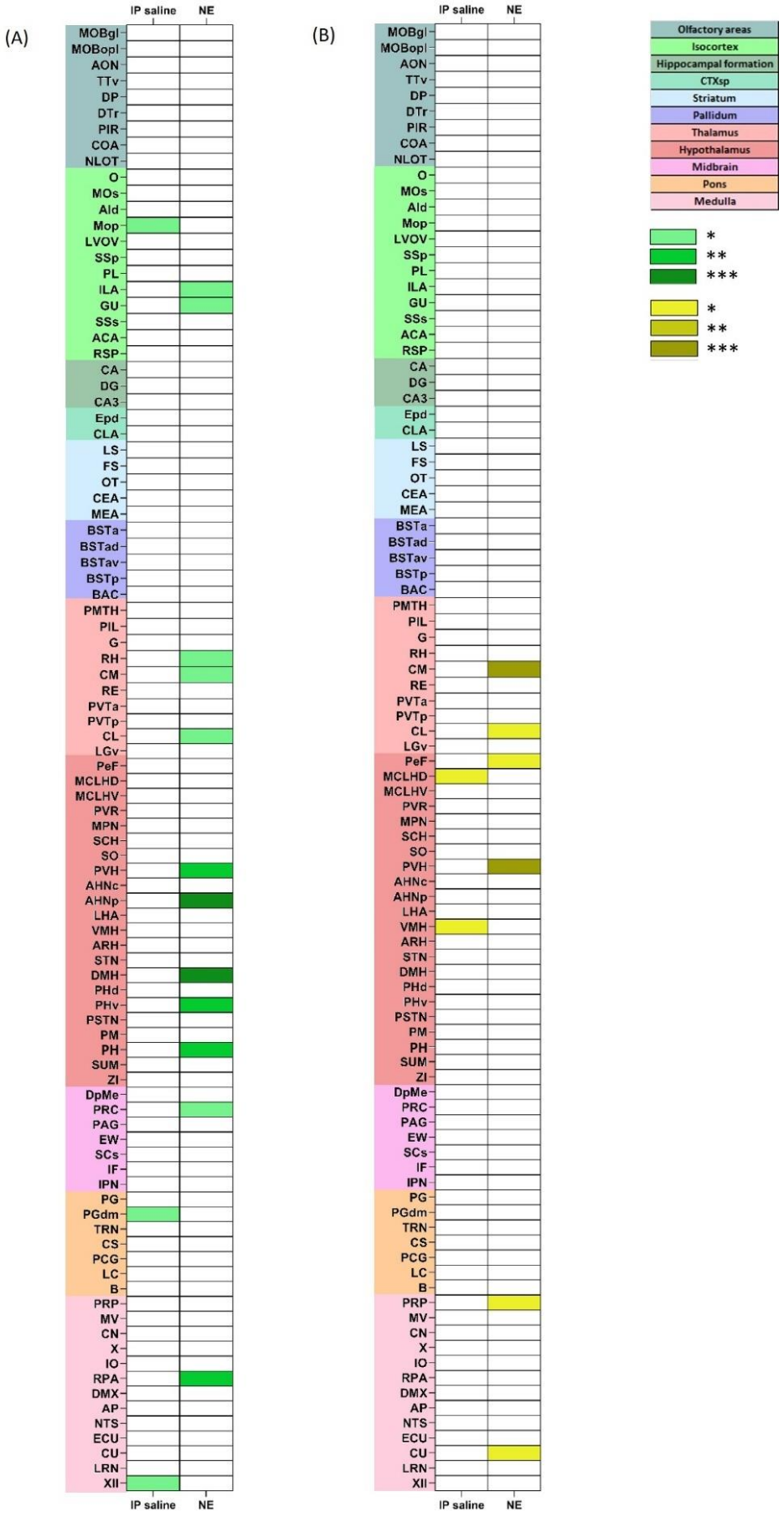

Figure 12. ***Levels of significance seen between animals exposed to novel environment (NE) or intraperitoneal injection of saline compared to non-stressed (absolute) controls.*** *(**A**) neuronal activation (FOS) and (**B**) colocalization (FOS + tdTomato). *p < 0.05; **p < 0.01; ***p < 0.001.*

4.2.2. Stress-induced neuronal activation

Figure 13 shows the proportion of FOS-immunoreactive neurons relative to their respective controls in response to the following stressors: hypertonic salt, LPS, ether exposure, restraint and predator odor.

Twelve brain areas have been found to be significantly activated by all stressors. These are as follows: the anterior cingulate area (ACA) (94); claustrum (CLA) (95); medial amygdalar nucleus (MEA) (96); bed nucleus of stria terminalis anteroventral division (BSTav) (97); geniculate nucleus (G) (98); anterior hypothalamic nucleus (AHNp) (99); paraventricular nucleus of the hypothalamus (PVH); lateral hypothalamic area (LHA) (100); dorsomedial nucleus of the hypothalamus (DMH) (101); posterior hypothalamic nucleus, ventral part (PHv) (102); parasubthalamic nucleus (PSTN) (103) and nucleus of the solitary tract (NTS) (73).

Areas that have been exclusively recruited by psychological stressors (restraint and predator odor) include: primary somatosensory area (SSp) (104); posteromedial thalamic area (PMTH) (105, 106); perifornical nucleus (PeF) (107); zona incerta (ZI) (108-110) and tegmental reticular nucleus (TRN) (111).

The supraoptic nucleus was the only region which has been exclusively activated by systemic (hypertonic salt and LPS), but not by psychogenic stressors.

Figure 14 summarizes the significance of stressor induced activation level differences in each region in which significant discrepancy was observed. Overall, among the used stressors, predator odor proved to activate the largest proportion of neurons in most of the observed areas compared to the appropriate control group.

DOI:10.14753/SE.2024.3001

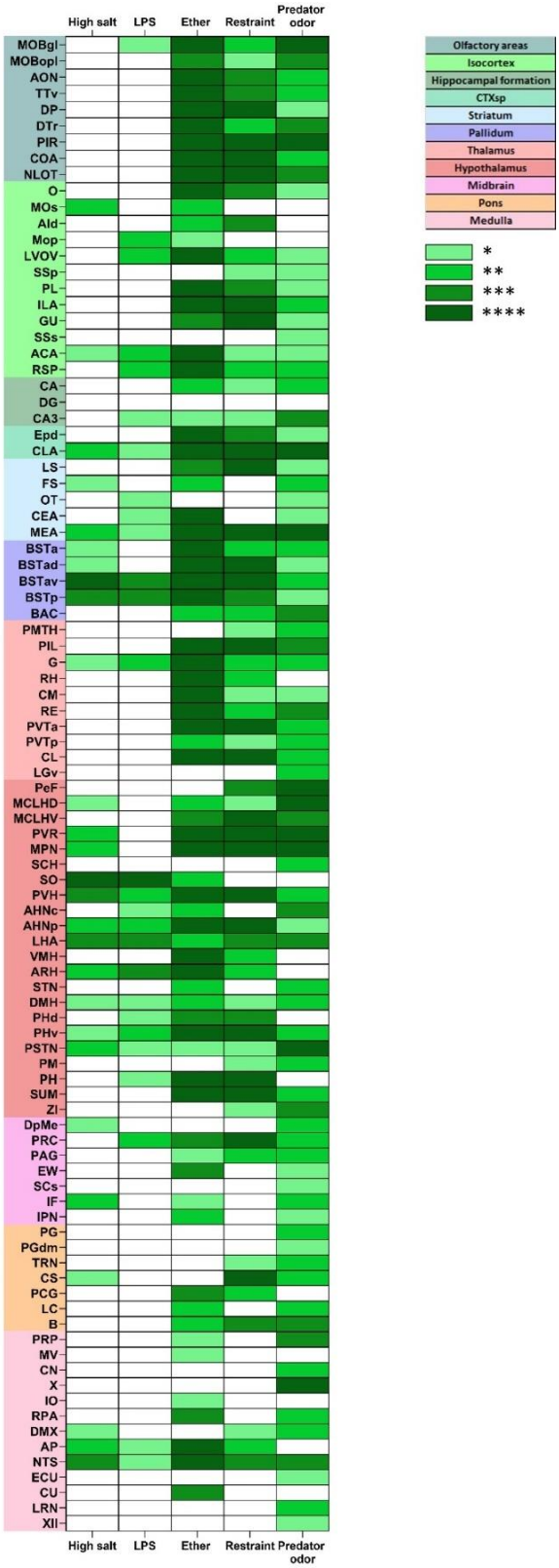

<u>Figure 13.</u> FOS expression in the stressed Crh-IRES-Cre;Ai9 mouse brain. *Color-coding refers to the levels of significance between stress-induced FOS density as compared to respective controls. *p < 0.05; **p < 0.01; ***p < 0.001; ****p < 0.0001.*

DOI:10.14753/SE.2024.3001

<	Restraint	Ether exposition	Hypertonic salt	LPS	Predator odor
Restraint		DP**, DTr****, PIR*, COA*, PL****, G**, RH**, CM***, RE***, PVTa**, CL**, EW*	BSTav*, SO****, LHA**, NTS****	BSTp*, G**, SO****, LHA***, NTS*	MOBgl****, DP**, DTr*, NLOT**, MOs*, SSp***, SSs***, RSP*, CA**, CLA**, BSTa****, BAC**, PMTH***, PIL****, G**, RE**, LGv****, MCLHD**, MPN****, SCH****, LHA***, STN****, PHd*, PSTN****, PM*, ZI****, DpMe****, PRC*, SCs***, IPN*, PG****, PGdm***, TRN*, CS****, LC****, B**, PRP****, MV***, CN***, X****, ECU****, DMX****, LRN****
Ether exposition	PeF*		BSTav**, SO****, LHA***, NTS****	SO****, LHA****, PRC*, NTS*	MOBgl****, NLOT*, MOs*, SSp***, SSs***, CLA**, BSTa***, BAC**, PMTH****, PIL****, LGv****, PeF***, MCLHD*, PVR*, MPN****, SCH****, LHA****, STN**, PHd*, PSTN****, PM**, ZI****, DpMe****, PRC***, PAG**, SCs***, IPN*, PG****, PGdm**, TRN***, CS****, LC****, B***, PRP****, MV***, CN***, X****, ECU****, DMX****, LRN****, XII*
Hypertonic salt	DP*, PIR***, COA**, O*, PL**, ILA*, CLA****, LS****, RH*, CL****, PeF*, MCLHV**, PVH**, DMH*, PH****, SUM**, PAG*, B*	MOBgl**, TTv**, DP****, DTr****, PIR****, COA****, NLOT*, O***, LVOV**, PL****, ILA**, RSP**, CA*, Epd*, CLA****, LS**, MEA*, RH****, CM****, RE****, PVTa****, PVTp**, CL****, PVH***, VMH**, PH****, EW**			MOBgl****, AON**, TTv**, DP****, DTr***, PIR**, COA**, NLOT****, LVOV**, SSp**, ILA***, SSs**, RSP**, CA***, Epd*, CLA****, BSTa****, BAC***, PMTH****, PIL****, RE***, PVTp**, LGv****, PeF***, MCLHV**, MPN****, SCH***, STN****, PHd*, PSTN***, PM**, ZI****, DpMe****, PRC**, PAG***, EW*, SCs***, PG****, PGdm*, TRN***, CS****, LC****, B****, PRP****, MV***, CN**, X****, ECU****, DMX****, LRN****, XII**
LPS	PIR***, COA**, O*, PL*, ILA*, CLA***, LS****, MEA*, CL****, MCLHV**, PVH**, DMH*, PH****, SUM**	DP***, DTr****, PIR****, COA****, NLOT*, O**, PL****, ILA**, CLA****, LS**, MEA***, RH****, CM****, RE****, PVTa****, CL****, PVH***, VMH**, PH*	SO***, NTS*		MOBgl****, AON*, TTv*, DP***, DTr*, PIR**, COA**, NLOT****, LVOV*, SSp**, ILA**, SSs**, RSP*, CA**, Epd*, CLA****, BSTa****, BAC***, PMTH****, PIL****, RE****, PVTp*, LGv****, PeF***, MCLHV**, PVR**, MPN****, SCH***, STN****, PHd*, PSTN****, PM**, ZI****, DpMe****, PAG**, SCs**, IPN*, PG**, TRN**, CS****, LC****, B***, PRP****, MV***, CN*, X****, DMX****, ECU****, LRN****, XII**
Predator odor	CL****, PVH**, DMH*, PH****	PL****, MEA**, RH****, CM***, PVTa*, CL****, PVH***, VMH**, PH***, AP*	BSTav*, SO****, NTS***	SO****	

Figure 14. ***Location and significance of stressor induced neuronal activation differences.*** *Columns represent the specific stressor after which the referred brain region showed significantly higher elevation of activated neuron rate (compared to the adequate control animals) than the stressor represented in the specific row. *p < 0.05; **p < 0.01; ***p < 0.001; ****p < 0.0001.*

4.2.3. Stress-induced activation of tdTomato positive profiles

In most of the brain areas, stress activated neurons were not tdTomato positive. In these areas the rate of colocalization was not significantly different from that seen in respective controls. In general, systemic stressors such as hypertonic salt and LPS injection resulted in fewer double-labeled areas than psychological (restraint, predator odor) stressors, as seen in Figure 15. All five stressors resulted in significant activation of putative CRH neurons in the orbital cortex and anterior cingulate area (ACA). Psychological, but not systemic challenges, activated tdTomato/CRH neurons in dorsal peduncular cortex, in the Barrington's nucleus and nucleus X. By contrast, putative CRH neurons in the periaqueductal gray were activated by LPS and high salt, not by psychogenic challenges.

Ether exposure, hypertonic salt, LPS and restraint but not predator odor resulted in significant colocalization of tdTomato signal and FOS in the hypothalamic paraventricular nucleus. Detailed analysis of the PVH however, revealed stressor-related heterogeneity in FOS/tdTomato coexpression (Figure 16). Significance of stressor induced CRH neuron activation level differences is demonstrated in Figure 17 by area.

Interestingly, certain tdTomato/CRH-rich brain areas, such as the piriform cortex, central amygdala, BNST and inferior olive, display heterogenous, stressor-specific colocalization of tdTomato and FOS markers.

DOI:10.14753/SE.2024.3001

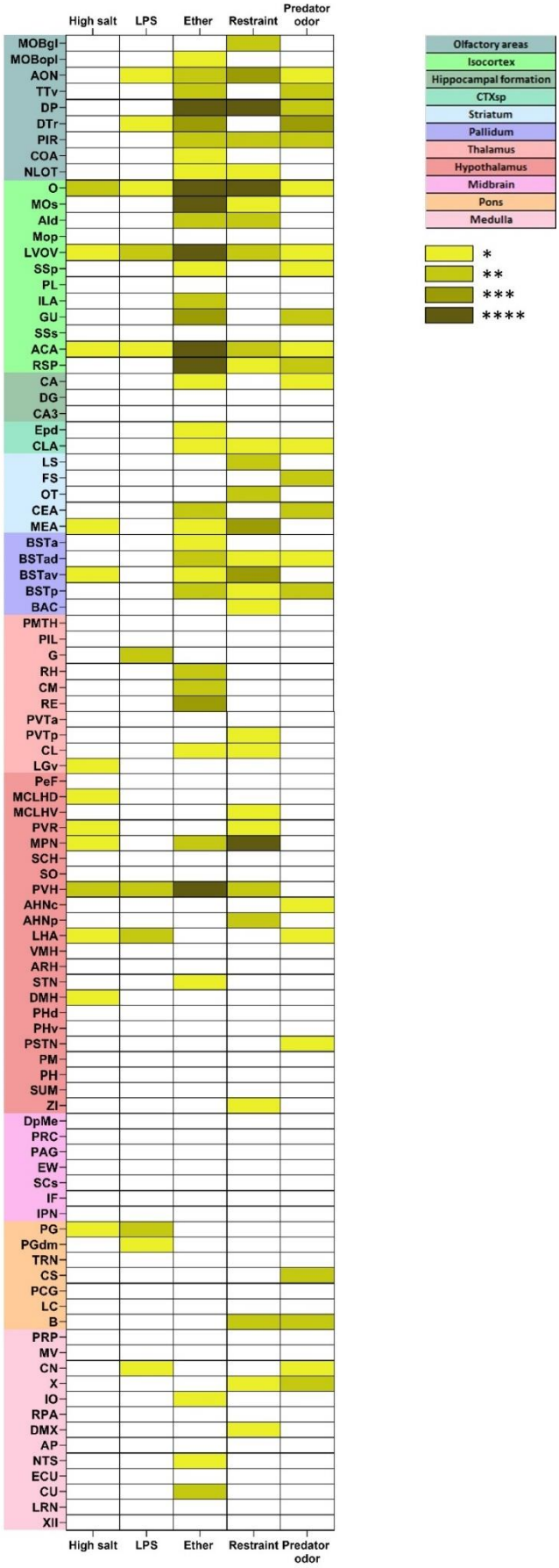

Figure 15. ***Stress-induced recruitment of putative CRH (tdTomato expressing) neurons in Crh-IRESCre;Ai9 mouse brain.*** *Color coding refers to significant differences between cell densities of neurons co-expressing tdTomato and FOS markers as compared to values of respective controls in the same area. *p < 0.05; **p < 0.01; ***p < 0.001; ****p < 0.0001.*

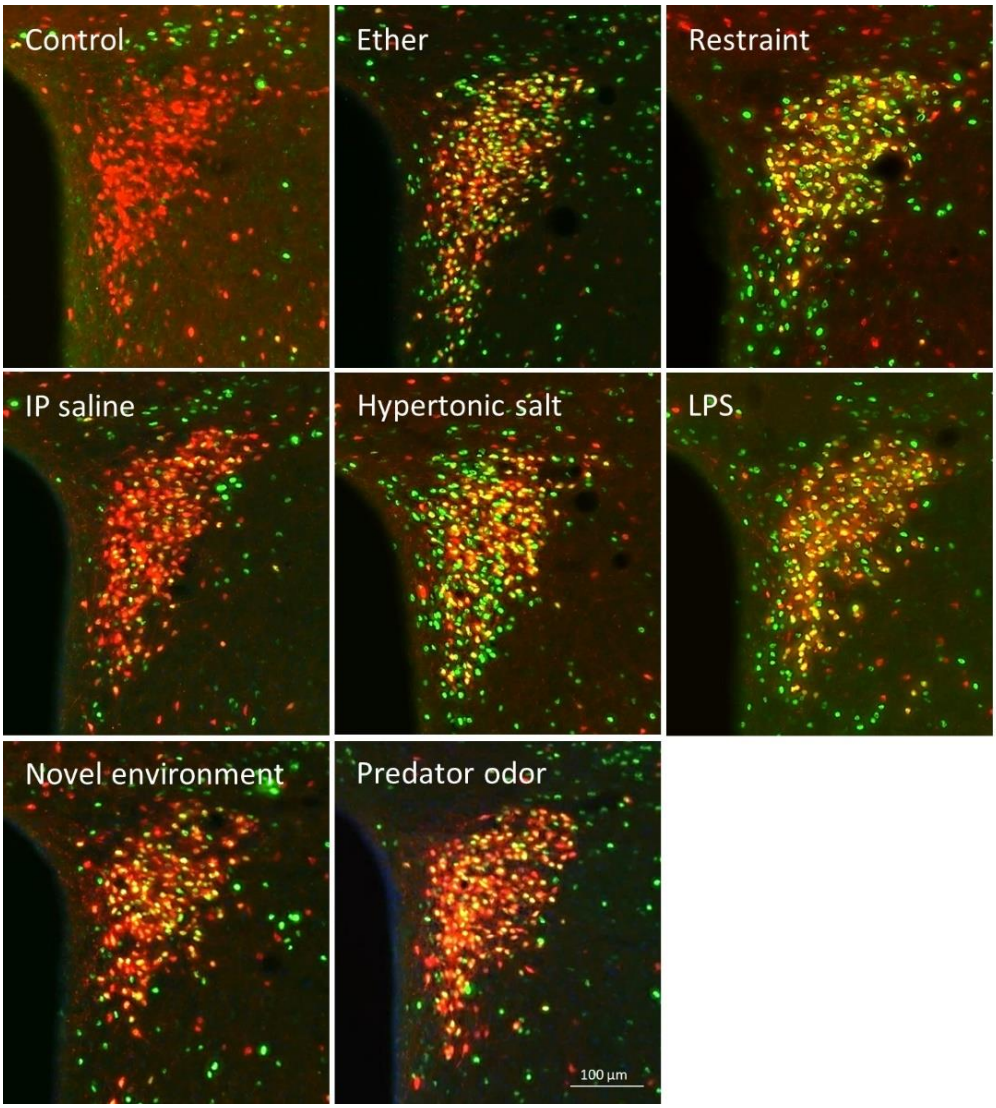

Figure 16. ***Colocalization of tdTomato (CRH) marker and FOS in the hypothalamic paraventricular nucleus of Crh-IRES-Cre;Ai9 mice in response to different stressors.***

<	Restraint	Ether exposition	Hypertonic salt	LPS	Predator odor
Restraint		ACA*, RSP*, CM*, SCs**, CU*	NLOT*, MOs*, LGv*, VMH*	DP**, DTr**, G*, LHA****, PGdm*, CN**	TTv*, DTr***, NLOT**, CA*, DpMe*, B****, PRP*
Ether exposition	MPN*		NLOT*, LGv*, PVR*, LHA**, VMH*, DpMe*, PGdm**	DP**, DTr**, G*, LHA****, PGdm**, CN**	DTr***, NLOT**, DpMe**, B****, PRP*, DMX*
Hypertonic salt	AON*, O***, OT*, PVH**, MV*	O****, LVOV*, SSp*, ACA****, RSP***, CM*, RE*, PVH****, SCs*, MV*, CU*		DP**, LHA*, CN*	TTv*, LVOV*, CA*, BSTad*, B****, DMX*
LPS	O**, MPN**, PVH**, MV*	O****, SSp*, ACA***, RSP**, RE*, PVH***, CU*			CA*, BSTad*, B****, PRP*, X*, DMX*
Predator odor	O**, MPN***, PVH*	O***, ACA**, RSP*, PVH***, SCs*, CU*	MOs*, LGv*, LHA*	DP*, LHA****, PGdm*	

Figure 17. ***Location and significance of stressor induced tdTomato positive neuron activation differences.*** *Columns represent the specific stressor after which the referred brain region showed significantly higher elevation of activated tdTomato positive neuron rate (compared to the adequate control animals) than the stressor represented in the specific row. *p < 0.05; **p < 0.01; ***p < 0.001; ****p < 0.0001.*

4.2.4. Acute stress-induced corticosterone

A separate set of Crh-IRES-Cre;Ai9 mice was exposed to ether (n = 4), hypertonic salt (n = 3), LPS (n = 3), restraint (n = 2) or predator odor (n = 3). Control mice (n = 3) were left undisturbed until sacrifice.

All applied acute stress exposure resulted in robust elevation of corticosterone level compared to the control animals (Figure 18).

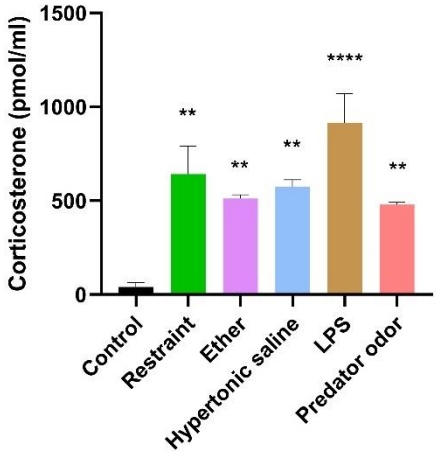

Figure 18. ***Mean ± SEM values of plasma corticosterone in animals exposed to different stressors****. **p < 0.01; ****p < 0.0001 compared to unstressed control mice.*

4.3. Chronic stress

It is important to distinguish that pathophysiological differences exist between a short-term challenge generated acute and a prolonged or frequent stressors-induced chronic stress paradigm (14). As so we decided to investigate the probable stress response differences. During acute and chronic repeated stress, C57BL/6J mice were exposed to one hour restraint stress once (n = 5) or on a daily basis for three weeks (n = 8). The group of chronic variable stressed animals was exposed twice daily to different psychogenic stressors (n = 13) (Table 1). Control animals (n = 5; n = 8; n = 13) were left undisturbed except for changing the bedding. Chronic stress is one of the major external factors, which precipitates anxiety or depression. Therefore, we aimed to elucidate differences in anxiety-related behavior of mice exposed to homotypic (chronic repeated restraint stress; CRS) vs heterotypic (chronic variable stress; CVS) chronic stress. To reveal the molecular mechanism underlying behavioral response to acute and chronic stress, we have measured hypothalamic expression of specific stress-related transcription factors of AP-1 family, which are responsible for acute- and lasting adaptations in target gene expression (34).

DOI:10.14753/SE.2024.3001

4.3.1. Chronic stress induced behavioral changes

The unpredictable chronic variable stress (CVS) protocol resulted in anxiety-like behavior with a decrease of centrum preference and in the latency to first time entrance into the corners of the open field arena (Figure 19).

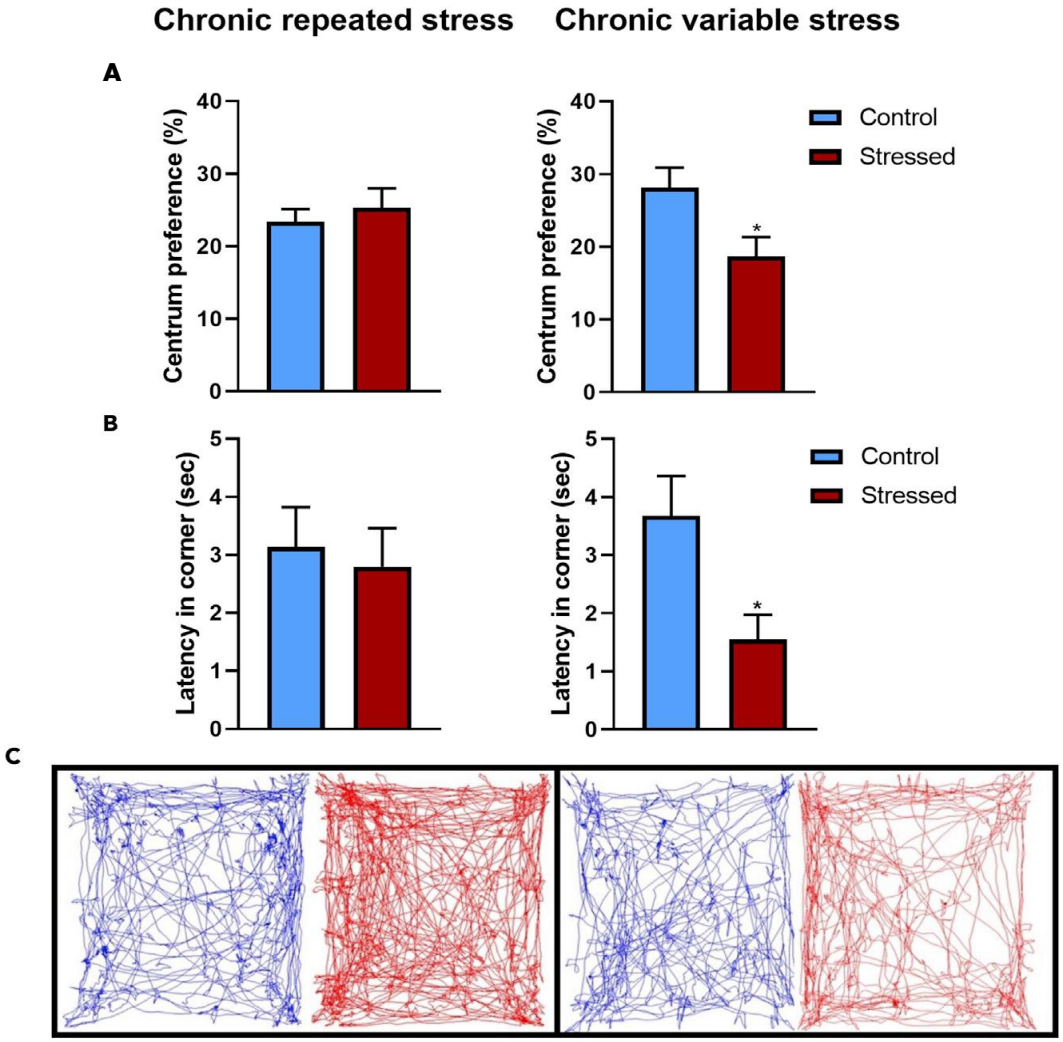

Figure 19. ***Chronic variable stress (CVS) but not chronic repeated restraint stress (CRS) increases anxiety-like behavior.*** *In the OF test, reduced centrum preference (**A**) and latency of the first entrance into the corner (**B**) were recorded in CVS exposed mice, while these parameters were unchanged in CRS exposed mice. Representative trajectory diagrams for control (blue) and chronically stressed (CRS and CVS) mice are shown on (**C**). Data are presented as mean ± SEM. *p < 0.05 vs. the control group.*

DOI:10.14753/SE.2024.3001

4.3.2. Fos-related transcription factors in the stressed hypothalamus

We have confirmed that c-Fos mRNA was induced in acutely restrained mice. By contrast, repeated restraint evoked significantly attenuated c-Fos response, while no response was detected in CVS exposed mice (Figure 20). Dramatic elevation of Fosl2 expression was detected exclusively in the CRS group. All stress paradigms increased hypothalamic expression of FosB, however the responses were significantly lower in chronically stressed groups, than that of acutely restrained groups.

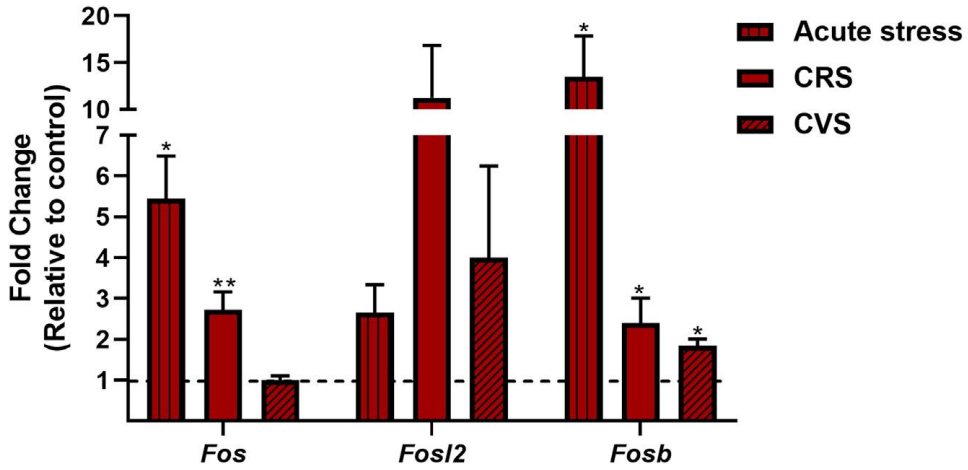

Figure 20. ***Acute- and chronic stress exposure differentially affects the expression of neuronal activation markers in the hypothalamus****. Fold change values, relative to controls, are shown in acutely restrained animals and mice exposed to repeated restraint (CRS) or chronic unpredictable variable (CVS) stress. Data are presented as mean ± SEM. *p < 0.05; ***p < 0.001; ****p < 0.0001 vs. control group.*

DOI:10.14753/SE.2024.3001

4.4. Investigation of CRH^{PVH} neurons

While neuroendocrine stress response is the outcome of a rather complex interplay of diverse cell types and neuronal networks across distinct brain regions, the key regulatory role of CRH^{PVH} neurons is well established. PVH, after integrating external and internal stress-related information, activates the HPA axis through the initiation of CRH release from the hypophyseotropic parvocellular neurons.

Next, we addressed special functional significance of CRH^{PVH} in mediating/initiating hormonal/activational and behavioral stress responses. We have compared responses evoked by acute or repeated restraint stress to those evoked by acute or repeated chemogenetic activation of CRH^{PVH} neurons.

For chemogenetic activation, Cre-dependent adeno-associated virus (AAV) construct (pAAV8/hSyn-DIO-hM3D(Gq)-mCherry) was stereotaxically administered bilaterally into the hypothalamic paraventricular nucleus of Crh-IRES-Cre mice. After three weeks of recovery, CRH^{PVH} neurons were either activated once or repeatedly once daily for 2 weeks with C21 actuator. Stressed animals received pAAV-hSyn-DIO-mCherry (control virus) into the PVH and were acutely or repeatedly exposed to restraint stress along with C21 intraperitoneal injection(s).

DOI:10.14753/SE.2024.3001

4.4.1. Validation of stereotaxic virus administration

Cre-dependent uptake and transcriptional activity of AAV virus constructs in the PVH was confirmed by red fluorescent protein (RFP) immunostaining. In the evaluation, only animals with correct injection placement and with clear bilateral RFP staining covering the PVH, were included (Figure 21).

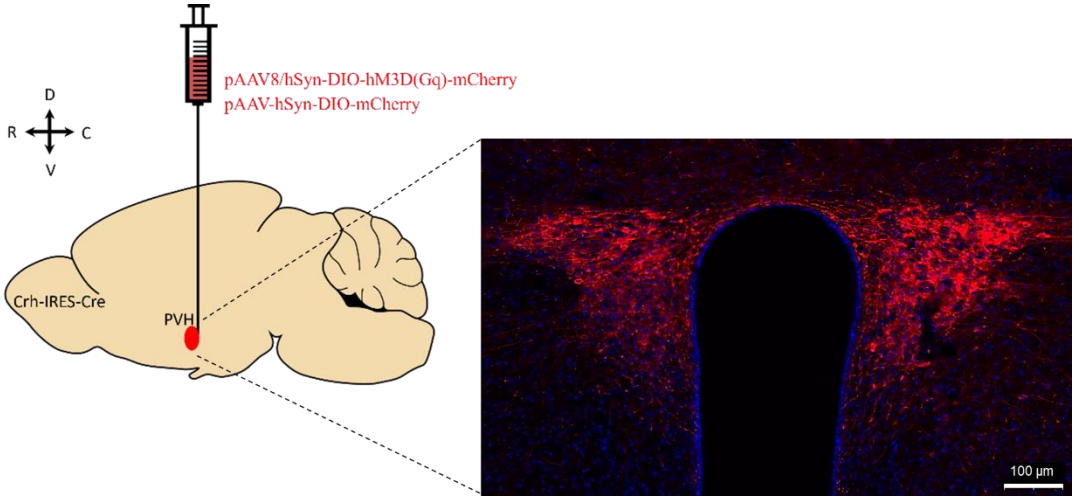

Figure 21. ***Successful bilateral administration of Cre-dependent adeno-associated virus (AAV) into hypothalamic paraventricular nucleus of a Crh-IRES-Cre mouse.***

Figure 22 shows that the pattern of the virus infected CRH^{PVH} cells entirely overlaps with the distribution of tdTomato+ neurons observed in Crh-IRES-Cre;Ai9 mice.

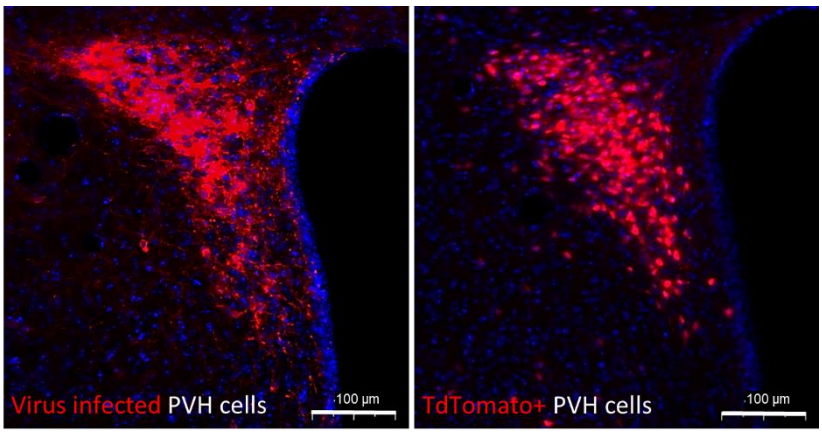

Figure 22. ***Location of virus infected PVH cells in Crh-IRES-Cre and tdTomato+ PVH cells in Crh-IRES-Cre;Ai9 mice.***

DOI:10.14753/SE.2024.3001

4.4.2. CRH^{PVH} neurons in acute stress reactions

After three weeks of recovery, animals injected with pAAV8/hSyn-DIO-hM3D(Gq)-mCherry (act. DREADD group; *n* = 5) were treated with DREADD agonist C21 for chemogenetic activation of CRH^{PVH} neurons. Mice injected with pAAV-hSyn-DIO-mCherry were also treated with DREADD agonist C21, while they also endured one hour restraint stress (Restraint group; *n* = 4). Animals were sacrificed 90 minutes post-injection/or stress. Neuronal activation was revealed by FOS-immunostaining. The timeline of the experiment is shown on Figure 23.

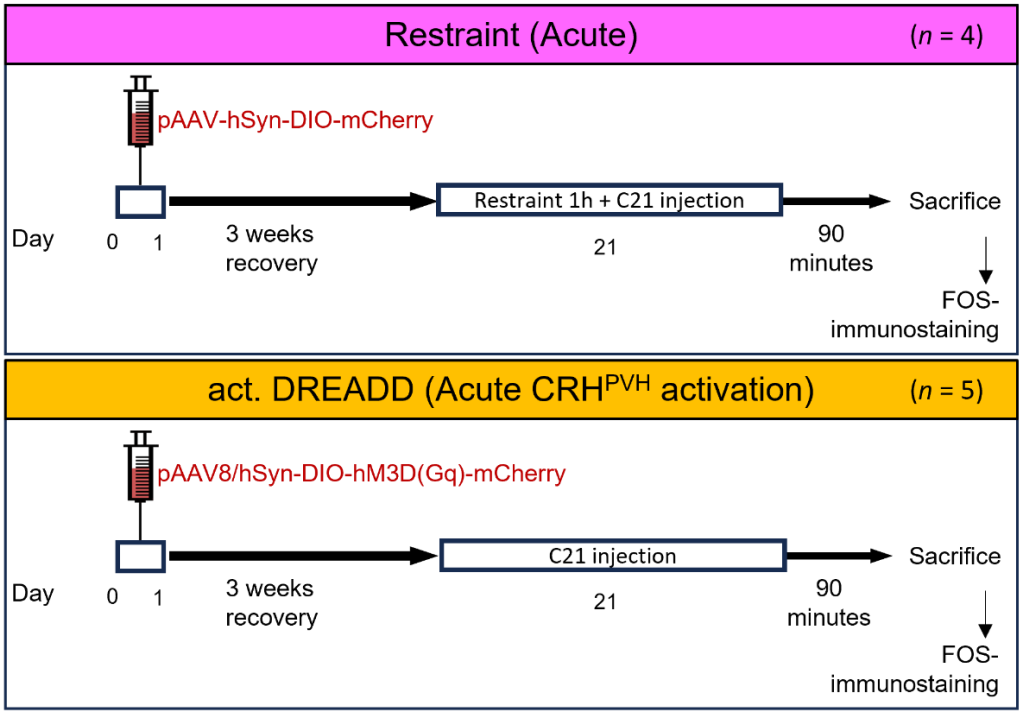

***Figure 23.** Experimental design of functional analysis of CRH^{PVH} in acute challenges.*

4.4.2.1. Neuronal activation

Both chemogenetic and restraint stress-induced activation of the animals resulted in c-Fos induction throughout the mouse brain. The number and distribution of c-Fos positive neurons in the PVH were comparable in mice exposed to chemogenic or stress-induced activation. A thorough comparison of c-Fos activational patterns in the stress-related neuronal circuit revealed areas that have been differentially activated. There were more areas that have been activated by acute restraint than those that became c-Fos positive following chemogenetic activation of CRH^{PVH} neurons. The areas that contained more c-Fos positive profiles in response to stress than activation of CRH^{PVH}

neurons are listed in Table 4. Activation of these areas means that they are involved in the brain stress system(circuit) but their activation is independent from the PVH. Microcopic image of the activated neurons of PVH, medial amygdalar nucleus (MEA), lateral septal nucleus (LS), supramammillary nucleus (SUM) and locus coeruleus (LC) can be seen on in Figure 24.

Table 4. ***Comprehensive list of brain regions, in which neuronal activation differed.*** *Brain regions were ranked on a "+" - "+++++" scale, where "+" = number of FOS+ cells/mm^2 < 50 and "+++++" = number of FOS+ cells/mm^2 > 200.*

	Act. DREADD	Restraint
MOBgl	++++	+++++
AON	+++	+++++
TTv	++	+++
SSp	+++	++++
ILA	++	++++
CA	+++	++++
CLA	++	++++
LS	+++	+++++
BSTa	+	+++
BSTav	++	+++
BSTp	+	++
BAC	++	+++
CM	+++	++++
PVTa	+++	++++
CL	++	+++
MPN	++	++++
ARH	+	++
DMH	+++	+++++
PHd	+++	++++
SUM	+++	+++++
DpMe	++	++++
PRC	+++	++++
EW	+++	++++
LC	++	+++
B	++	+++
RPA	+	++
AP	+	++

Olfactory areas
Isocortex
Hippocampal formation
CTXsp
Striatum
Pallidum
Thalamus
Hypothalamus
Midbrain
Pons
Medulla

DOI:10.14753/SE.2024.3001

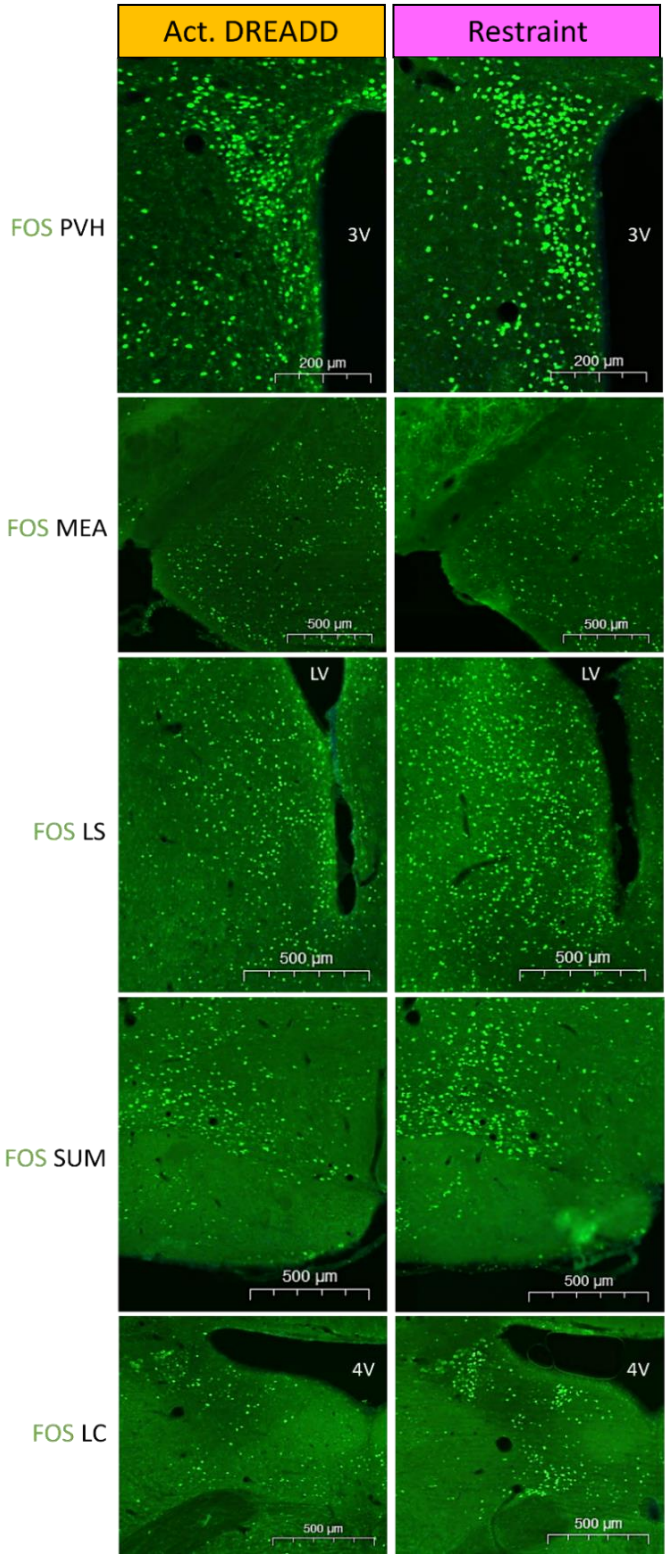

Figure 24. ***DREADD agonist 21 (C21) vs acute restraint induced neuronal activation in the mouse brain.*** *PVH-paraventricular hypothalamic nucleus; MEA-medial amygdalar nucleus; LS-lateral septal nucleus; SUM-supramammillary nucleus; LC-locus coeruleus; third ventricle (3V); lateral ventricles (LV); fourth ventricle (4V).*

DOI:10.14753/SE.2024.3001

4.4.3. CRH^{PVH} neurons in chronic stress reaction

To address the role of CRH^{PVH} neurons in organizing chronic stress responses, animals were injected with pAAV8/hSyn-DIO-hM3D(Gq)-mCherry into the PVH (act. DREADD group; n = 14). After 3 weeks of recovery, mice were injected daily for two additional weeks with DREADD agonist C21 for repeated chemogenetic activation of CRH^{PVH} neurons. Additional group of mice were injected with control virus pAAV-hSyn-DIO-mCherry treated for two additional weeks with DREADD agonist C21 daily and exposed to one hour restraint stress each day (Repeated Restraint group; n = 10). Control animals (n = 7) were not virus injected, but received intraperitoneal saline injection daily, for two weeks. The timeline of the experiment is shown in Figure 25. Body weight (BW) and nest building (NB) behavior of the animals were observed at the beginning and at the end of the two weeks treatment. To investigate anxiety and depression-like behavior, open field (OF) and tail suspension (TST) tests were carried out at the end of experiment. Blood samples from retro-orbital sinus were collected at two different time points: we sacrificed half of the mice after the TST, which test can be also considered as an acute stressor (Sacrifice I.), while the rest of the animals were sacrificed on the following day under basal (no-stress) conditions (Sacrifice II.).

DOI:10.14753/SE.2024.3001

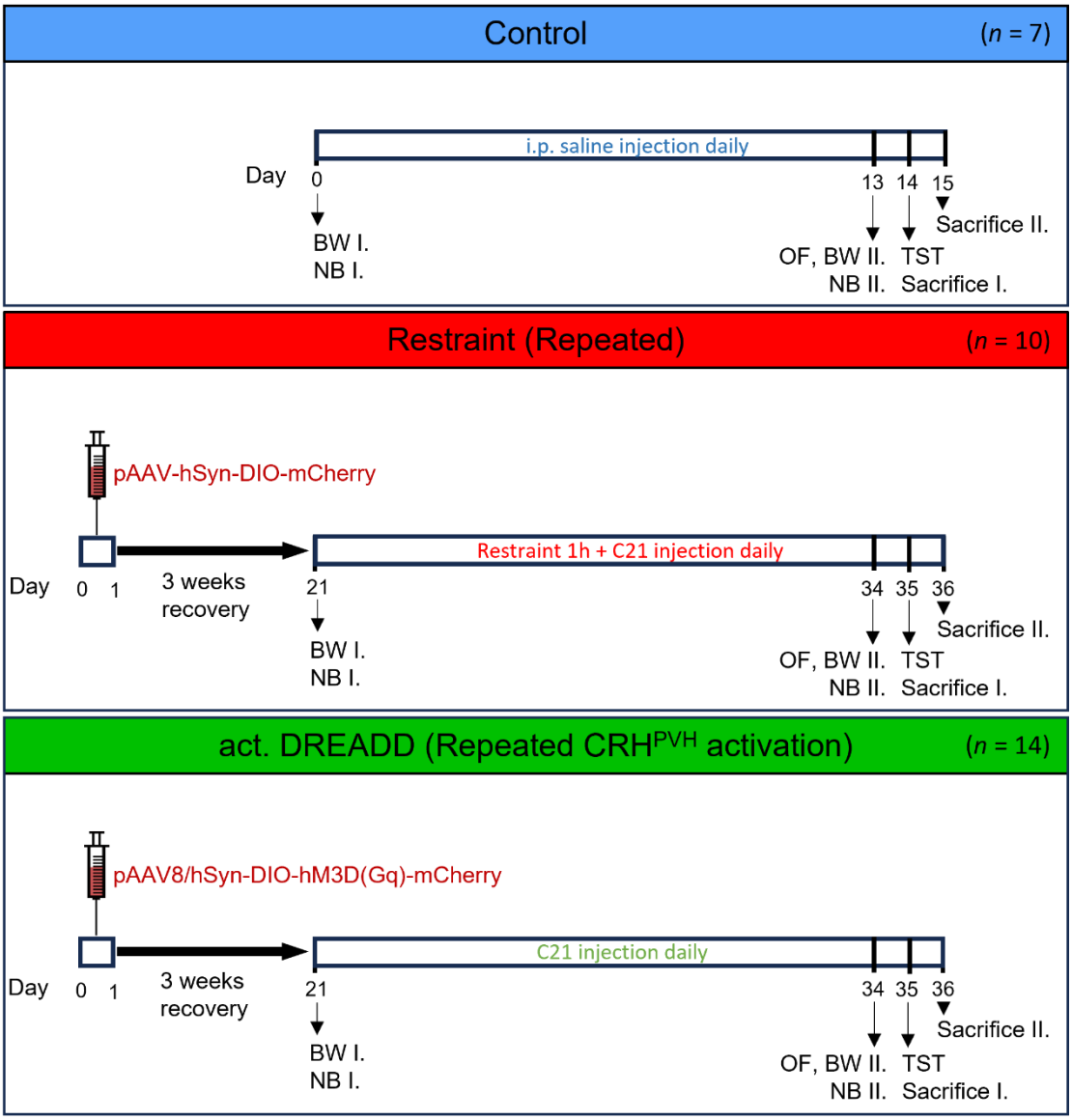

Figure 25. ***Experimental design of functional analysis of CRH^{PVH} in chronic challenges.*** *Nest building (NB I-II. time point), open field (OF) and tail suspension (TST) tests were performed on the indicated days of the trial. Body weight (BW) of the animals was measured at the beginning and at the end of the experiment.*

4.4.3.1. Body weight changes

Both repeated restraint and repeated chemogenetic activation of CRH^{PVH} neurons resulted in decrease of body weight of the mice by the end of the two weeks treatment. Their body weight change was significantly different from that of controls (Figure 26).

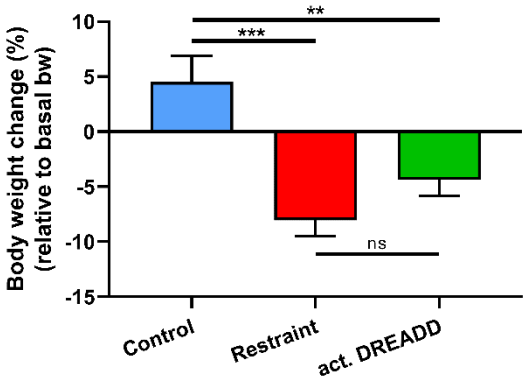

Figure 26. ***Change of body weight due to repeated restraint and repeated chemogenetic activation of CRH^{PVH} neurons.*** *Data are presented as mean ± SEM. **p < 0.01; ***p < 0.001 vs. control group; ns = not significant.*

4.4.3.2. Behavioral changes

4.4.3.2.1. Nest building (NB) test

The quality of the nests, built by the animals was scored (1-5) before and after exposure to repeated challenges. Two weeks of repeated chemogenetic CRH^{PVH} neuron activation reduced the quality of the nests built by the animals. By contrast, chronic restraint stress did not induce significant changes in this type of behavior (Figure 27).

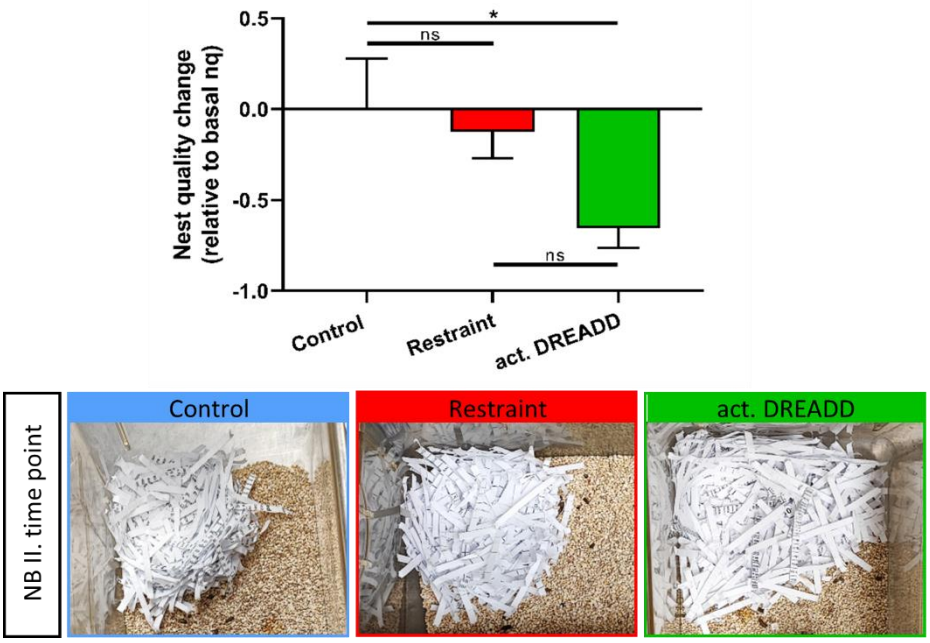

DOI:10.14753/SE.2024.3001

Figure 27. ***Quality of nests significantly dropped after two weeks of chemogenetic activation of CRH^{PVH} neurons.*** *Change in nest quality scores obtained after and before the repeated challenges. Data are presented as mean ± SEM. *p < 0.05 vs. control group, ns = not significant. Representative photographs of the nests were taken at the end of the experiment (NB II. time point).*

4.4.3.2.2. Open field (OF) test

The activity pattern of control mice was not significantly different from those exposed to repeated challenges tested in a novel open field environment for 10 minutes. All experimental mice had similar centrum preference and latency to first step into the corner region (Figure 28A). Representative trajectory diagrams also showed no outstanding pattern difference among the treatment groups (Figure 28B).

However a more detailed analysis of open field behavior: surveying, walking, rearing and grooming revealed significant differences. As a result of two weeks restraint stress, mice groomed significantly more frequently and for a longer period of time compared to the animals in the other two groups. Furthermore, we observed that the duration of surveying was significantly elevated in case of animals that received act. DREADD virus injection compared to the restrained ones. Duration and frequency of walking and rearing remained alike in all treatment groups (Figure 28C-D).

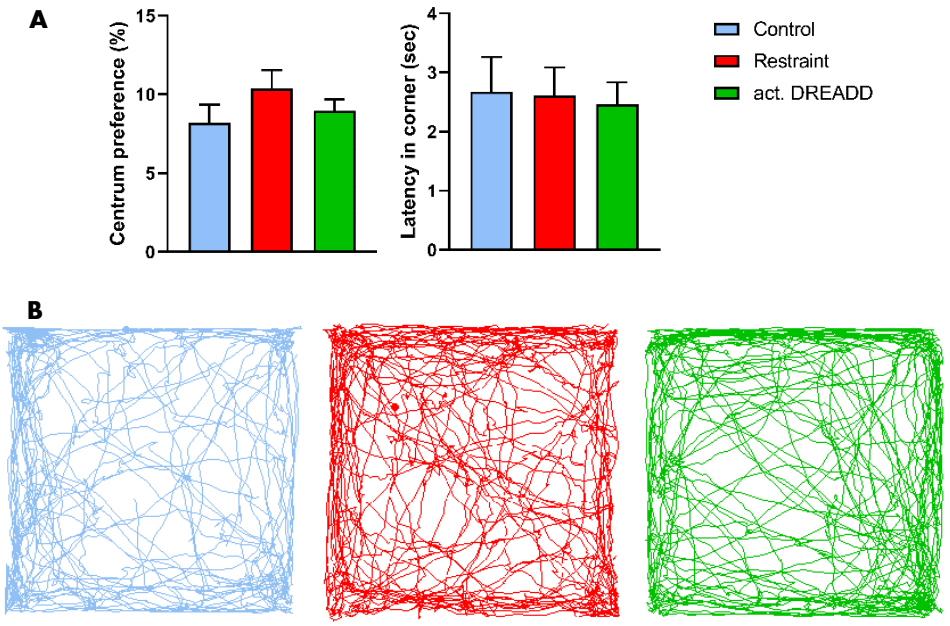

DOI:10.14753/SE.2024.3001

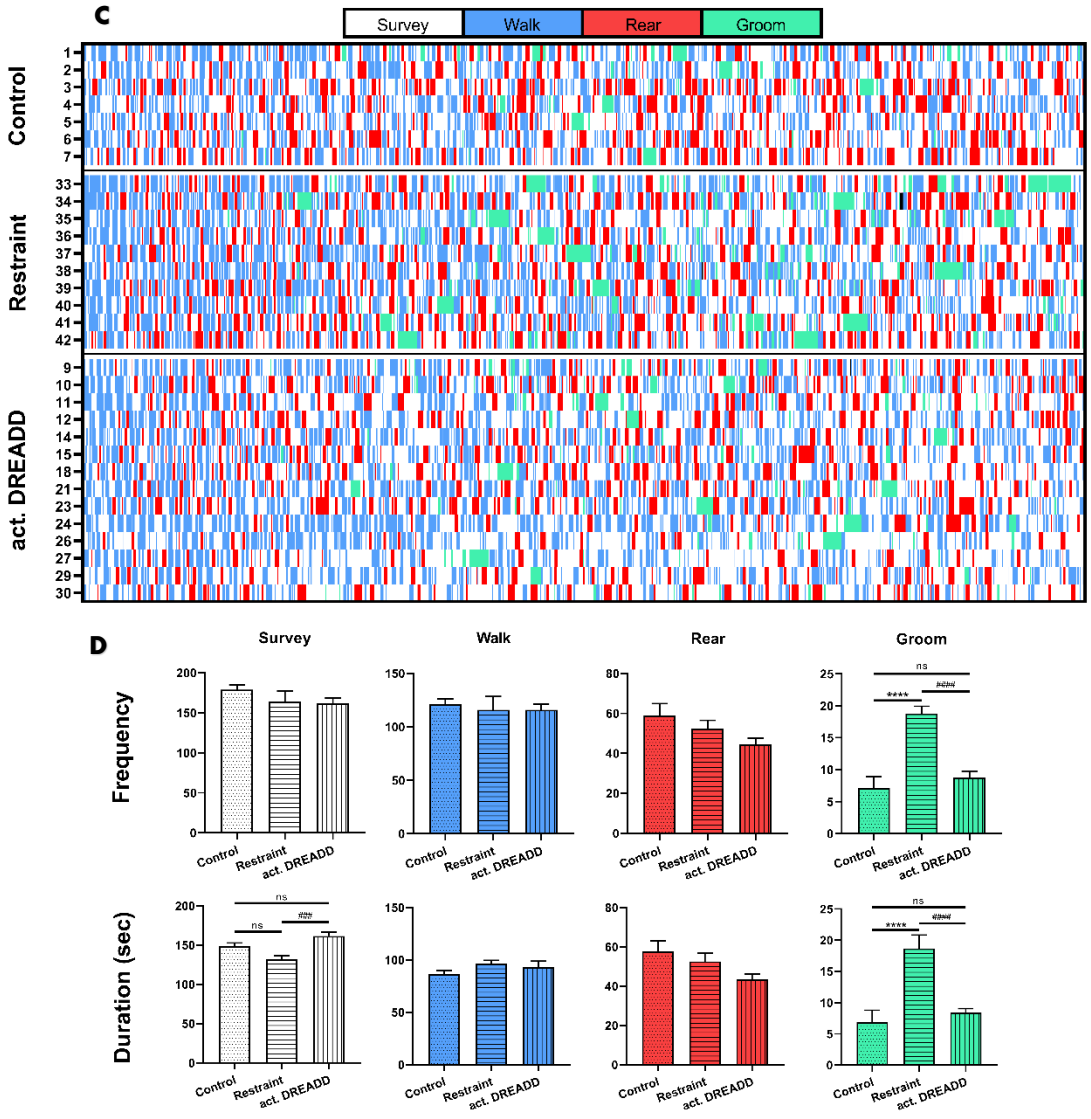

Figure 28. ***Repeated restraint and repeated chemogenetic CRH^{PVH} activation induced behavioral changes observed in open field arena.*** *Centrum preference and latency of the first entrance into the corner (**A**), representative trajectory diagrams (**B**) and ethograms (**C**). Occurrence of the selected behavioral element (survey, walk, real, grooming) during the test can be seen on **C**, where each row represents one mouse. Frequency and duration of specific elements are seen on **D**. Data are presented as means ± SEM. ****p < 0.0001 vs. control group. ###p < 0.001; ####p < 0.0001 between Restraint and act. DREADD groups; ns = not significant.*

DOI:10.14753/SE.2024.3001

4.4.3.2.3. Tail suspension (TST) test

During the 6 minutes long tail suspension test, moving and immobile state of the animals were monitored and quantified. As Figure 29 shows, moving frequency of the mice exposed to repeated chemogenetic activation of CRH^{PVH} neurons were significantly higher compared to that of the restrained mice. During the second half of the test, observed immobility duration of the act. DREADD group was also significantly elevated compared to the control animals.

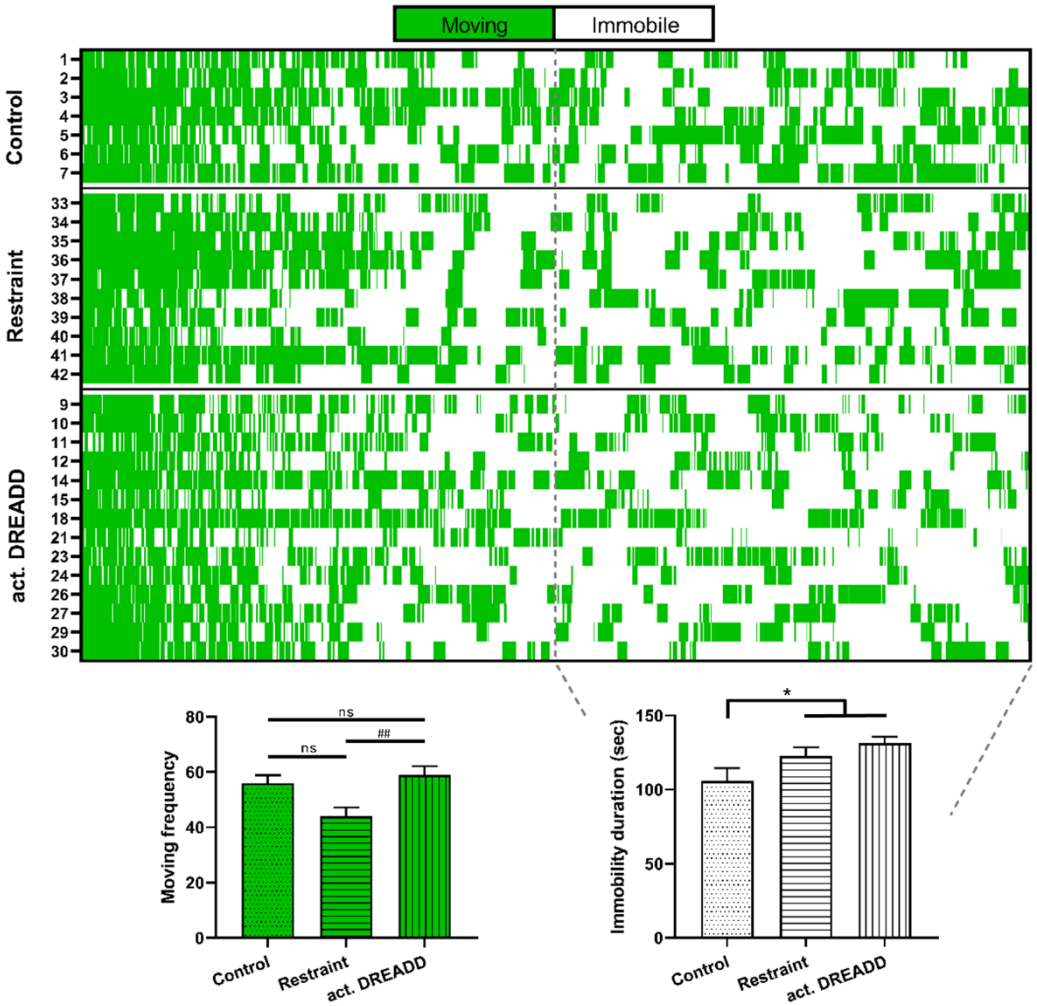

Figure 29. ***Detailed ethogram of moving and immobility behavioral elements of the animals during tail suspension test.*** *On the ethogram each row represents one mouse. Diagram of moving frequency represents the data collected over the entire six-minute duration of the test, while the immobility duration diagram specifically represents data observed during the 4th-6th minutes of the test. Data are presented as mean ± SEM. *p < 0.05 vs. control group. ##p < 0.01 between Restraint and act. DREADD groups; ns = not significant.*

DOI:10.14753/SE.2024.3001

4.4.3.3. Corticosterone measurement

Basal serum corticosterone level (sampled at Sacrifice II. time point) did not differ significantly among the groups at the end of the two weeks treatment.

Tail suspension test (as an acute stress) evoked significant corticosterone elevation in all groups. In chronically restrained mice, acute stress induced CORT level was significantly higher compared to that of the other two groups (Figure 30).

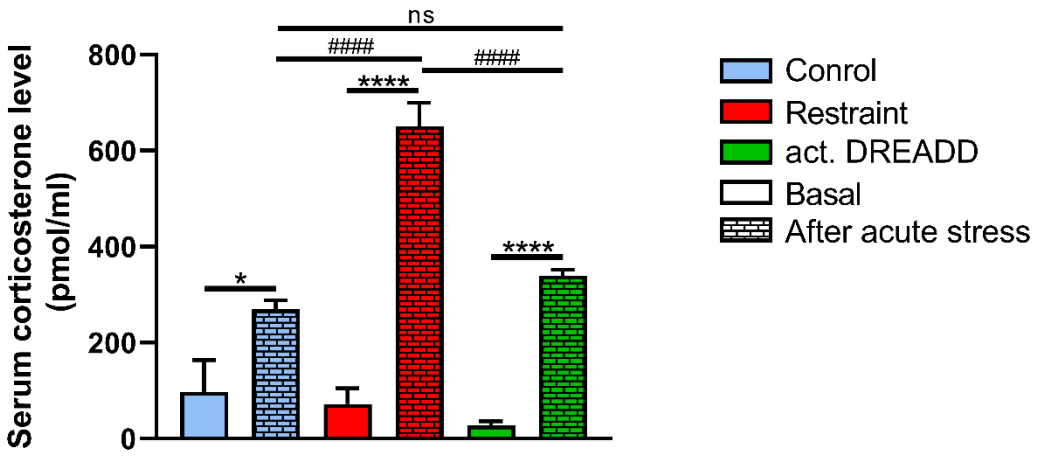

Figure 30. ***Basal and acute stress induced serum corticosterone level of control, repeatedly restrained mice and animals in which CRH^{PVH} neurons were repeatedly activated.*** *Data are presented as mean ± SEM. *p < 0.05; ****p < 0.0001 between Basal and After acute stress states; $^{\#\#\#\#}$p < 0.0001 vs. After acute stress states; ns = not significant.*

DOI:10.14753/SE.2024.3001

5. Discussion

5.1. CRH involvement in the organization of acute stress responses

Here we provide a detailed analysis of stress-dependent recruitment of corticotropin-releasing hormone (CRH) neurons in the mouse brain. Putative CRH-producing neurons have been identified using Cre reporter transgenic mice (Crh-IRES-Cre;Ai9) in which a CAG-LoxStopLox-tdTomato construct is integrated into Gt(Rosa)26Sor locus (112). Because Cre recombinase and CAG promoter are active throughout the whole ontogenesis, it is likely that neurons, which are active during embryonic development, but not in adults, express the tdTomato marker. Nevertheless, there was a good correlation between tdTomato and CRH mRNA expressions in most of the areas except the thalamus, striatum and midbrain. In these structures, the fluorescent marker expression exceeded that of the mRNA. Chen et al. reported an almost complete overlap of native peptide and the tdTomato reporter in the Crh-IRES-Cre;Ai14 mouse, although their analysis was limited to PVH, BNST, amygdala and the hippocampus (69).

Previous studies used Ai14 reporter line (68, 69, 113), while we found that the Ai9 is more suitable for colocalization studies, due to the moderate expression of the fluorescent marker gene. Importantly, tdTomato expression is independent of the strength of CRH expression, because the marker gene is driven by a constitutively active CAG promoter. Indeed, neither adrenalectomy nor acute stress exposure, which are known as strong activators of CRH neurons, affected tdTomato staining intensity.

FOS-immunostaining was used as a functional anatomical marker of stress-activated neurons. c-Fos is an immediate early gene, which became activated in response to various acute stimuli and peaks at 90–120 min post-challenge (86). Cell population commonly displaying stress-induced c-Fos-immunoreactivity in response to all kinds of stressors is regarded as a core stress-related circuit. Various parts of this core stress circuit have been analyzed in detail in the forebrain and brainstem (77, 79, 114, 115). Similar commonly activated brain structures have been identified by Pacak and Palkovits (14) using different stressors (immobilization, cold, insulin-induced hypoglycemia, hemorrhage and pain). It should be noted however, that the strength of

FOS induction is very heterogeneous even in a commonly activated area of the hypothalamic paraventricular nucleus. Although the functional domains of the PVH in mice are not as well distinguishable as in rats, it is likely that the hypophysiotropic neuron population has been ubiquitously activated. Indeed, all stressors used here resulted in significant elevation of plasma CORT.

In addition to the core system, stressor-specific regions have also been revealed. For instance, contribution of olfactory areas was evident in ether vapor and predator odor exposed animals, which were not activated at all in hypertonic salt or LPS-injected animals. By contrast, magnocelluar neurosecretory cells in the supraoptic nucleus displayed significant FOS staining in response to systemic challenges but not to psychological insults. Comparison of FOS patterns in the mouse brain responding to systemic vs. neurogenic stimuli revealed them as highly distinct with more widespread neuronal activation seen after neurogenic stressors. Such differential activation by interleukin-1 (systemic) vs. foot shock (neurogenic) stressors has been described in rats (116).

The neurobiological function of CRH goes far beyond the initiation of the neuroendocrine stress cascade. CRH has been highly implicated in mediation of behavioral, emotional and affective aspects of the stress response (117). For instance, central delivery of CRH results in changes in locomotion, arousal, anxiety, reward, learning and memory (62, 118, 119). However, the distribution of extrahypophyseotropic stress-related CRH neurons remains to be precisely located and functionally tested. Colocalization of tdTomato signal with FOS protein was used to identify such stress-related CRH neuron population. Among the 95 areas studied, anterior cingulate and orbital/orbitofrontal cortices showed significant colocalization of the two markers in response to all stressors. These cortical areas have been shown to be stress sensitive and implicated in regulation of cognitive functions and affect (120). In response to psychological stressors CRH neurons in another prefrontal cortical area, the dorsal peduncular cortex, became activated. This cell population has been referred to as master regulator, which connects emotion-related cortical structures with the sympathoexcitatory preganglionic neurons in the dorsomedial hypothalamic nucleus (121). This circuit has been shown to mediate thermogenic and cardiovascular responses to psychological challenges.

External and internal threats commonly mobilize both the hypophyseotropic and brain CRH systems. CRH containing, median eminence projecting, parvocellular neurons in the PVH initiate the neuroendocrine stress response, while the widespread brain CRH system governs autonomic and behavioral aspects of stress (29-31). It should also be noted that these functions are not completely distinct, since glucocorticoid hormones, the end-products of the neuroendocrine stress cascade, also have profound central effects on behavior (122). Furthermore, a subpopulation of PVH^{CRH} neurons that possess angiotensin I receptor via projections to the lower brainstem orchestrate neuroendocrine and cardiovascular (autonomic) axes (123).

Brain CRH is involved in arousal and affects the sleep–wake cycle. Noradrenergic output from the locus coeruleus (LC) has been implicated as the major regulator of the arousal. LC is innervated by CRH-positive fibers and CRH injections to LC results in sympatomedullary activation. Furthermore, CeA^{CRH} neurons have been revealed as the source of stress-related CRH into LC (124). The very same LC projecting CRH neurons have also been implicated in stress-induced anxiety, despair and aversion.

More recently, chemogenetic inhibition $BNST^{CRH}$ neurons enhanced fear behavior to predator odor (125), although the target of this CRH-positive neuron population remains to be established. By contrast, systemic IL-1, but not foot shock, resulted in the activation of cells in the same BNST subfield, although the neurochemical nature of these neurons has not been directly addressed (73).

Another interesting finding of this study is the relative weakness of brain CRH recruitment to systemic (LPS and hypertonic salt) challenges compared to stressors with strong psychological components. Indeed, a number of observations suggest the involvement of brain CRH in different psychopathologies. Abnormal levels of CRH were found in the cerebrospinal fluid (CSF) of depressed patients. Melancholic depression was associated with hypersecretion of central CRH and a positive correlation was found between CRH level and the severity of depression. On the other hand, atypical depression is characterized by hypoactive brain CRH activity and suppressed HPA axis. By contrast, PTSD patients have hyperactive central- and blunted neuroendocrine CRH activities (90). It is very likely that CSF CRH originates from the cortical CRH neurons; however, further functional studies are needed to clarify the recruitment of central CRH neurons in these psychopathologies.

In summary, our present comprehensive analysis of the stress-dependent recruitment of brain CRH neurons provides starting points for functional characterization of the brain stress system and for the development of new targets to treat stress-related mental disorders.

5.2. Comparison of acute and chronic stress responses

In everyday life, stress is not an only event. It occurs either repeatedly or chronically. Subsequently, we aimed to model these scenarios and to highlight the differences between hormonal, and behavioral changes induced by acute- repeated- or chronic stress. With comparison of chronic repeated restraint (CRS) and chronic variable stress (CVS), we aimed to observe differences resulting from the variability and unpredictability of chronic stressors.

Variation in the characteristics of stress responses are contingent upon diverse molecular mechanisms underlying the reactions. Fos-related transcription factors, which modulate both acute- and lasting adaptations in gene expression in the target neurons, exhibit distinct expression patterns in the stressed hypothalamus (34). Our current data validate a significantly higher elevation in c-Fos mRNA levels following acute stress compared to chronic challenges. In the latter case, induction of Fosl2 and FosB as markers of chronic neuronal activation could be detected. Most prominent increase in Fosl2 expression could be observed in the hypothalamus of CRS exposed mice. While all stress paradigms led to an elevation in hypothalamic expression of FosB, responses were significantly lower in chronically stressed groups compared to acutely restrained mice. Indeed, Fosl2 encodes Fra-2, a Fos-related protein, which has been shown to mediate gene expression changes in response to repeated immobilization stress (126). FosB has been previously identified as a factor critical for long-term neural and behavioral plasticity to chronic stimuli and in stress resilience (127, 128).

Chronic (variable) mild stress is often co-mentioned with anxiety and depression-like/anhedonic behaviour (129). In our study, anxiety-like behavior developed in response to heterotypic unpredictable- (CVS), but not to homotypic chronic repeated stressors.

In summary, in contrast to the acute stressed animals, in chronically stressed mice, induction of transient transcription factor (c-Fos) is desensitized, while mRNA of

chronic markers is differentially activated in CRS vs CVS exposed mice. Our findings on comparison of mouse behavior in open field test, may support the evidence that chronic exposure to variable stressors induces anxiety and depressive symptoms, unlike the same quality repeated stressors.

5.3. CRH^{PVH} neurons in distinct stress reactions

Besides CRH^{PVH} neurons, the major drivers of neuroendocrine stress response, several diverse cell types and neuronal networks participate in the generation and regulation of the stress cascade. Here, we investigated the specific role of CRH^{PVH} cells in the organization of acute and chronic stress reactions by comparing the activational and behavioral changes seen after acute or repeated restraint stress with those seen after exclusive activation of CRH^{PVH} neurons. For chemogenetic studies, pAAV8/hSyn-DIO-hM3D(Gq)-mCherry viral particle was injected into the PVH of Crh-IRES-Cre mice. This experimental scenario results in Gq-DREADD (hM3D(Gq)) receptor expression exclusively in CRH^{PVH} neurons. DREADD mediated neuronal activation of these neurons was induced by intraperitoneal injection of compound 21 (C21) actuator. In contrast to clozapine N-oxide (CNO) the classic ligand of DREADD, C21 has minimal off-target activity and has exclusive effect on hM3D(Gq) activation (81). It has been shown that CNO is converted to clozapine and may exert clozapine-like behavioral effects (130) and therefore it is not well suited for stress experiments. For this reason, we have used the more specific DREADD agonist compound 21 for activation of hypothalamic neurons. The used dose (1 mg/kg) was recommended by HelloBio, however recent studies report some off-target effects of this compound as well (131).

Comparing the effects of selective CRH^{PVH} neuron activation and one hour restraint-induced acute responses showed that the two treatments resulted in comparable degree of CRH neuron activation, as similar number of FOS+ neurons could be observed in the PVH of the animals. Interestingly, several brain regions (e.g. LS, SUM, LC) showed higher level of neuronal activation in the restrained mice compared to the CRH^{PVH} neuron activated animals. The observation, that neuronal activation pattern of the two groups differ, underlies the importance of brain regions other than the PVH in the organization of acute stress response. Areas, which became c-Fos positive in response to CRH^{PVH} activation are members of a circuit whose activation is dependent

on CRH^{PVH} master cells. By contrast, neurons that display c-Fos after restraint but express much less or no IEG after chemogenetic CRH^{PVH} activation, are stress-responsive, but CRH^{PVH}-independent and/or situated upstream to CRH^{PVH} neurons. Further experiments are needed to identify the neurochemical phenotype, connections and functional relevance of these neurons. For instance, the lateral septum (LS) is among the basal forebrain structures that was activated by restraint but not by CRH^{PVH} stimulation. LS integrates aboundant stress-related cortical/subcortical information and projects to downstream targets to generate appropriate behavioral stress responses independent from CRH^{PVH} activation (132).

Chronic stressors, due to their extended duration, are more prone to instigate enduring physical and behavioral alterations. These changes serve as valuable indicators for observing the underlying processes (133, 134). Repeated stress and repeated stimulation of CRH^{PVH} neurons resulted in decrease of body weight gain. Body weight is a sensitive marker of chronic stress as previously reported (135). CRH is involved in the web of neuropeptides and neurotransmitters regulating food intake and metabolism. CRH itself is anorexigenic, central administration of this neuropeptide results in depressed appetite and increased energy expenditure (136). Furthermore, CRH neurons through their projections to hypothalamic feeding centers and descending projections to the brainstem and spinal cord are capable to inhibit food intake and increase energy expenditure (137), which alignes with our current observations. The fact that both repeated challenges resulted in comparable body weight loss, suggests that effect of chronic stress on the body weight regulation is partly or might entirely mediated through CRH^{PVH} neuron population.

Chronic/repeated stress precipitates anxiety, anhedonia and depressive behavior in human and in laboratory rodents (138). Although we did not reveal major differences in specific markers of anxious behavior (centum preference, latency in corners) in openfield test, detailed analysis of ethograms, revealed a tendency for decreased rearing in both repeatedly challenged groups and tendency for decreased survey in the group of repeatedly restrained animals. Decreased rearing and exporatory behavior in a novel environment are also a sign of anxiety (64). Significant difference was found in grooming, where both frequency and duration of this behavior was higher in repeatedly restrained animals compared to controls or animals in which CRH^{PVH} neurons were

repeatedly activated. Mouse self grooming is a complex innate behavior, a specific sequence of stereotyped movements. It has been shown that aversive stimuli, including stress, precipitate grooming (139). This observation is in line with our results, showing increased grooming in repeatedly restrained animals. It has also been reported that the patterning of self grooming is different in stressed animals compared to those that are „in comfort" (139). Although grooming is a stress-related behavior in a novel environment, based on our present findings, it is not very likely that CRH^{PVH} neurons are involved in the neuronal circuit which regulates grooming in a repeated stress paradigm. By contrast, data reported by Füzesi et al. (140) have shown that foot shock stress-induced grooming is suppressed by optogenetic inhibition of CRH^{PVH} neurons. Furthermore, acute optogenetic activation of CRH^{PVH} neurons significantly increased grooming activity in the homecage. The reason why these findings are different, remains to be systematically revealed. It may be a difference between optogenetic vs. chemogenetic activation of PVH CRH neurons. Alternatively, in our experiment, CRH^{PVH} neurons were repeatedly stimulated for two weeks, not only once for a short period of time. Additional difference may originate from the location where the experiments have been performed. Füzesi et al. tested their mice in the homecage, while our data were obtained in an open field arena. Indeed, grooming was context-dependent also in optogenetically activated animals. It should also be noted that stress hormones, ACTH and corticosterone have been shown to induce self-grooming behavior. Thus, the difference between our results and that of Füzesi et al. may originate from hormone-release differences in response to optogenetic vs chemogenetic activation of HPA axis.

Decrease in nest's quality in chronically challenged mice is also indicative of disturbed well-being, loss of motivation, or disturbed goal-oriented performance. Nest building is an innate behavior, which is seen in both sexes (141). It has been shown that the nest building behavior is reduced by stress (142). In line with this information, we found that the quality of nests was reduced in both repeatedly challenged groups. Although the neuronal circuit which mediates nest building behavior is not fully established, our present results suggest that direct, repeated (chemogenetic) activation of CRH neurons in the hypothalamic paraventricular nucleus may interfere with nest building.

Data obtained in the tail suspension test (TST) also indicate some behavioral despair. This test has been developed for mice to examine the effects of antidepressants in preclinical setting, however there are still debates about the interpretation of immobility and escape seen during TST (143). The moving frequency was significantly higher in animals with activated CRH^{PVH} neurons (compared to repeatedly restrained animals). These data, together with the finding of significantly higher duration of immobility in both chronically challenged animals reveals that the immobile state is more frequently interrupted by attempts of escape in mice, whose CRH^{PVH} neurons have been repeatedly activated.

Restraint − as a psychological stressor – recruits numerous brain regions to formulate an adequate stress response, including stress-induced behavioral adaptation. Several limbic (e.g. BNST and amygdala), cortical- (sensory and motor cortex) and subcortical structures exert their impact via interconnections among each other (32, 33). Many brain regions play essential role in organization of chronic restraint-induced behavioral elements. For instance, basolateral amygdala, CEA and the anterior division of bed nuclei of stria terminalis (BSTa) play essential role in the initiation of movement patterns associated with stress responses (139, 144, 145). In contrast, behaviors observed after C21 actuator-induced selective CRH^{PVH} activation represents the exclusive action of these neurons. With the comparison of behavioral elements that are differentially affected by restraint vs the specific activation of CRH^{PVH} neurons, one can start to tease apart the neuronal circuit involved in organization of stress response. Thus, the observed stress response differences are likely to arise from the differences of neuronal network and/or differences in signal transduction pathways and molecular cascades in stress-related neurons.

Tail suspension test is not only a behavioral test, but also a robust stressor. This allowed us to investigate hormonal responses to a novel, heterotypic stressor (i.e. tail suspension). Prior exposure to severe stressors results in a hyperresponsive state to further novel stressors. This sensitization provides a basis of certain stress-induced psychopathologies such as post-traumatic stress disorder (PTSD) or psychosis (146). As expected, the heterotypic stressor resulted in significant elevation of serum corticosterone in all groups. However, the corticosterone (CORT) response was highly sensitized in mice, which have been repeatedly restrained for 2 weeks before exposure

to tail suspension. By contrast, tail suspension induced CORT elevation of mice with repeated chemogenetic activation of CRH^{PVH} neurons, was not sensitized. Therefore, sensitization of hormonal responses might be mediated by hyperactivity of the stress-related neuronal input projecting upon the paraventricular nucleus, rather than the CRH^{PVH} neurons itself. Bhatanagar et al. (147) provided a strong, c-Fos based evidence that the posterior part of the paraventricular thalamic nucleus (postPVTh) is involved in the chronic stress-induced sensitization of hormonal responses to novel stress. Moreover, an increased activity through the parabrachial nucleus-, posterior paraventricular thalamic nucleus-, amygdala- and hypothalamic PVH circuit has been proposed to cause sensitization of HPA activity. Radley and Sawchenko (148) provided functional anatomical evidence for decreased GABAergic inhibitory input originating in the anterior BNST to the hypophyseotropic neurosecretory neurons as the main cause of exaggregated hormonal response to novel stress in rats.

Orexin and cholecystokinin are the neuropeptides that have been hypothesized to mediate facilitated stress response. It has also been shown that impaired fast or delayed glucocorticoid negative feedback may not be involved. Although the extraparaventricular brain CRH pathways (i.e. brain-stress system) appear to influence cross-sensitization between chronic stress and drugs of abuse (146), the recruitment of extrahypothalamic CRH neurons in facilitation of hormonal stress response needs to be established.

In summary, our study revealed that cells in distinct brain regions – in addition to CRH^{PVH} neurons – do play significant role in the modulation of stress cascade management: different behavioral characteristics and stress-induced sensitization develop in response to chronic restraint, but not to exclusive CRH^{PVH} activation. To distinguish the exact circuits that are exclusively CRH^{PVH} neuron activated, cross-correlation and network connectivity analysis on c-Fos immunostained brain sections is needed.

DOI:10.14753/SE.2024.3001

6. Conclusion

Main conclusions of my thesis:

1. Crh-IRES-Cre;Ai9 is a proper mouse model for examining stress-induced CRH neuron recruitment of the brain.
2. CRH neurons are widely spread throughout the mouse brain.
3. Different neuronal circuits and CRH clusters take part in the organization of stress cascade in heterotypic acute stress reactions.
4. Neurogenic stimuli result in highly distinct with more widespread neuronal activation compared to the systemic stressors.
5. Recruitment of brain CRH to systemic (LPS and hypertonic salt) challenges shows relative weakness compared to stressors with strong psychological components.
6. In chronically stressed mice induction of neuronal activity marker: transient transcription factor (c-Fos) is desensitized, while mRNA of chronic markers is differentially activated in chronic repeated restraint stress (CRS) vs chronic variable stress (CVS) exposed mice.
7. Chronic exposure to heterotypic unpredictable stressors (CVS) provokes anxiety/depressive symptoms in contrast to repeated stressors.
8. Selective chemogenetic activation of CRH^{PVH} induces neuroendocrine stress response, which justifies key role of CRH^{PVH} in initiation of stress cascade.
9. Exclusively CRH^{PVH} neuron driven stress cascade differs from restraint induced response in many aspects, that highlights the importance of the interplay of additional brain regions.

DOI:10.14753/SE.2024.3001

7. Summary

Corticotropin-releasing hormone (CRH) neurons in the paraventricular hypothalamic nucleus (PVH) are in the position to integrate stress-related information and initiate adaptive neuroendocrine-, autonomic-, metabolic- and behavioral responses. In addition to hypophysiotropic cells, CRH is widely expressed in the CNS, however their involvement in the organization of the stress response is not fully understood. In our experiments, we used the recently available Crh-IRES-Cre;Ai9 mouse line to study the recruitment of hypothalamic and extrahypothalamic CRH neurons in categorically distinct, acute stress reactions. To investigate the role of CRH^{PVH} neurons in the initiation of stress reaction, we compared hormonal, behavioral and molecular responses of mice in which CRH^{PVH} neurons were chemogenetically activated with those exposed to single or repeated restraint. Differences of acute-, chronic variable (CVS)- and chronic repeated restraint (CRS)-induced stress cascade features were also examined. 95 brain regions in the adult male mouse brain have been identified as containing putative CRH neurons with significant expression of tdTomato marker gene. With comparison of CRH mRNA and tdTomato distribution, we found match and mismatch areas. Reporter mice were then exposed to restraint, ether, high salt, lipopolysaccharide or predator odor stressors and neuronal activation was revealed by FOS immunohistochemistry. In addition to a core stress system, stressor-specific areas have been revealed to display activity marker FOS. A stressor-specific differential activation pattern was observed in CRH neurons in extrahypothalamic regions. Comparison of acute selective chemogenetic CRH^{PVH} activation and acute restraint-induced stress cascade revealed several neurons, whose activation is CRH^{PVH}-independent and/or are situated upstream to CRH^{PVH} neurons. Hormonal and behavioral responses induced by repeated activation of CRH^{PVH} differed from those, which were produced by repeted restraint stress, highlighting the importance of additional brain regions in organizing the stress response. In chronic stress (CRS and CVS) the expression of FOS was desensitized, while the mRNA of chronic markers (Fosl2 and Fosb) was differentially activated. Comprehensive description of stress-related CRH neurons in the mouse brain provides a starting point for a systematic functional analysis of the brain stress system and its relation to stress-induced psychopathologies.

DOI:10.14753/SE.2024.3001

8. Összefoglalás

A paraventricularis hypothalamus mag (PVH) corticotropin-releasing hormont (CRH) termelő neuronjai képesek a stresszel kapcsolatos információk integrálására, majd adaptív neuroendokrin, autonóm, metabolikus és viselkedési válaszok indukálására. CRH széles körben expresszálódik a központi idegrendszerben a hipofiziotróp sejteken kívül is, azonban ezen neuronok stresszválaszban betöltött szerepe nem eléggé tisztázott. Kísérleteink során Crh-IRES-Cre;Ai9 egerek segítségével feltérképeztük és összehasonlítottuk különböző stresszorok hatására indukálódó hypotalamikus és extrahypothalamikus CRH neuronok eloszlását. Az egerek agyában 95 régiót azonosítottunk, melyek neuronjai jelentős mértékben fejeztek ki tdTomato markergént, azaz potenciális CRH-t expresszálnak. Egyes területeken egyezett, míg máshol eltért a CRH mRNS és a tdTomato eloszlása. A riporter egereket restrainnek, éternek, magas koncentrációjú sóoldat-, és lipopoliszacharid injekciónak, valamint ragadozószagnak tettük ki. Az aktivált sejteket FOS immuncitokémia segítségével azonosítottuk: alapvető stresszreaktív régiókat és stresszor-specifikus területeket mutattunk ki. A CRH^{PVH} neuronok mind az 5 akut stresszor hatására aktiválódtak; azonban az extrahypothalamikus régiók CRH neuronjainak aktivációs mintázata eltért. A CRH^{PVH} neuronok stresszválaszban betöltött szerepének vizsgálata céljából összehasonlítottuk restraint stressznek kitett állatok hormonális, FOS mintázatbeli- és viselkedési változásait azokkal az egerekkel, melyekben kizárólag a CRH^{PVH} neuronokat aktiváltuk kemogenetikailag. Megfigyeltük az akut, a krónikus változó (CVS) és a krónikus ismételt restraint (CRS) stressz által kiváltott stresszkaszkád jellemzőit is. Az akut szelektív kemogenetikai CRH^{PVH} aktiváció és az akut restraint indukálta stresszkaszkád összehasonlításával kimutattunk agyterületeket, melyek aktivációja független CRH^{PVH} neuronokétól. A CRH^{PVH} sejtek ismétlődő aktivációja indukálta krónikus stresszreakció számos aspektusban eltér a krónikus restraint indukáltától, mely kiemeli az egyéb agyterületek sztresszreakció megszervezésében betöltött szerepét. Krónikus stressz esetén (CRS és CVS) a FOS expresszió deszenzitizált, míg a krónikus markerek (Fosl2 és Fosb) mRNS szintje eltérő volt. Az egéragy stresszel kapcsolatos CRH neuronjainak azonosítása kiindulópontot ad az agyi stresszrendszer szisztematikus funkcionális elemzéséhez, valamint a stressz által kiváltott pszichopatológiai betegségek hátterében húzódó folyamatok megértéséhez.

9. References

1. Bernard C, Greene HC, Henderson LJ, Cohen IB. An Introduction to the Study of Experimental Medicine: Dover Publications; 1957.
2. Cannon W, Pettit A. A Charles Richet: ses amis, ses collègues, ses élèves. Paris: Les Éditions Médicales. 1926.
3. Cannon WB. The wisdom of the body1939.
4. Cannon WB. ORGANIZATION FOR PHYSIOLOGICAL HOMEOSTASIS. Physiological Reviews. 1929;9(3):399-431.
5. Richter CP. Total self-regulatory functions in animals and human beings. Harvey Lecture Series. 1943;38(63):1942-3.
6. Hardy JD. Control of heat loss and heat production in physiologic temperature regulation. Harvey Lect. 1953;49:242-70.
7. Selye H. Stress without Distress. In: Serban G, editor. Psychopathology of Human Adaptation. Boston, MA: Springer US; 1976. p. 137-46.
8. Selye H. Stress and the general adaptation syndrome. Br Med J. 1950;1(4667):1383-92.
9. Selye H. The general adaptation syndrome and the diseases of adaptation. J Clin Endocrinol Metab. 1946;6:117-230.
10. Selye H. A Syndrome produced by Diverse Nocuous Agents. Nature. 1936;138(3479):32-.
11. Nawe J. DUAL RESPONSIBILITY OF MANAGING STRESS, EUSTRESS, DISTRESS, RUST-OUT AND BURN-OUT IN LIBRARIES. University of Dar es Salaam Library Journal. 2003;4(1&2):43-57.
12. Bienertova-Vasku J, Lenart P, Scheringer M. Eustress and Distress: Neither Good Nor Bad, but Rather the Same? BioEssays. 2020;42(7):1900238.
13. Kovács KJ, Miklós IH, Bali B. Chapter 6.1 - Psychological and physiological stressors. In: Steckler T, Kalin NH, Reul JMHM, editors. Techniques in the Behavioral and Neural Sciences. 15: Elsevier; 2005. p. 775-92.
14. Pacák K, Palkovits M. Stressor specificity of central neuroendocrine responses: implications for stress-related disorders. Endocr Rev. 2001;22(4):502-48.
15. Nederhof E, Schmidt MV. Mismatch or cumulative stress: toward an integrated hypothesis of programming effects. Physiol Behav. 2012;106(5):691-700.

16. Santarelli S, Lesuis SL, Wang XD, Wagner KV, Hartmann J, Labermaier C, Scharf SH, Müller MB, Holsboer F, Schmidt MV. Evidence supporting the match/mismatch hypothesis of psychiatric disorders. Eur Neuropsychopharmacol. 2014;24(6):907-18.
17. Ketchesin KD, Stinnett GS, Seasholtz AF. Corticotropin-releasing hormone-binding protein and stress: from invertebrates to humans. Stress. 2017;20(5):449-64.
18. Masood A, Nadeem A, Mustafa SJ, O'Donnell JM. Reversal of oxidative stress-induced anxiety by inhibition of phosphodiesterase-2 in mice. J Pharmacol Exp Ther. 2008;326(2):369-79.
19. Tyng CM, Amin HU, Saad MNM, Malik AS. The Influences of Emotion on Learning and Memory. Front Psychol. 2017;8:1454.
20. Godoy LD, Rossignoli MT, Delfino-Pereira P, Garcia-Cairasco N, de Lima Umeoka EH. A Comprehensive Overview on Stress Neurobiology: Basic Concepts and Clinical Implications. Front Behav Neurosci. 2018;12:127.
21. Chu B, Marwaha K, Sanvictores T, Ayers D. Physiology, Stress Reaction. StatPearls. Treasure Island (FL): StatPearls Publishing
Copyright © 2023, StatPearls Publishing LLC.; 2023.
22. Christensen NJ. The biochemical assessment of sympathoadrenal activity in man. Clin Auton Res. 1991;1(2):167-72.
23. Tsigos C, Kyrou I, Kassi E, Chrousos GP. Stress: Endocrine Physiology and Pathophysiology. In: Feingold KR, Anawalt B, Blackman MR, Boyce A, Chrousos G, Corpas E, de Herder WW, Dhatariya K, Dungan K, Hofland J, Kalra S, Kaltsas G, Kapoor N, Koch C, Kopp P, Korbonits M, Kovacs CS, Kuohung W, Laferrère B, Levy M, McGee EA, McLachlan R, New M, Purnell J, Sahay R, Shah AS, Singer F, Sperling MA, Stratakis CA, Trence DL, Wilson DP, editors. Endotext. South Dartmouth (MA): MDText.com, Inc.
Copyright © 2000-2024, MDText.com, Inc.; 2000.
24. Cannon WB. Bodily changes in pain, hunger, fear and rage: An account of recent researches into the function of emotional excitement. New York, NY, US: D Appleton & Company; 1915. xiii, 311-xiii, p.

25. Tank AW, Lee Wong D. Peripheral and central effects of circulating catecholamines. Compr Physiol. 2015;5(1):1-15.
26. Wadsworth ME, Broderick AV, Loughlin-Presnal JE, Bendezu JJ, Joos CM, Ahlkvist JA, Perzow SED, McDonald A. Co-activation of SAM and HPA responses to acute stress: A review of the literature and test of differential associations with preadolescents' internalizing and externalizing. Dev Psychobiol. 2019;61(7):1079-93.
27. MUNCK A, NÁRAY-FEJES-TÓTH A. Glucocorticoids and Stress: Permissive and Suppressive Actions. Annals of the New York Academy of Sciences. 1994;746(1):115-30.
28. Munck A, Náray-Fejes-Tóth A. The ups and downs of glucocorticoid physiology. Permissive and suppressive effects revisited. Mol Cell Endocrinol. 1992;90(1):C1-4.
29. Sawchenko PE, Brown ER, Chan RK, Ericsson A, Li HY, Roland BL, Kovács KJ. The paraventricular nucleus of the hypothalamus and the functional neuroanatomy of visceromotor responses to stress. Prog Brain Res. 1996;107:201-22.
30. Swanson LW, Sawchenko PE, Rivier J, Vale WW. Organization of ovine corticotropin-releasing factor immunoreactive cells and fibers in the rat brain: an immunohistochemical study. Neuroendocrinology. 1983;36(3):165-86.
31. Kovács KJ. CRH: the link between hormonal-, metabolic- and behavioral responses to stress. J Chem Neuroanat. 2013;54:25-33.
32. Herman JP, Figueiredo H, Mueller NK, Ulrich-Lai Y, Ostrander MM, Choi DC, Cullinan WE. Central mechanisms of stress integration: hierarchical circuitry controlling hypothalamo-pituitary-adrenocortical responsiveness. Front Neuroendocrinol. 2003;24(3):151-80.
33. Sheng JA, Bales NJ, Myers SA, Bautista AI, Roueinfar M, Hale TM, Handa RJ. The Hypothalamic-Pituitary-Adrenal Axis: Development, Programming Actions of Hormones, and Maternal-Fetal Interactions. Front Behav Neurosci. 2020;14:601939.
34. Kovács KJ. Measurement of Immediate-Early Gene Activation- c-fos and Beyond. Journal of Neuroendocrinology. 2008;20(6):665-72.

35. Levy B, Tasker J. Synaptic regulation of the hypothalamic–pituitary–adrenal axis and its modulation by glucocorticoids and stress. Frontiers in Cellular Neuroscience. 2012;6.
36. Cole RL, Sawchenko PE. Neurotransmitter regulation of cellular activation and neuropeptide gene expression in the paraventricular nucleus of the hypothalamus. J Neurosci. 2002;22(3):959-69.
37. Gjerstad JK, Lightman SL, Spiga F. Role of glucocorticoid negative feedback in the regulation of HPA axis pulsatility. Stress. 2018;21(5):403-16.
38. Di S, Malcher-Lopes R, Halmos KC, Tasker JG. Nongenomic glucocorticoid inhibition via endocannabinoid release in the hypothalamus: a fast feedback mechanism. J Neurosci. 2003;23(12):4850-7.
39. Focke CMB, Iremonger KJ. Rhythmicity matters: Circadian and ultradian patterns of HPA axis activity. Mol Cell Endocrinol. 2020;501:110652.
40. Pierre K, Rao RT, Hartmanshenn C, Androulakis IP. Modeling the Influence of Seasonal Differences in the HPA Axis on Synchronization of the Circadian Clock and Cell Cycle. Endocrinology. 2018;159(4):1808-26.
41. Sandi C. Stress, cognitive impairment and cell adhesion molecules. Nat Rev Neurosci. 2004;5(12):917-30.
42. Lupien SJ, de Leon M, de Santi S, Convit A, Tarshish C, Nair NP, Thakur M, McEwen BS, Hauger RL, Meaney MJ. Cortisol levels during human aging predict hippocampal atrophy and memory deficits. Nat Neurosci. 1998;1(1):69-73.
43. McIntyre CK, McGaugh JL, Williams CL. Interacting brain systems modulate memory consolidation. Neurosci Biobehav Rev. 2012;36(7):1750-62.
44. Katsu Y, Baker ME. Subchapter 123D - Cortisol. In: Ando H, Ukena K, Nagata S, editors. Handbook of Hormones (Second Edition). San Diego: Academic Press; 2021. p. 947-9.
45. Vale W, Spiess J, Rivier C, Rivier J. Characterization of a 41-residue ovine hypothalamic peptide that stimulates secretion of corticotropin and beta-endorphin. Science. 1981;213(4514):1394-7.

46. Schmidt M, Enthoven L, van der Mark M, Levine S, de Kloet ER, Oitzl MS. The postnatal development of the hypothalamic–pituitary–adrenal axis in the mouse. International Journal of Developmental Neuroscience. 2003;21(3):125-32.
47. Kuperman Y, Weiss M, Dine J, Staikin K, Golani O, Ramot A, Nahum T, Kühne C, Shemesh Y, Wurst W, Harmelin A, Deussing JM, Eder M, Chen A. CRFR1 in AgRP Neurons Modulates Sympathetic Nervous System Activity to Adapt to Cold Stress and Fasting. Cell Metab. 2016;23(6):1185-99.
48. Merchenthaler I. Corticotropin releasing factor (CRF)-like immunoreactivity in the rat central nervous system. Extrahypothalamic distribution. Peptides. 1984;5 Suppl 1:53-69.
49. Van Bockstaele EJ, Colago EE, Valentino RJ. Amygdaloid corticotropin-releasing factor targets locus coeruleus dendrites: substrate for the co-ordination of emotional and cognitive limbs of the stress response. J Neuroendocrinol. 1998;10(10):743-57.
50. Boorse GC, Denver RJ. Widespread tissue distribution and diverse functions of corticotropin-releasing factor and related peptides. General and Comparative Endocrinology. 2006;146(1):9-18.
51. Stengel A, Taché Y. Corticotropin-releasing factor signaling and visceral response to stress. Exp Biol Med (Maywood). 2010;235(10):1168-78.
52. Laryea G, Arnett MG, Muglia LJ. Behavioral Studies and Genetic Alterations in Corticotropin-Releasing Hormone (CRH) Neurocircuitry: Insights into Human Psychiatric Disorders. Behav Sci (Basel). 2012;2(2):135-71.
53. Rassouli O, Liapakis G, Lazaridis I, Sakellaris G, Gkountelias K, Gravanis A, Margioris AN, Karalis KP, Venihaki M. A novel role of peripheral corticotropin-releasing hormone (CRH) on dermal fibroblasts. PLoS One. 2011;6(7):e21654.
54. Taché Y, Bonaz B. Corticotropin-releasing factor receptors and stress-related alterations of gut motor function. J Clin Invest. 2007;117(1):33-40.
55. Kalantaridou S, Makrigiannakis A, Zoumakis E, Chrousos GP. Peripheral corticotropin-releasing hormone is produced in the immune and reproductive systems: actions, potential roles and clinical implications. Front Biosci. 2007;12:572-80.

56. Suda T, Tomori N, Tozawa F, Mouri T, Demura H, Shizume K. Distribution and characterization of immunoreactive corticotropin-releasing factor in human tissues. J Clin Endocrinol Metab. 1984;59(5):861-6.
57. Peng J, Long B, Yuan J, Peng X, Ni H, Li X, Gong H, Luo Q, Li A. A Quantitative Analysis of the Distribution of CRH Neurons in Whole Mouse Brain. Front Neuroanat. 2017;11:63.
58. Kono J, Konno K, Talukder AH, Fuse T, Abe M, Uchida K, Horio S, Sakimura K, Watanabe M, Itoi K. Distribution of corticotropin-releasing factor neurons in the mouse brain: a study using corticotropin-releasing factor-modified yellow fluorescent protein knock-in mouse. Brain Struct Funct. 2017;222(4):1705-32.
59. Alon T, Zhou L, Pérez CA, Garfield AS, Friedman JM, Heisler LK. Transgenic mice expressing green fluorescent protein under the control of the corticotropin-releasing hormone promoter. Endocrinology. 2009;150(12):5626-32.
60. Dunn AJ, Berridge CW. Physiological and behavioral responses to corticotropin-releasing factor administration: is CRF a mediator of anxiety or stress responses? Brain Research Reviews. 1990;15(2):71-100.
61. Koob GF. A Role for Brain Stress Systems in Addiction. Neuron. 2008;59(1):11-34.
62. Linthorst ACE, Flachskamm C, Hopkins SJ, Hoadley ME, Labeur MS, Holsboer F, Reul JMHM. Long-Term Intracerebroventricular Infusion of Corticotropin-Releasing Hormone Alters Neuroendocrine, Neurochemical, Autonomic, Behavioral, and Cytokine Responses to a Systemic Inflammatory Challenge. The Journal of Neuroscience. 1997;17(11):4448-60.
63. Devilbiss DM, Waterhouse BD, Berridge CW, Valentino R. Corticotropin-Releasing Factor Acting at the Locus Coeruleus Disrupts Thalamic and Cortical Sensory-Evoked Responses. Neuropsychopharmacology. 2012;37(9):2020-30.
64. Sztainberg Y, Chen A. Chapter 15 - Neuropeptide Regulation of Stress-Induced Behavior: Insights from the CRF/Urocortin Family. In: Fink G, Pfaff DW, Levine JE, editors. Handbook of Neuroendocrinology. San Diego: Academic Press; 2012. p. 355-75.

65. Antoni FA, Palkovits M, Makara GB, Linton EA, Lowry PJ, Kiss JZ. Immunoreactive Corticotropin-Releasing Hormone in the Hypothalamoinfundibular Tract. Neuroendocrinology. 2008;36(6):415-23.
66. Ann-Judith Silverman AH-YDDK. Modofication of hypothalamic neurons by behavioral stress. In: Tache IMJE, Brown, M.R., editor. Neuropeptides and Stress. pp. Springer: Berlin/Heidelberg, Germany1989. p. 23–37.
67. Taniguchi H, He M, Wu P, Kim S, Paik R, Sugino K, Kvitsani D, Fu Y, Lu J, Lin Y, Miyoshi G, Shima Y, Fishell G, Nelson Sacha B, Huang ZJ. A Resource of Cre Driver Lines for Genetic Targeting of GABAergic Neurons in Cerebral Cortex. Neuron. 2011;71(6):995-1013.
68. Wamsteeker Cusulin JI, Füzesi T, Watts AG, Bains JS. Characterization of corticotropin-releasing hormone neurons in the paraventricular nucleus of the hypothalamus of Crh-IRES-Cre mutant mice. PLoS One. 2013;8(5):e64943.
69. Chen Y, Molet J, Gunn BG, Ressler K, Baram TZ. Diversity of Reporter Expression Patterns in Transgenic Mouse Lines Targeting Corticotropin-Releasing Hormone-Expressing Neurons. Endocrinology. 2015;156(12):4769-80.
70. Morgan JI, Curran T. Stimulus-Transcription Coupling in the Nervous System: Involvement of the Inducible Proto-Oncogenes fos and jun. Annual Review of Neuroscience. 1991;14(1):421-51.
71. Chan R, Brown E, Ericsson A, Kovacs K, Sawchenko P. A comparison of two immediate-early genes, c-fos and NGFI-B, as markers for functional activation in stress-related neuroendocrine circuitry. The Journal of Neuroscience. 1993;13(12):5126-38.
72. Park AY, Park YS, So D, Song IK, Choi JE, Kim HJ, Lee KJ. Activity-Regulated Cytoskeleton-Associated Protein (Arc/Arg3.1) is Transiently Expressed after Heat Shock Stress and Suppresses Heat Shock Factor 1. Sci Rep. 2019;9(1):2592.
73. Sawchenko PE, Li HY, Ericsson A. Circuits and mechanisms governing hypothalamic responses to stress: a tale of two paradigms. Prog Brain Res. 2000;122:61-78.

74. Rivest S, Rivier C. Stress and Interleukin-1 β-Induced Activation of c-fos, NGFI-B ann CRF Gene Expression in the Hypothalamic PVN: Comparison Between Sprague-Dawley, Fisher-344 and Lewis Rats. Journal of Neuroendocrinology. 1994;6(1):101-17.
75. Radley JJ, Arias CM, Sawchenko PE. Regional Differentiation of the Medial Prefrontal Cortex in Regulating Adaptive Responses to Acute Emotional Stress. The Journal of Neuroscience. 2006;26(50):12967-76.
76. Ericsson A, Kovács KJ, Sawchenko PE. A functional anatomical analysis of central pathways subserving the effects of interleukin-1 on stress-related neuroendocrine neurons. J Neurosci. 1994;14(2):897-913.
77. Dayas CV, Buller KM, Crane JW, Xu Y, Day TA. Stressor categorization: acute physical and psychological stressors elicit distinctive recruitment patterns in the amygdala and in medullary noradrenergic cell groups. European Journal of Neuroscience. 2001;14(7):1143-52.
78. Cullinan WE, Helmreich DL, Watson SJ. Fos expression in forebrain afferents to the hypothalamic paraventricular nucleus following swim stress. J Comp Neurol. 1996;368(1):88-99.
79. Campeau S, Watson SJ. Neuroendocrine and behavioral responses and brain pattern of c-fos induction associated with audiogenic stress. J Neuroendocrinol. 1997;9(8):577-88.
80. Lara Aparicio SY, Laureani Fierro ÁdJ, Aranda Abreu GE, Toledo Cárdenas R, García Hernández LI, Coria Ávila GA, Rojas Durán F, Aguilar MEH, Manzo Denes J, Chi-Castañeda LD, Pérez Estudillo CA. Current Opinion on the Use of c-Fos in Neuroscience. NeuroSci. 2022;3(4):687-702.
81. Roth BL. DREADDs for Neuroscientists. Neuron. 2016;89(4):683-94.
82. Naso MF, Tomkowicz B, Perry WL, 3rd, Strohl WR. Adeno-Associated Virus (AAV) as a Vector for Gene Therapy. BioDrugs. 2017;31(4):317-34.
83. Li H, Illenberger JM, Cranston MN, Mactutus CF, McLaurin KA, Harrod SB, Booze RM. Posterior ventral tegmental area-nucleus accumbens shell circuitry modulates response to novelty. PLoS One. 2019;14(3):e0213088.

84. Krashes MJ, Koda S, Ye C, Rogan SC, Adams AC, Cusher DS, Maratos-Flier E, Roth BL, Lowell BB. Rapid, reversible activation of AgRP neurons drives feeding behavior in mice. J Clin Invest. 2011;121(4):1424-8.
85. Lightman SL, Young WS, 3rd. Corticotrophin-releasing factor, vasopressin and pro-opiomelanocortin mRNA responses to stress and opiates in the rat. J Physiol. 1988;403:511-23.
86. Kovacs KJ, Sawchenko PE. Sequence of stress-induced alterations in indices of synaptic and transcriptional activation in parvocellular neurosecretory neurons. J Neurosci. 1996;16(1):262-73.
87. Matsuo T, Isosaka T, Tang L, Soga T, Kobayakawa R, Kobayakawa K. Artificial hibernation/life-protective state induced by thiazoline-related innate fear odors. Commun Biol. 2021;4(1):101.
88. Neely CLC, Pedemonte KA, Boggs KN, Flinn JM. Nest Building Behavior as an Early Indicator of Behavioral Deficits in Mice. J Vis Exp. 2019(152).
89. Brown JM, Phan BA, Aalling N, Morton GJ, Schwartz MW, Scarlett JM. Combined micro-osmotic pump infusion and intracerebroventricular injection to study FGF1 signaling pathways in the mouse brain. STAR Protoc. 2022;3(2):101329.
90. Kasckow JW, Baker D, Geracioti TD, Jr. Corticotropin-releasing hormone in depression and post-traumatic stress disorder. Peptides. 2001;22(5):845-51.
91. Andersen CL, Jensen JL, Ørntoft TF. Normalization of real-time quantitative reverse transcription-PCR data: a model-based variance estimation approach to identify genes suited for normalization, applied to bladder and colon cancer data sets. Cancer Res. 2004;64(15):5245-50.
92. Zelena D, Mergl Z, Foldes A, Kovács KJ, Tóth Z, Makara GB. Role of hypothalamic inputs in maintaining pituitary-adrenal responsiveness in repeated restraint. Am J Physiol Endocrinol Metab. 2003;285(5):E1110-7.
93. Kier A, Han J, Jacobson L. Chronic treatment with the monoamine oxidase inhibitor phenelzine increases hypothalamic-pituitary-adrenocortical activity in male C57BL/6 mice: relevance to atypical depression. Endocrinology. 2005;146(3):1338-47.

94. Ito H, Nagano M, Suzuki H, Murakoshi T. Chronic stress enhances synaptic plasticity due to disinhibition in the anterior cingulate cortex and induces hyper-locomotion in mice. Neuropharmacology. 2010;58(4-5):746-57.
95. Niu M, Kasai A, Tanuma M, Seiriki K, Igarashi H, Kuwaki T, Nagayasu K, Miyaji K, Ueno H, Tanabe W, Seo K, Yokoyama R, Ohkubo J, Ago Y, Hayashida M, Inoue KI, Takada M, Yamaguchi S, Nakazawa T, Kaneko S, Okuno H, Yamanaka A, Hashimoto H. Claustrum mediates bidirectional and reversible control of stress-induced anxiety responses. Sci Adv. 2022;8(11):eabi6375.
96. Zhang WH, Zhang JY, Holmes A, Pan BX. Amygdala Circuit Substrates for Stress Adaptation and Adversity. Biol Psychiatry. 2021;89(9):847-56.
97. Crestani CC, Alves FH, Gomes FV, Resstel LB, Correa FM, Herman JP. Mechanisms in the bed nucleus of the stria terminalis involved in control of autonomic and neuroendocrine functions: a review. Curr Neuropharmacol. 2013;11(2):141-59.
98. Campeau S, Akil H, Watson SJ. Lesions of the medial geniculate nuclei specifically block corticosterone release and induction of c-fos mRNA in the forebrain associated with audiogenic stress in rats. J Neurosci. 1997;17(15):5979-92.
99. Bang JY, Zhao J, Rahman M, St-Cyr S, McGowan PO, Kim JC. Hippocampus-Anterior Hypothalamic Circuit Modulates Stress-Induced Endocrine and Behavioral Response. Frontiers in Neural Circuits. 2022;16.
100. Gomes-de-Souza L, Costa-Ferreira W, Mendonça MM, Xavier CH, Crestani CC. Lateral hypothalamus involvement in control of stress response by bed nucleus of the stria terminalis endocannabinoid neurotransmission in male rats. Sci Rep. 2021;11(1):16133.
101. DiMicco JA, Samuels BC, Zaretskaia MV, Zaretsky DV. The dorsomedial hypothalamus and the response to stress: part renaissance, part revolution. Pharmacol Biochem Behav. 2002;71(3):469-80.
102. Myers B, Carvalho-Netto E, Wick-Carlson D, Wu C, Naser S, Solomon MB, Ulrich-Lai YM, Herman JP. GABAergic Signaling within a Limbic-

Hypothalamic Circuit Integrates Social and Anxiety-Like Behavior with Stress Reactivity. Neuropsychopharmacology. 2016;41(6):1530-9.

103. Nagashima T, Tohyama S, Mikami K, Nagase M, Morishima M, Kasai A, Hashimoto H, Watabe AM. Parabrachial-to-parasubthalamic nucleus pathway mediates fear-induced suppression of feeding in male mice. Nat Commun. 2022;13(1):7913.
104. McGirr A, LeDue J, Chan AW, Boyd JD, Metzak PD, Murphy TH. Stress impacts sensory variability through cortical sensory activity motifs. Translational Psychiatry. 2020;10(1):20.
105. Hsu DT, Lombardo KA, Bakshi VP, Balachandran JS, Roseboom PH, Kalin NH. Acute stress-induced increases in thalamic CRH mRNA are blocked by repeated stress exposure. Brain Res. 2001;915(1):18-24.
106. Hsu DT, Lombardo KA, Herringa RJ, Bakshi VP, Roseboom PH, Kalin NH. Corticotropin-releasing hormone messenger RNA distribution and stress-induced activation in the thalamus. Neuroscience. 2001;105(4):911-21.
107. Nunez A, Tortorella S, Rodrigo-Angulo M, Garzón M. Synaptic interactions between perifornical lateral hypothalamic area, locus coeruleus nucleus and the oral pontine reticular nucleus are implicated in the stage succession during sleep-wakefulness cycle. Frontiers in Neuroscience. 2013;7.
108. Venkataraman A, Brody N, Reddi P, Guo J, Gordon Rainnie D, Dias BG. Modulation of fear generalization by the zona incerta. Proc Natl Acad Sci U S A. 2019;116(18):9072-7.
109. Zhang L, Zhang P, Qi G, Cai H, Li T, Li M, Cui C, Lei J, Ren K, Yang J, Ming J, Tian B. A zona incerta-basomedial amygdala circuit modulates aversive expectation in emotional stress-induced aversive learning deficits. Front Cell Neurosci. 2022;16:910699.
110. Zhou H, Xiang W, Huang M. Inactivation of Zona Incerta Blocks Social Conditioned Place Aversion and Modulates Post-traumatic Stress Disorder-Like Behaviors in Mice. Front Behav Neurosci. 2021;15:743484.
111. Romero-Leguizamón CR, Kohlmeier KA. Stress-related endogenous neuropeptides induce neuronal excitation in the Laterodorsal Tegmentum. Eur Neuropsychopharmacol. 2020;38:86-97.

112. Madisen L, Zwingman TA, Sunkin SM, Oh SW, Zariwala HA, Gu H, Ng LL, Palmiter RD, Hawrylycz MJ, Jones AR, Lein ES, Zeng H. A robust and high-throughput Cre reporting and characterization system for the whole mouse brain. Nat Neurosci. 2010;13(1):133-40.
113. Walker LC, Cornish LC, Lawrence AJ, Campbell EJ. The effect of acute or repeated stress on the corticotropin releasing factor system in the CRH-IRES-Cre mouse: A validation study. Neuropharmacology. 2019;154:96-106.
114. Abrahám IM, Kovács KJ. Postnatal handling alters the activation of stress-related neuronal circuitries. Eur J Neurosci. 2000;12(8):3003-14.
115. Li HY, Sawchenko PE. Hypothalamic effector neurons and extended circuitries activated in "neurogenic" stress: a comparison of footshock effects exerted acutely, chronically, and in animals with controlled glucocorticoid levels. J Comp Neurol. 1998;393(2):244-66.
116. Li HY, Ericsson A, Sawchenko PE. Distinct mechanisms underlie activation of hypothalamic neurosecretory neurons and their medullary catecholaminergic afferents in categorically different stress paradigms. Proc Natl Acad Sci U S A. 1996;93(6):2359-64.
117. Heinrichs SC, Koob GF. Corticotropin-releasing factor in brain: a role in activation, arousal, and affect regulation. J Pharmacol Exp Ther. 2004;311(2):427-40.
118. Roozendaal B, Schelling G, McGaugh JL. Corticotropin-releasing factor in the basolateral amygdala enhances memory consolidation via an interaction with the beta-adrenoceptor-cAMP pathway: dependence on glucocorticoid receptor activation. J Neurosci. 2008;28(26):6642-51.
119. Servatius RJ, Beck KD, Moldow RL, Salameh G, Tumminello TP, Short KR. A Stress-Induced Anxious State in Male Rats: Corticotropin-Releasing Hormone Induces Persistent Changes in Associative Learning and Startle Reactivity. Biological Psychiatry. 2005;57(8):865-72.
120. Sequeira MK, Gourley SL. The stressed orbitofrontal cortex. Behav Neurosci. 2021;135(2):202-9.
121. Kataoka N, Shima Y, Nakajima K, Nakamura K. A central master driver of psychosocial stress responses in the rat. Science. 2020;367(6482):1105-12.

122. Korte SM, Bouws GA, Bohus B. Central actions of corticotropin-releasing hormone (CRH) on behavioral, neuroendocrine, and cardiovascular regulation: brain corticoid receptor involvement. Horm Behav. 1993;27(2):167-83.
123. Elsaafien K, Kirchner MK, Mohammed M, Eikenberry SA, West C, Scott KA, de Kloet AD, Stern JE, Krause EG. Identification of Novel Cross-Talk between the Neuroendocrine and Autonomic Stress Axes Controlling Blood Pressure. J Neurosci. 2021;41(21):4641-57.
124. McCall JG, Al-Hasani R, Siuda ER, Hong DY, Norris AJ, Ford CP, Bruchas MR. CRH Engagement of the Locus Coeruleus Noradrenergic System Mediates Stress-Induced Anxiety. Neuron. 2015;87(3):605-20.
125. Bruzsik B, Biro L, Sarosdi KR, Zelena D, Sipos E, Szebik H, Török B, Mikics E, Toth M. Neurochemically distinct populations of the bed nucleus of stria terminalis modulate innate fear response to weak threat evoked by predator odor stimuli. Neurobiol Stress. 2021;15:100415.
126. Nankova BB, Rivkin M, Kelz M, Nestler EJ, Sabban EL. Fos-related antigen 2: potential mediator of the transcriptional activation in rat adrenal medulla evoked by repeated immobilization stress. J Neurosci. 2000;20(15):5647-53.
127. Perrotti LI, Hadeishi Y, Ulery PG, Barrot M, Monteggia L, Duman RS, Nestler EJ. Induction of deltaFosB in reward-related brain structures after chronic stress. J Neurosci. 2004;24(47):10594-602.
128. Vialou V, Robison AJ, Laplant QC, Covington HE, 3rd, Dietz DM, Ohnishi YN, Mouzon E, Rush AJ, 3rd, Watts EL, Wallace DL, Iñiguez SD, Ohnishi YH, Steiner MA, Warren BL, Krishnan V, Bolaños CA, Neve RL, Ghose S, Berton O, Tamminga CA, Nestler EJ. DeltaFosB in brain reward circuits mediates resilience to stress and antidepressant responses. Nat Neurosci. 2010;13(6):745-52.
129. Schweizer MC, Henniger MS, Sillaber I. Chronic mild stress (CMS) in mice: of anhedonia, 'anomalous anxiolysis' and activity. PLoS One. 2009;4(1):e4326.
130. Manvich DF, Webster KA, Foster SL, Farrell MS, Ritchie JC, Porter JH, Weinshenker D. The DREADD agonist clozapine N-oxide (CNO) is reverse-metabolized to clozapine and produces clozapine-like interoceptive stimulus effects in rats and mice. Sci Rep. 2018;8(1):3840.

131. Goutaudier R, Coizet V, Carcenac C, Carnicella S. Compound 21, a two-edged sword with both DREADD-selective and off-target outcomes in rats. PLoS One. 2020;15(9):e0238156.
132. Rizzi-Wise CA, Wang DV. Putting Together Pieces of the Lateral Septum: Multifaceted Functions and Its Neural Pathways. eneuro. 2021;8(6):ENEURO.0315-21.2021.
133. Mangiavacchi S, Masi F, Scheggi S, Leggio B, De Montis MG, Gambarana C. Long-term behavioral and neurochemical effects of chronic stress exposure in rats. J Neurochem. 2001;79(6):1113-21.
134. Mesa-Gresa P, Ramos-Campos M, Redolat R. Corticosterone levels and behavioral changes induced by simultaneous exposure to chronic social stress and enriched environments in NMRI male mice. Physiology & Behavior. 2016;158:6-17.
135. Fell R, Gelling M, Macdonald DW, Mathews F, McLaren GW. Body weight change as a measure of stress: a practical test. Animal Welfare. 2004;13(3):337-41.
136. Levine AS, Rogers B, Kneip J, Grace M, Morley JE. Effect of centrally administered corticotropin releasing factor (CRF) on multiple feeding paradigms. Neuropharmacology. 1983;22(3):337-9.
137. Qu N, He Y, Wang C, Xu P, Yang Y, Cai X, Liu H, Yu K, Pei Z, Hyseni I, Sun Z, Fukuda M, Li Y, Tian Q, Xu Y. A POMC-originated circuit regulates stress-induced hypophagia, depression, and anhedonia. Mol Psychiatry. 2020;25(5):1006-21.
138. Tran I, Gellner AK. Long-term effects of chronic stress models in adult mice. J Neural Transm (Vienna). 2023;130(9):1133-51.
139. Kalueff AV, Stewart AM, Song C, Berridge KC, Graybiel AM, Fentress JC. Neurobiology of rodent self-grooming and its value for translational neuroscience. Nat Rev Neurosci. 2016;17(1):45-59.
140. Füzesi T, Daviu N, Wamsteeker Cusulin JI, Bonin RP, Bains JS. Hypothalamic CRH neurons orchestrate complex behaviours after stress. Nat Commun. 2016;7:11937.
141. Deacon RM. Assessing nest building in mice. Nat Protoc. 2006;1(3):1117-9.

142. Jirkof P. Burrowing and nest building behavior as indicators of well-being in mice. Journal of Neuroscience Methods. 2014;234:139-46.
143. Cryan JF, Mombereau C, Vassout A. The tail suspension test as a model for assessing antidepressant activity: Review of pharmacological and genetic studies in mice. Neuroscience & Biobehavioral Reviews. 2005;29(4):571-625.
144. Lebow MA, Chen A. Overshadowed by the amygdala: the bed nucleus of the stria terminalis emerges as key to psychiatric disorders. Molecular Psychiatry. 2016;21(4):450-63.
145. Stamatakis AM, Sparta DR, Jennings JH, McElligott ZA, Decot H, Stuber GD. Amygdala and bed nucleus of the stria terminalis circuitry: Implications for addiction-related behaviors. Neuropharmacology. 2014;76 Pt B(0 0):320-8.
146. Belda X, Nadal R, Armario A. Critical features of acute stress-induced cross-sensitization identified through the hypothalamic-pituitary-adrenal axis output. Scientific Reports. 2016;6(1):31244.
147. Bhatnagar S, Dallman M. Neuroanatomical basis for facilitation of hypothalamic-pituitary-adrenal responses to a novel stressor after chronic stress. Neuroscience. 1998;84(4):1025-39.
148. Radley JJ, Sawchenko PE. Evidence for involvement of a limbic paraventricular hypothalamic inhibitory network in hypothalamic-pituitary-adrenal axis adaptations to repeated stress. J Comp Neurol. 2015;523(18):2769-87.

DOI:10.14753/SE.2024.3001

10. Publications of the author

Publications that form the basis of the Ph.D. dissertation:

Horváth K, Juhász B, Kuti D, Ferenczi S, Kovács KJ.
Recruitment of Corticotropin-Releasing Hormone (CRH) Neurons in Categorically Distinct Stress Reactions in the Mouse Brain. ***INTERNATIONAL JOURNAL OF MOLECULAR SCIENCES*** 2023 Jul 21;24(14):11736.

Kuti D, Winkler Z, **Horváth K**, Juhász B, Szilvásy-Szabó A, Fekete C, Ferenczi S, Kovács KJ.
The metabolic stress response: Adaptation to acute-, repeated- and chronic challenges in mice. ***ISCIENCE*** 2022 Jun 30;25(8):104693.

Other Publications:

Chaves T, Fazekas CL, **Horváth K**, Correia P, Szabó A, Török B, Bánrévi K, Zelena D.
Stress Adaptation and the Brainstem with Focus on Corticotropin-Releasing Hormone. ***INTERNATIONAL JOURNAL OF MOLECULAR SCIENCES*** 2021 Aug 23;22(16):9090.

Josa V, Ferenczi S, Szalai R, Fuder E, Kuti D, **Horvath K**, Hegedus N, Kovacs T, Bagamery G, Juhasz B, Winkler Z, Veres DS, Zrubka Z, Mathe D, Baranyai Z. Thrombocytosis and Effects of IL-6 Knock-Out in a Colitis-Associated Cancer Model. ***INTERNATIONAL JOURNAL OF MOLECULAR SCIENCES*** 2020 Aug 27;21(17):6218.

Kuti D, Winkler Z, **Horváth K**, Juhász B, Paholcsek M, Stágel A, Gulyás G, Czeglédi L, Ferenczi S, Kovács KJ.
Gastrointestinal (non-systemic) antibiotic rifaximin differentially affects chronic stress-induced changes in colon microbiome and gut permeability without effect on behavior. ***BRAIN BEHAVIOR AND IMMUNITY*** 2020 Feb 84:218-228.

Korsós G, **Horváth K**, Likács A, Vezér T, Glávits R, Fodor K, Fekete SG.
Effects of accelerated human music on learning and memory performance of rats. ***APPLIED ANIMAL BEHAVIOUR SCIENCE*** 2018 May 202:94-99.

Fekete SGy, Lukács A, **Horváth K**, Korsós G, Vezér T.
Effects of Mozart Sonata on the rats' learning and memory performance.
MAGYAR ÁLLATORVOSOK LAPJA 2014 March 136(3):167-176.

DOI:10.14753/SE.2024.3001

11. Acknowledgement

First, I would like to thank my supervisor Krisztina Kovács for guiding and supporting me over the years.

I am indebted to all my past and present colleagues, who supported and helped me along my way: Dániel Kuti, Balázs Juhász, Szilamér Ferenczi, Ágnes Polyák, Dóra Kővári and Zsuzsanna Winkler.

I am also very grateful for Pál Vági and László Barna for their unlimited help through the past years. Special thanks to Dóra Zelena, Bibiána Török, Eszter Sipos and Sándor György Fekete for giving me the opportunity to learn from them through our joint work. Furthermore, I am thankful to all the assistants and workers of the institute.

But mainly, this thesis would not have been finished without the support and help of my family and friends. Finally, I owe thanks to all the laboratory animals.